Katsiaryna Marhelava, MSc

Evaluation of the anticancer efficacy of a chimeric antigen receptor targeting PD-L1 molecule

Dissertation on Doctorate in Medical and Health Sciences

in the discipline of Medical Science

Supervisor: Radoslaw Zagozdzon, MD, PhD

Co-supervisor: Malgorzata Bajor, PhD

Department of Clinical Immunology

Defending the doctoral dissertation

before the Medical Science Discipline Council

Medical University of Warsaw

Warsaw 2022

Key words: immunotherapy, breast cancer, chimeric antigen receptor, PD-L1 molecule

Słowa kluczowe: immunoterapia, nowotwór piersi, chimeryczny receptor antygenowy, cząsteczka PD-L1

The work was supported by the grant from the National Science Centre within the funding scheme OPUS 12 – “The Evaluation of the anticancer efficacy of a new chimeric antigen receptor targeting PD-L1 molecule” No 2016/23/B/NZ6/02535.

The studies presented in the current thesis were conducted as a part of the project published as:

Bajor M*, Graczyk- Jarzynka A*, Marhelava K*, et al. PD- L1 CAR effector cells induce self-amplifying cytotoxic effects against target cells. J Immunother Cancer. 2022 Jan;10(1):e002500. doi:10.1136/jitc-2021-002500.

* the authors contributed equally.

ACKNOWLEDGEMENTS

I would like to thank my supervisor, Dr Radoslaw Zagozdzon, for his guidance throughout this project and for sharing his enormous knowledge and creative ideas. I am also very grateful to my co-supervisor, Dr Malgorzata Bajor, for her valuable advice and feedback and for teaching me multiple laboratory techniques.

I would like to thank Dr Agnieszka Graczyk-Jarzynka, with whom I had pleasure to collaborate, for sharing her expertise and for her support and encouragement. I would also like to thank Dr Magdalena Winiarska, whose knowledge, persistence and optimism helped a lot in the realization of this project.

As the research was mainly conducted at the Department of Immunology, I would like to thank all the members and the head of the Department Prof. Jakub Golab for creation of the unique and inspiring environment, for providing advice, assistance, and access to the advanced research facilities.

Finally, I would like to express gratitude towards Postgraduate School of Molecular Medicine and all its member's staff for all the guidance and support during my PhD studies.

TABLE OF CONTENTS

LIST OF FIGURES

LIST OF TABLES

ABBREVIATIONS

Abbreviation	Description
ACT	adoptive cell therapy
ADCC	antibody-dependent cell-mediated cytotoxicity
ALL	acute lymphoblastic leukemia
allo-HSCT	allogeneic hematopoietic stem cell transplantation
ALPPL2	alkaline phosphatase placental-like 2
AML	acute myeloid leukemia
APC	antigen-presenting cell
ATZ	atezolizumab
BMA	bone marrow aspirate
BPE	bovine pituitary extract
BSA	bovine serum albumin
CAF	cancer-associated fibroblast
CAR	chimeric antigen receptor
CARD	caspase recruitment domain
CCL2	C-C motif chemokine ligand 2
cHL	classical Hodgkin lymphoma
CLL	chronic lymphocytic leukemia
CR	complete remission
CRS	cytokine release syndrome
CTLA4	cytotoxic T lymphocyte-associated antigen 4
DC	dendritic cell
DLBCL	diffuse large B-cell lymphoma
DMSO	dimethyl sulfoxide
dsDNA	double-stranded DNA
EGFR	epidermal growth factor receptor
ER+	estrogen receptor-positive
Fab	antigen-binding fragment of an antibody
Fc	fragment crystallizable fragment of an antibody
FDA	US Food and Drug Administration
FRα	folate receptor α
Fv	variable region of an antibody

GM-CSF	granulocyte-macrophage colony-stimulating factor
HCAb	heavy-chain antibody
hEGF	human epidermal growth factor
HIF1-α	hypoxia-inducible-1 factor alpha
HNSCC	head and neck squamous cell carcinoma
HRE	hypoxia-responsive element
ICANS	immune effector cell-associated neurotoxicity syndrome
iCasp9	caspase 9/AP1903 suicide system
ICI	immune checkpoint inhibitor
IFN	interferon
Ig	immunoglobulin
IL	interleukin
irAEs	immune-related adverse events
ITAM	immunoreceptor tyrosine-based activation motif
KO	knock-out
LAG-3	lymphocyte activation gene 3
LPS	lipopolysaccharide
MCAM	melanoma cell adhesion molecule
MCL	mantle cell lymphoma
MDSC	myeloid-derived suppressor cell
MHC	major histocompatibility complex
NHL	non-Hodgkin lymphoma
NK cell	natural killer cell
NSCLC	non–small cell lung cancer
PBMC	peripheral blood mononuclear cell
PBS	phosphate-buffered saline
PCR	polymerase chain reaction
PD-1	programmed cell death protein-1
PD-L1	programmed death-ligand 1
PD-L2	programmed cell death 1 ligand 2
R/R	relapsed or refractory
ROS	reactive oxygen species
scFv	single-chain variable fragment

SDS-PAGE	sodium dodecyl sulfate-polyacrylamide gel electrophoresis
sgRNA	single guide RNA
SMASh-CAR	small molecule-assisted shutoff CAR
SOC	super optimal catabolite repression medium
SWIFF-CAR	switch-off CAR
synNotch	synthetic Notch receptor
TAA	tumor associated antigen
TAM	tumor-associated macrophage
TCR	T-cell receptor
TIGIT	T-cell immunoglobulin and ITIM domain
TIL	tumor-infiltrating lymphocyte
TIM-3	T-cell immunoglobulin-3
TME	tumor microenvironment
TNBC	triple-negative breast cancer
TNF	tumor necrosis factor
Treg	regulatory T cell
TRUCK	T cells redirected for universal cytokine-mediated killing
VH	variable heavy chain of an antibody
VL	variable light chain of an antibody
WHO	World Health Organization

ABSTRACT

The adoptive transfer of T cells expressing chimeric antigen receptors (CARs) is an effective therapy, successfully applied recently in the treatment of hematological malignancies. However, the use of this approach is still limited in the treatment of solid tumors. One of the major challenges is the immunosuppressive environment at the tumor site, which impairs the effectiveness of CAR-T cells. Cancer cells prevent the immune attack by increasing the expression of immune checkpoint molecules, which serve them as natural “shields”. In particular, the immune checkpoint molecule programmed death-ligand 1 (PD-L1) is often selectively overexpressed on the surface of tumor cells and/or on the cells composing tumor microenvironment (TME). Thus, PD-L1 molecule is an attractive target for CAR-based therapy. In this study, the technology of primary human T cells modification with PD-L1-CAR was successfully implemented and optimized in our laboratory. The ability of modified PD-L1-CAR-T cells to recognize and attack PD-L1-expressing tumors was assessed using breast cancer cell lines with various levels of target protein expression. The non-malignant mammary cells were used to evaluate the safety of the PD-L1-CAR-based therapy. The obtained results indicate the efficiency of the PD-L1-CAR-T cells in the specific elimination of PD-L1-positive cells. Additionally, the CAR-bearing T cells were observed to induce PD-L1 expression on the surface of targeted cells, which demonstrates the self-amplifying mechanism of PD-L1-CAR-T cells action. Such a self-amplification phenomenon appears to be unique among the CAR-based strategies and can markedly broaden the potential spectrum of malignancies targeted with the PD-L1-CAR-based therapies. Concomitantly, the obtained data implies the potential cytotoxicity of the PD-L1-CAR-T cells towards non-malignant cells. In summary, the study demonstrates the feasibility of targeting breast cancer using PD-L1-CAR-T cells, while indicating, that this approach requires extensive caution in the introduction into clinical studies.

STRESZCZENIE

Adoptywny transfer limfocytów T, zmodyfikowanych genetycznie tak, aby dochodziło w nich do ekspresji chimerycznych receptorów antygenowych (CARs), jest skuteczną terapią z powodzeniem stosowaną w leczeniu nowotworów hematologicznych. Niemniej wykorzystanie tej metody w terapii guzów litych jest nadal ograniczone. Między innymi wyzwanie stanowi obecne w guzie immunosupresyjne mikrośrodowisko, które negatywnie wpływa na efektywność limfocytów CAR-T. Komórki nowotworowe bronią się przed eliminacją przez komórki układu immunologicznego poprzez zwiększenie ekspresji cząsteczek zwanych „punktami kontrolnymi układu odpornościowego". W szczególności, cząsteczka PD-L1 jest często obecna w nadmiernej ilości na powierzchni komórek nowotworowych oraz/lub innych komórek tworzących guz lity. Zatem białko PD-L1 jest atrakcyjnym celem dla terapii opartej na zastosowaniu chimerycznych receptorów antygenowych zdolnych do rozpoznania tej cząsteczki. W ramach przedstawionej pracy technologię modyfikacji pierwotnych limfocytów T konstruktem kodującym PD-L1-CAR wdrożono i zoptymalizowano w naszym laboratorium. Uzyskane komórki PD-L1-CAR-T zostały ocenione pod względem zdolności do rozpoznawania cząsteczki docelowej oraz do eliminacji komórek nowotworowych mających tę cząsteczkę na swojej powierzchni. Jako modele guzów litych wykorzystane zostały linie komórkowe raka piersi cechujące się zróżnicowaną ekspresją PD-L1. Bezpieczeństwo terapii zostało ocenione przy użyciu niezmienionych nowotworowo komórek pochodzących z gruczołu sutkowego. Otrzymane wyniki wskazują na zdolność limfocytów PD-L1-CAR-T do specyficznej eliminacji komórek charakteryzujących się obecnością białka PD-L1 na swojej powierzchni. Ponadto, zaobserwowano że limfocyty PD-L1-CAR-T wzmacniają własne działanie poprzez indukcję ekspresji PD-L1 na komórkach, które je otaczają. Taki mechanizm nie został wcześniej opisany dla żadnej innej terapii CAR-T i rozszerza potencjał dla wykorzystania limfocytów PD-L1-CAR-T w terapii różnorodnych fenotypowo guzów litych. Jednocześnie, zaobserwowany efekt wskazuje też na możliwą cytotoksyczność limfocytów PD-L1-CAR-T wobec komórek niezmienionych nowotworowo. Podsumowując, przedstawione w pracy badania pokazują, że komórki CAR-T, wyposażone w receptor wiążący cząsteczkę PD-L1, mogą być wykorzystane w terapii nowotworów piersi, jednocześnie, należy podkreslić

konieczność zachowania szczególnej ostrożności przy wprowadzaniu takiej terapii do badań klinicznych.

1. INTRODUCTION

Cancer remains the second worldwide cause of death after ischemic heart disease, but will likely become the first in 2060 considering the issue of an aging population in many countries. According to the World Health Organization (WHO) evaluation in 2019, currently cancer is the first or second leading cause of death under the age of 70 years in 112 of 183 countries, while in only 23 countries it occupies third or fourth place (1). Additionally, cancer has one of the highest clinical, social, and economic impacts among all human diseases, as measured by Disability-Adjusted Life Years (DALYs) index (2). Indeed, despite the existing methods of treatment, it has risen from sixth place in 1990 among the top causes for DALYs worldwide to second place in 2017 after only cardiovascular diseases (3).

1.1 Traditional cancer treatment

Traditional cancer therapy most often includes surgery, radiation therapy, and systemic chemotherapy, including modern molecularly targeted compounds. Each of these methods has several disadvantages that limit their efficacy in the clinic (4).

Surgery is most commonly used to remove the tumor with the margin of surrounding healthy tissue and in some cases, it may be the only treatment applied. However, surgical intervention may not only leave behind the locally invading and/or metastatic cancer cells but sometimes even promote the growth of these cells. This may occur due to the inflammatory state development following the surgical tissue damage, which leads to the release of growth factors, chemokines, and cytokines. The released molecules may act as inducers of tumor progression. Additionally, physiological consequences of surgery include tissue hypoxia and the production of reactive oxygen species (ROS). Altogether, these factors may promote cancer cell invasion, adhesion, and metastasis (5).

Radiation therapy is recommended for approximately half of all cancer patients as a form of treatment. Being a non-invasive treatment, radiotherapy is often chosen as an alternative to surgery for early-stage tumors, especially in cases where it can provide similar therapeutic effects as compared with surgery while preserving the function or

where surgery is not considered due to a patient's comorbidities (6). Radiotherapy can significantly prolong patient's survival and improve the local control rates of tumors; however, the disadvantages of this approach include higher radiation resistance of some tumors than that of the surrounding normal tissue, limited capacity of tumor pathoanatomical borders identification, and the adjustment of the treatment volume. Moreover, the individual heterogeneity in terms of tumor and normal tissue responses toward irradiation is quite significant (7).

In addition to surgery and radiation, chemotherapy is the first-line therapy for many types of cancers, especially those where metastasis is a primary target. Unlike localized tumor, which may be managed by surgery and/or radiotherapy, metastases are spread in distant tissues and organs and could be better reached with drugs that follow the pharmacological rules of distribution in the body (8). However, cytotoxic chemotherapy is considered to have a relatively narrow therapeutic window: if exposure levels are not within the optimal range, there is a risk of either toxicity or a lack of efficacy (9). The side effects of systemic chemotherapy used to treat cancer are often severe. Non-targeted drugs may suppress hematopoiesis and provoke cutaneous eruptions and vascular, lung, and liver injury. Generalized side effects of the newer molecularly targeted drugs occur less often and usually with less severity (10) as this approach is based on the use of agents that discriminate between non-cancer from cancer cells. The evolution of this precision medicine concept became possible due to the cumulating knowledge about cancer cell genetics and physiology. In contrast to normal cells, which functioning requires the involvement of various signaling pathways, cancer cells often preferably exploit a few selected pathways, which is conditioned by activation of several oncogenes and/or loss of genes that suppress tumor growth (11). For example, the first targeted drug tamoxifen binds to the estrogen receptor and thus inhibits the growth of estrogen receptor-positive (ER+) breast cancer (12). Other drugs target the epidermal growth factor receptor (EGFR), a receptor tyrosine kinase, which is overexpressed on over 90% of head and neck cancers and some bladder, ovarian and cervical cancers. Indeed, most of the approved molecularly-targeted chemotherapeutics are tyrosine kinase inhibitors (13). However, despite the advantage coming from decreased generalized toxicity, the application of molecularly targeted drugs may be

followed by tumor adaptation, increased malignancy, and the invasive metastatic switch (10).

Overall, the traditional approaches often result in damage to the tumor-bearing host and the host's immune system. Conversely, some of the novel strategies are aimed at the activation of the patients' immune system via so-called biological therapies, which are often more physiological and well tolerated (14).

1.2 Biological therapies in cancer treatment

The idea that the immune system may be stimulated into recognizing and eradicating neoplasia appeared already back in the 18th century when in the effort to develop a cancer vaccine, the surgeon to the Duke of Kent injected himself with malignant tissue to prevent the development of cancer. A few decades later, the doctor to Louis XVII inoculated himself with breast cancer trying to reverse a soft-tissue sarcoma. However, the first report of successful immunotherapy was published only in 1891 by an American clinician William Coley. The doctor was able to achieve a cure rate of 10% in soft-tissue sarcoma by injecting the heat-killed endotoxin-containing bacteria (15). In 1909, Paul Ehrlich went further and postulated, that the immune system itself is able to both recognize and protect against spontaneously occurring cancer. Fifty years later, Lewis Thomas suggested that the immune system recognizes newly arising tumors by detecting the expression of tumor-specific neo-antigens on tumor cells and eliminating them. At the same time, F. Macfarlane Burnet hypothesized that tumor cell neo-antigens induce an immunological reaction against cancer and subsequently formulated the immune surveillance theory (16). In 1953 two immunologists, Gross and Foley independently demonstrated the specific stimulation of the mice immune response following immunization against different tumors (17). During the subsequent decades, anticancer immunotherapy transformed from a promising therapeutic option into a clinical reality. Many immunotherapeutic regimens are now approved by the US Food and Drug Administration (FDA) and the European Medicines Agency for use in cancer patients, and many others are being investigated alone or in combination with traditional approaches (18). The examples of modern immunotherapy are presented in Figure 1.

Some types of immunotherapy, such as treatment based on using adoptive cells transfer, immune-modulating agents such as cytokines (19), immune checkpoint inhibitors, or small-molecule drugs (20) are aimed at the stimulation of the immune system to efficiently eliminate cancer cells. Other therapies, that target tumors directly, involve the administration of therapeutic antibodies (21,22), cancer vaccines (23), oncolytic viruses (24) or engineered T cells (https://www.cancer.gov).

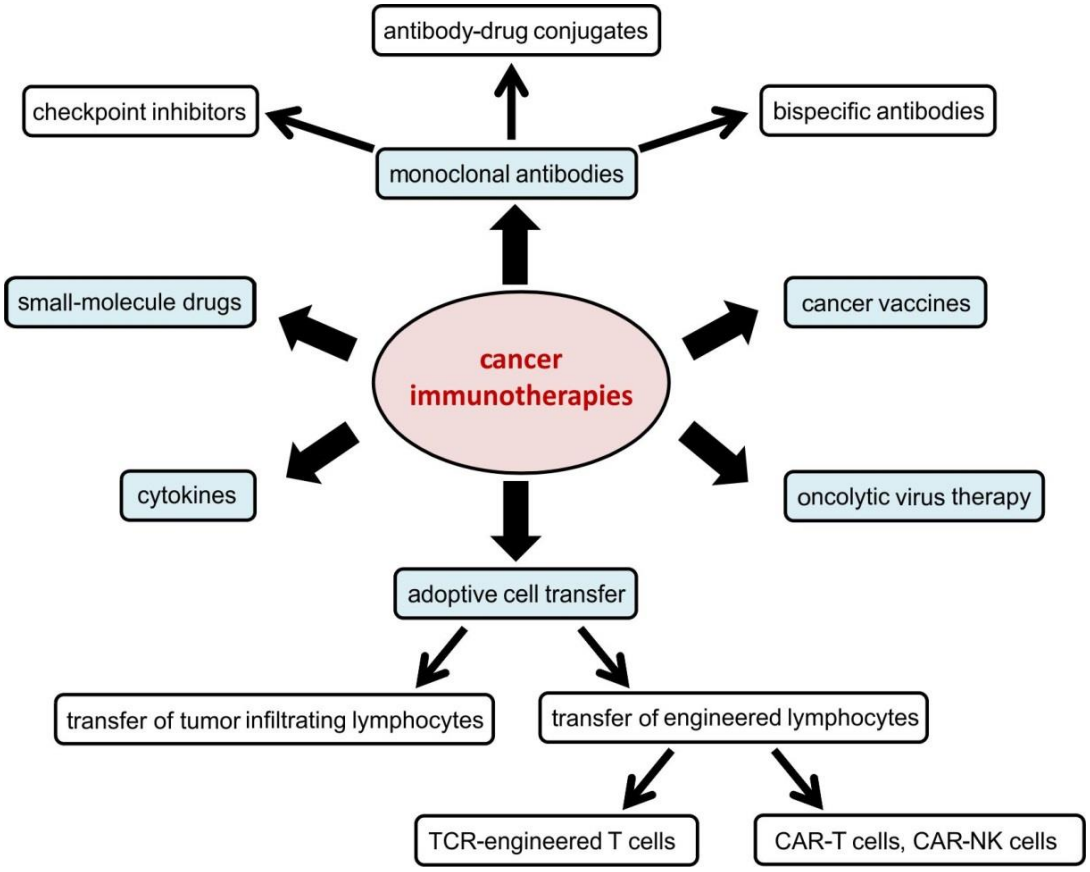

Figure 1 Types of cancer immunotherapy. Based on (23,25,26).

At present, two areas of anticancer immunotherapies develop most rapidly: adoptive immunotherapies and modulation of immune checkpoints.

1.2.1 Adoptive immunotherapies

In 1986, studies showed that some of the murine tumor-infiltrating lymphocytes (TILs) expanded *in vitro* were capable of specific recognition of autologous tumors (27). In 1988, similar effect was observed in clinics, when the adoptive cell therapy (ACT) using autologous TILs mediated objective regression of cancer in patients with metastatic melanoma (28).

Currently, most tumor cells are known to express antigens that host T cells are able to recognize. The presence of point mutations in cancer cell genes may lead to changes in the amino acid sequence of the encoded proteins. Thus, the generated proteins become so-called tumor neo-antigens which are unique to individual tumors. Several studies indicated a subset of patients that can generate a spontaneous CD8+ T cell-mediated response against tumor-associated antigens, independently from pathogen involvement (29). Additionally, the number of mutations harbored by tumors was observed to positively correlate with the probability of endogenous T cell activation. In this case, neo-antigens are recognized as foreign molecules, thereby becoming targets for T cell attack (30). Since neo-antigens differ from non-mutated self-antigens, the quality of the T cell pool that is available for these antigens is not affected by central T cell tolerance (31). However, spontaneous T cell responses against mutant antigens are relatively inefficient and fail to mediate tumor rejection in most cases. Additionally, the clinical evidence suggests that not all patients have tumor-primed T cells that are sufficient to eradicate tumors (32).

Classical adoptive immunotherapy of cancer is based on a transfer of either autologous patient-derived TILs or infusion of allogeneic donor lymphocytes following bone marrow transplantation. The therapy allows for the selection of the T cell populations with the highest tumor recognition ability and necessary effector functions. Moreover, in contrast to other forms of cancer immunotherapy that rely on the *in vivo* development of sufficient numbers of antitumor T cells, large numbers of antitumor T cells for the ACT can be readily grown *in vitro*. After the re-infusion to patients, the cells continue to proliferate *in vivo* with improved antitumor functions (33). The other benefits of this strategy include the possibility of T cell trafficking to the site of antigen and generation of memory T cells, which maintain the therapeutic effect years after initial treatment. Most importantly, the responses of such T cells are specific, and thus can potentially distinguish between healthy and cancerous tissue (34). Cell transfer therapy with autologous TILs was found to be especially efficient for the patients with metastatic melanoma (35), likely because melanomas harbor more mutations as compared to any other type of cancer (36).

The weakness of this strategy comes from the fact, that the majority of tumor-specific antigens that have been identified so far are self-antigens found also in normal tissues. Thus, the potent anti-tumor T cell response to such antigens, often overexpressed or aberrantly expressed by tumors, is restricted within the central tolerance mechanism (37). The T-cells repertoire capable of the highest-avidity interactions between self-peptide, major histocompatibility complex, and T cell antigen receptor is deleted during the T cell development. The remaining T cells are able to generate the immune response restricted to lower-avidity interactions with such antigens, which results in the limited therapeutic efficacy of TILs (29). Indeed, the induction of the successful immune response against the tumor cells expressing self-antigens is the main challenge for cancer immunotherapy (38).

The ability of cancers to escape the immune response by losing the major histocompatibility complex (MHC) class I molecules generates another limitation for using primary T cells in adoptive cell transfer. As mentioned, the antigens expressed on cancer cells can only be recognized by antigen-specific cytotoxic T cells when presented in the context of the MHC. A Darwinian type of immune selection following the tumor infiltration by T cells results in survival of mostly MHC class I-negative cells from an initially heterogeneous population of cancer cells (39).

The solution for overcoming adoptive T-cell therapy deficiencies came in the form of chimeric antigen receptor (CAR)-T-cell therapy, which is based on primary T-cell engineering and the use of synthetic receptors. These artificial constructs are able to recognize any cell surface structure independently of MHC presentation, which greatly broadens the array of antigens that can activate a CAR-T cell with resultant cytotoxicity (40).

1.3 Chimeric antigen receptors

Canonical T cell activation requires multiple signals in order to achieve complete and optimal effector function. First, the T-cell receptor (TCR) is engaged, next the co-stimulation is required and finally, cytokine sensing is needed (41). Chimeric antigen receptors (CARs) were conceived to mimic the function of the TCR complex and progressively evolved to integrate additional signals (42). The CAR is a hybrid antigen

receptor, part antibody-like, and part TCR-like, and is composed of an extracellular antigen-binding domain and intracellular signaling domain(s) (Figure 2). The first construct was presented in 1993 by Schindler's group. The variable regions (Fv) of an antibody were combined with the constant regions of the TCR chains, which allowed the T cell to precisely recognize tumor antigens. The whole structure was linked with gamma or zeta chains, the common signal-transducing subunits of the immunoglobulin receptor and the TCR. The construct generated a functional surface receptor, which triggered interleukin 2 secretion upon encountering antigen and mediated non-major-histocompatibility-complex-restricted hapten-specific target cell lysis (43).

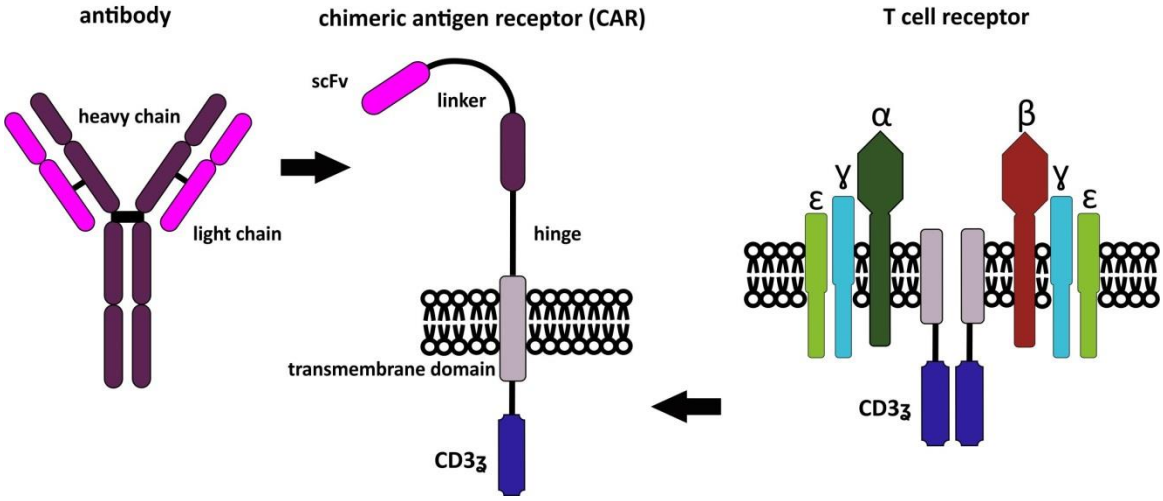

Figure 2 Schematic presentation of the Ist generation chimeric antigen receptor construct (see details in text). Based on (44).

Genetic retargeting of a T cell with a CAR allows for a high level of antigen-specificity, usually through the single-chain variable fragment (scFv) which is derived from a tumor-specific antibody and allows for MHC-independent antigen recognition (45). Another feature of the broad applicability of CARs is their ability to bind not only to proteins but also to carbohydrate and glycolipid structures, additionally expanding the range of potential targets. The domains used to bind to an antigen can be divided into several main categories. Among them, there are scFv sequences derived from antibodies, antigen-binding fragments (Fabs) selected from libraries, and natural ligands that engage their cognate receptor (46). Recently the heavy-chain antibodies (HCAbs) initially found in camelids have expanded the list. HCAbs were discovered to contain only heavy chains with two constant domains (CH2 and CH3) and a short single variable

hinge termed VHH or nanobody, which is the smallest functional antigen-binding fragment of the antibody (47). Successful examples in each of these categories have been reported. However, the scFv fragments obtained from murine immunoglobulins remain the most commonly used, as they are easily derived from well-characterized monoclonal antibodies (46). Antigen recognition is therefore directed to native cell-surface structures (38). The scFv ectodomain of a CAR presents as a small synthetic functional module composed of a variable heavy (VH) and variable light (VL) chain portion of an antibody. The two chain portions are combined with a long flexible linker. The most commonly used linker in several CAR constructs is (Gly4Ser). Glycine residues provide flexibility and serine residues provide solubility. This ensures a properly folded scFv while maintaining the antigen-binding capability of the parental antibody. Differences in the orientation of the VH, linker, and VL may affect the scFv's affinity and specificity, thus being important in CAR-T cell efficacy and safety (48).

The antigen recognition and ligand binding by scFv trigger phosphorylation of the immunoreceptor tyrosine-based activation motifs (ITAM) in the CD3ζ -derived intracellular region of the molecule, activating a signaling cascade (38). The process of T-cell activation involves the induction of proliferation, cytokine secretion, and cytolysis (45). Thus, CAR-T cells combine the dynamics of T cells with the antigen specificity of an antibody. They can bind the tumor antigen without antigen processing and independently of an HLA-mediated antigen presentation (44).

In order to increase the stability of a CAR and to avoid spontaneous activation, a non-signaling extracellular spacer domain is inserted between the scFv and the transmembrane domain. The spacer domain often consists ofimmunoglobulin G (IgG) hinge domain and CH2-CH3 domain of an IgG-Fc. The length and composition of the spacer domain can influence the CAR-T cell function independently of the intracellular domain (44).

As it was mentioned above, the most basic CAR design, known as first-generation CAR, contained an antigen-binding domain directly fused to the intracellular portion of the TCR invariant chain, CD3ζ. This signal was insufficient to activate resting T cell and required exogenous administration of cytokines (42). Although the antigen-specific activation of T cells occurs primarily via TCR aggregation and phosphorylation of TCR-

associated CD3 proteins, the final T cell response is highly influenced by the signaling from a range of co-stimulatory and co-inhibitory molecules present on the T cell surface. Co-stimulatory signals enhance T cell proliferation, cytokine secretion, cytotoxic function, memory formation, or survival (49). In order to provide the co-stimulation lacking in tumor cell targets, several groups have incorporated co-stimulatory endodomains into CAR molecules, creating so-called second-generation CARs. Both preclinical and clinical studies demonstrated the superiority of CARs with dual signal domains. *In vitro*, the T cells bearing this construct were observed to undergo robust proliferation and produce large amounts of interleukin-2 (IL-2) following their stimulation with the target antigen (50–52). In patients, the second-generation CAR-expressing T cells showed remarkably enhanced expansion and persistence as compared to first-generation CAR-expressing lymphocytes (53). Most co-stimulatory receptors belong to the immunoglobulin or tumor necrosis factor receptor (TNFR) superfamilies that bind to ligands expressed by activated or licensed APCs. Table 1 presents examples of co-stimulatory molecules expressed by T cells and exploited in CAR-T (49).

Table 1 The list of co-stimulatory molecules employed within chimeric antigen receptors (CARs).

Receptor family	Costimulatory molecule	Ligand(s)	T cell expression	Functional characteristics within CAR-T cells
Ig superfamily	CD28	CD80/CD86	Resting and activated T cells	Potent cytotoxic function; IL-2 production; may favor CD4+ T cell expansion
	ICOS (CD278)	ICOS-L (CD275)	Activated T cells	May favor Th1 and Th17 polarisation
TNF receptor superfamily	4-1BB (CD137)	4-1BBL (CD137L)	Memory and CD8+ T cells; activated CD4+ cells	Stimulates CD8+ central memory T cell generation; favors CAR-T cell persistence
	OX40 (CD134)	OX40L (CD252)	Activated T cells	Suppresses Treg development
	CD27	CD70	Activated T cells	Upregulates Bcl-X(L) protein expression; favors CAR-T cell persistance
	CD40	CD40L (CD154)	Activated T cells	Increases proliferation and secretion of pro-inflammatory Th1 cytokines
Others	CD40L	CD40	Activated T cells	Acts indirectly on tumor cells or APC cells through the enhancement of costimulatory activity
	TLRs	TLR agonists	Activated T cells	Enhances effector function and cytotoxicity; increases IL-2, IFNγ and GM-CSF production

Subsequent side-by-side comparison of the most frequently used CAR endodomains showed, that CD28 reinforced T cell proliferation and is mandatory to induce IL-2. It was observed, that without IL-2 supplementation, CD28 and OX40 (CD137), but not 4-1BB (CD134) enhanced specific cytolysis. While CD28, 4-1BB, and

OX40 similarly improved pro-inflammatory cytokine secretion, OX40 most efficiently prevented activation-induced cell death of the effector memory T cells. Concomitantly, even though CD28 was superior to initiating the T cell response, OX40 and 4-1BB sustained the response in long term with OX40 being most effective. To combine all the beneficial functions in one CAR, a 3rd generation CD28-OX40 construct was created. This "third-generation" CAR was shown to have improved antitumor response without losing specificity due to a combination of costimulatory domains, and additionally provided some benefit in sustaining the survival of more matured T cells (54).

Recently, CAR-T cells are additionally engineered with an expression cassette for a transgenic protein. The solution allows delivering the protein to the targeted tissue in a therapeutic concentration while keeping the protein concentration low in the surrounding tissue or systemically. The generated "T cells redirected for universal cytokine-mediated killing", so-called TRUCKs or the "fourth generation" of CAR-bearing cells, combine the redirected CAR-T cell attack with the locally restricted release of a biologically active protein while avoiding its systemic toxicity (55). Thus, approach can be used to modulate the tumor microenvironment in solid tumor treatment (56). The protein for the release can be produced in a constitutive or inducible manner following the CAR activation and subsequent signaling. Nearly every protein can be produced and released by the TRUCK-T cells. So far, the concept was proven by the generation of the cells able to deliver IL-12, IL-15, and IL-18 to the targeted tissue. Each of the approaches had a beneficial effect on CAR-T cell antitumor activity (57). The summary of existing CAR construct types is presented in Figure 3.

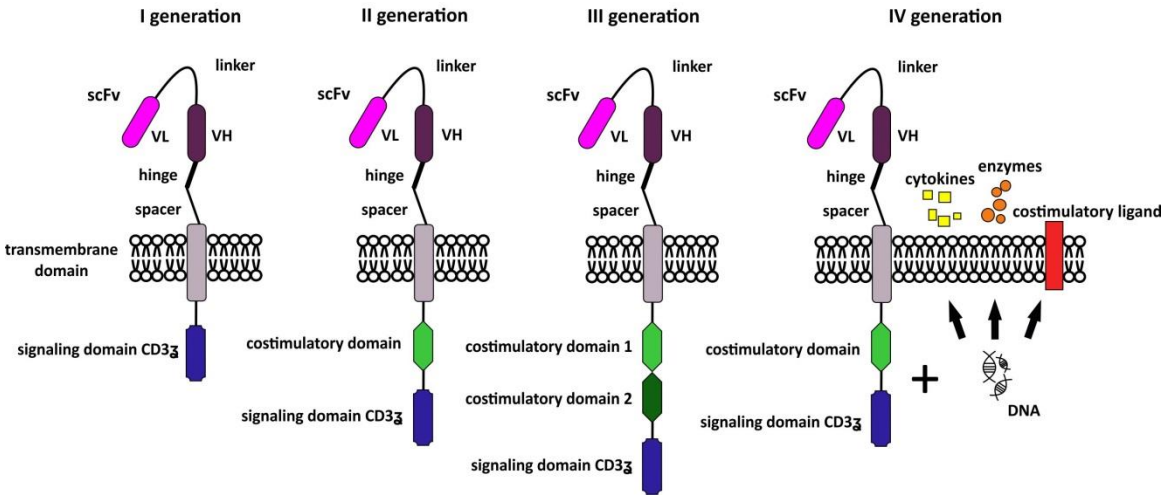

Figure 3 Structures of the four generations of CARs. *The binding domain of CAR consists of an scFv, comprising the light and heavy variable fragments of a monoclonal antibody joined by a flexible linker. The intracellular parts are different between the three generations of CAR. The first-generation CAR only has the signal transduction domain of the CD3-zeta chain (CD3ζ) or Fc receptor γ (FcRγ) which mediated transient persistence, inefficient cytotoxicity, and low-level cytokine secretion. The second- and third-generation CAR add one or more co-stimulatory domains (CD28, 4-1BB, or OX40) to the first generation, which lead to enhanced cytotoxicity and cytokine secretion along with prolonged T cell persistence. The fourth-generation CAR combines the CAR-T cell-mediated attack with the locally restricted release of a biologically active protein* (44,58).

Besides effectiveness, also the issue of CAR-T therapy safety needs to be addressed, and the focus is primarily concentrated on the possibility of quick CAR-T cells elimination once the immune-related severe adverse effects are triggered (59). The introduction of the inducible caspase 9 (iCasp9)/AP1903 suicide system into modified T cells allows for rapid induction of their apoptosis. In the construct, the caspase activation and recruitment domain (CARD) of pro-apoptotic caspase-9 is replaced with a mutated drug-binding domain from the human FK506-binding protein (FKBP12). The obtained fusion protein has a very high affinity for the small molecular dimerizer drugs AP20187 or AP1903, designed specifically for FKBP12 binding. Therefore, the administration of these drugs induces iCasp9 and cell apoptosis (60). Autologous iCasp9-expressing CAR-T cells are currently being evaluated in several clinical trials (61).

The most recent strategy to control CAR-T cell function is based on the incorporation of a protease and protease target site in the CAR construct, together with a ‘degron’ moiety that promotes degradation of the CAR protein. In this case, the CAR construct is expressed while the target site is cleaved and thus the degron is removed

from the protein. However, once an exogenous small molecule protease inhibitor is administered, the CAR protein is no longer cleaved, resulting in the preservation of the degron, which leads to the CAR degradation via the proteolysis. The modified construct was named small molecule-assisted shutoff CAR (SMASh-CAR), it is also known as switch-off CAR (SWIFF-CARs) (62).

1.3.1 Currently approved CAR-T therapies

Currently, there are five CAR-T cell therapies clinically approved by both FDA and the European Commission. Kymriah (tisagenlecleucel) and Yescarta (axicabtagene ciloleucel) are approved for the treatment of B-cell non-Hodgkin lymphomas (NHLs). Both products are second-generation CD19-targeting CARs (63). Tecartus (brexucabtagene autoluecel) is the first CD19 chimeric antigen receptor T-cell therapy for relapsed or refractory mantle cell lymphoma (MCL) (64)**.** Recently**,** CD19-CAR-based therapy Breyanzi (lisocabtagene maraleucel) was also approved for the treatment of adults with relapsed or refractory (R/R) large B-cell lymphoma after two or more lines of systemic therapy, and BCMA-CAR-T cell therapy Abecma (Idecabtagene vicleucel) – for the treatment of relapsed or refractory multiple myeloma after 4 or more prior lines of therapy (65).

Moreover, there are at least two CAR-T-based therapies approved locally. One of them is relmacabtagene autoleucel (relma-cel) in China –CD-19-CAR-T cell therapy to treat large B-cell lymphoma after at least two prior lines of systemic therapy (66). Another one is CD19-CAR-T ARI-0001, approved in 2021 by The Spanish Agency of Medicines and Medical Devices (AEMPS) to treat acute lymphoblastic leukemia (ALL) that is resistant to conventional treatments in patients older than 25 (67).

The therapy procedure is presented in Figure 4. The patient's T cells are collected via leukapheresis, stimulated, and then genetically modified to express the CD19-CAR, usually with a lentiviral or retroviral vector (68). Following leukapheresis, most patients receive bridging chemotherapy while awaiting CAR-T cell infusion, to provide the disease control while the T cells are being modified and expanded (69). CAR-T-cells are typically prepared for the infusion 3-4 weeks following apheresis, at which time patients undergo lymphodepleting fludarabine-cyclophosphamide chemotherapy (69). Such lymphodepleting therapy appears necessary to prevent cell-mediated immune response

against the genetically modified CAR-T cells which are not completely identical to the initially extracted host T cells. The incorporation of lymphodepleting therapy was also shown to promote the expansion and proliferation of CAR-T cells upon reinfusion. The mechanisms underlying this process include the greater availability of IL-7, IL-15, and possibly IL-21, which activate and expand tumor-reactive T cells; the impairment of CD4+CD25+ regulatory T cells (Treg) that suppress tumor-reactive T cells; and the induction of tumor apoptosis and necrosis in conjunction with antigen-presenting cell activation (70). Finally, CAR-T-cells are infused as a one-time treatment, after which the patient is monitored for toxicity and efficacy (68).

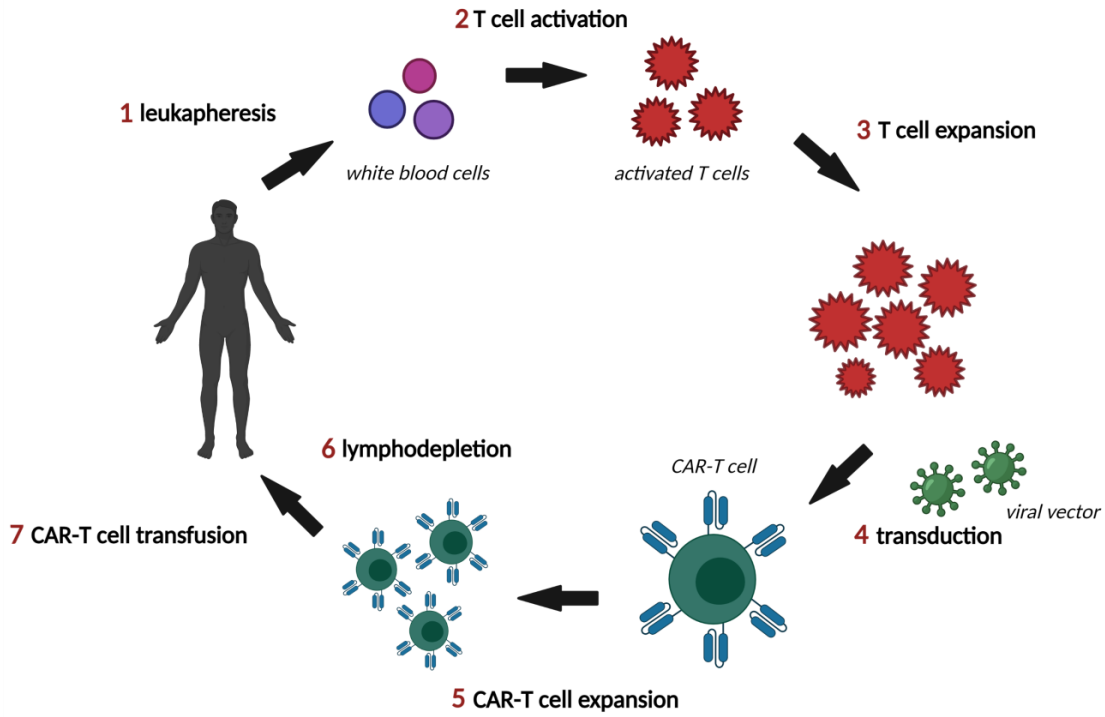

Figure 4 CAR-T cell-based treatment process. Based on (44). Created with BioRender.com.

The main toxicity issue of the therapy is cytokine release syndrome (CRS) that occurs in patients following *in vivo* CAR-T activation and expansion and is triggered by antigen recognition followed by generalized immune activation. At the early stages, CRS symptoms include fever, myalgias, and fatigue. Further, the patients' condition can worsen as the CRS can progress to capillary leak, hypoxia, and vasodilatory shock, leading even to organ disfunction (71). The pathophysiology of CRS remains mostly unknown, but it was noticed that a broad range of cytokines is involved in the dynamics of this condition. In particular, interferon-γ (IFN-γ), IL-6, tumor necrosis factor-alpha

(TNF-α), IL-10, granulocyte-macrophage colony-stimulating factor (GM-CSF), and C-C motif chemokine ligand 2 (CCL2) are released by the activated T cells and bystander normal immunocompetent cells, such as macrophages, natural killer cells (NK cells), and endothelial cells (72). CRS may also be accompanied or followed by the development of immune effector cell-associated neurotoxicity syndrome (ICANS), which is the second most frequently seen undesirable result of CAR-T cell activation. Neurotoxicity may present as a wide range of symptoms. Mild symptoms include headaches, diminished attention, and handwriting changes, while in severe cases patients may suffer from aphasia, seizures, and cerebral edema (73). The mechanisms underlying the ICANS development are not fully studied. One of the hypotheses suggests cytokine diffusion to the brain, another one the possible T cell trafficking into the central nervous system. Patients with CRS and ICANS usually receive immunosuppressive treatment (74).

Another side effect of most of the CAR-T cell therapies currently applied in clinics comes from the fact, that CD19 molecule is not only uniformly expressed by the majority of B-cell malignancies, which makes it an attractive target, but also by mature B cells, B-cell precursors, and a fraction of plasma cells (75,76). Therefore, normal B-lineage cells are also eliminated after CD19-CAR-T infusion, which is a typical “on-target off-tumor” side effect of CD19-CAR-T therapy. B-cell aplasia results in long-lasting hypogammaglobulinemia, which, however, may be treated with intermittent immunoglobulin replacement required occasionally to prevent severe infections (77).

1.3.2 Solid tumor microenvironment as a limitation to CAR-T cell therapy

The clinical and preclinical experience with CAR-T cell therapy for solid tumors has been much less successful so far. The meta-analysis performed in 2018 showed, that the response rate of CAR-T cell therapy among solid tumors reaches only 9% (95% CI: 4%-16%) (78). The limitations include a little number of potential target antigens as well as their heterogeneous expression, which often results in “on-target off-tumor” toxicity of CAR-T cells targeted against antigens that are found on solid tumors, but also non-malignant tissues. It is also a side effect of CD19-CAR-T cell therapy, but whilst the loss of normal B cells can be compensated with intravenous immunoglobulin infusions, targeting more abundant molecules may be fatal for the patient (74).

Another challenge is to ensure T cell fitness and survival before reaching tumor sites, their efficient trafficking to the tumor site, and physical barriers penetration (79). A tumor is composed not only of cancer cells themselves but also of a large number of non-transformed cells recruited by malignant cells, which generates the specific tumor microenvironment (80). Depending on the levels of proinflammatory cytokine production and T cell infiltration, the TME could be divided into two categories: cold (low T cells presence) and hot (high T cells presence). The differences between those two types are presented in Figure 5. Hot tumors exhibit molecular signatures of immune activation, whereas cold tumors are characterized by T cell absence or exclusion (81). Solid tumor cells are rarely present in the circulation system but accumulate in the districts which are difficult to infiltrate by T cells. In addition to the physical barriers, chemokines secreted by solid tumor cells are usually abnormal, which results in insufficient T cell recruitment (82). Adoptive cell therapy was shown to be able to establish an infiltrate to solve this problem (83). However, even after solving these problems, there is a need to address the issue of an immunosuppressive tumor microenvironment (79). In the case of hot tumors (T cell-infiltrated), which are characterized by the production of IFN and chemokines that attract T cells, these infiltrating CD8+ T cells commonly have a dysfunctional phenotype due to induced inhibitory pathways (84).

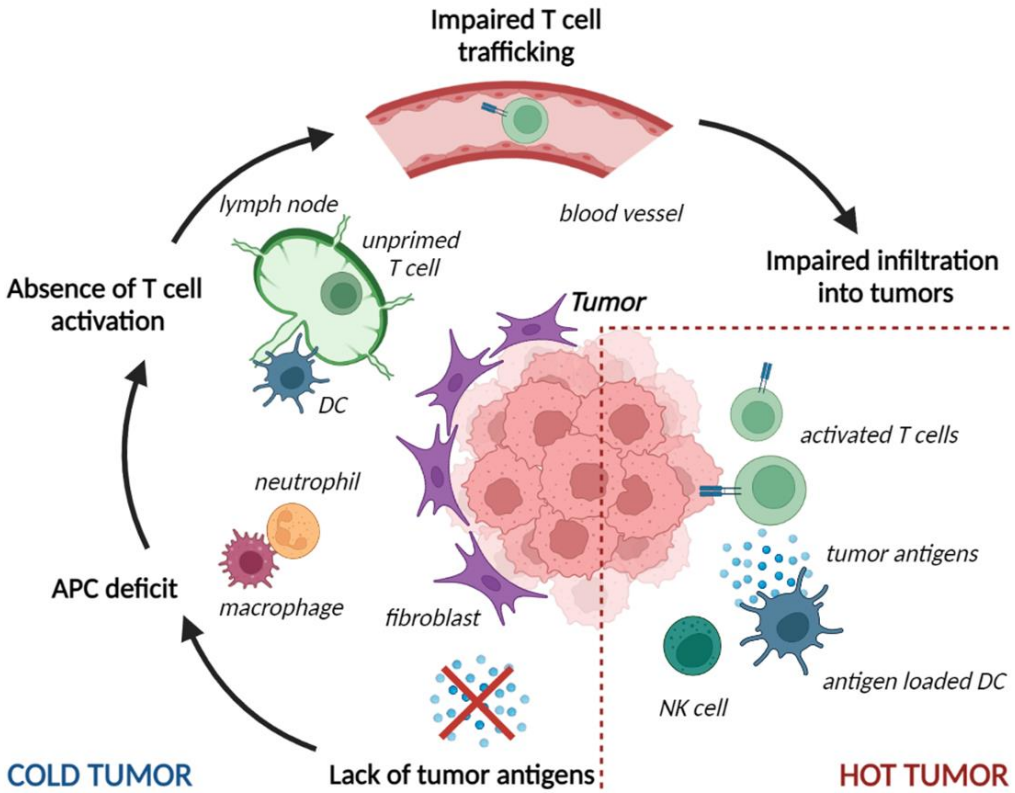

Figure 5 Tumor immunophenotypes (see details in text). Based on* (25,85)*. Created with BioRender.com.

The tumor microenvironment is the main location in which tumor cells and the host immune system interact. Characterization of the nature of immune responses in the human cancer microenvironment is necessary to understand tumor immunity and to further improve current cancer immunotherapy (86). Cancer immunotherapy is based on the exploitation of the immune system mechanisms in order to restore or induce the activity of cytotoxic T cells and other immune effector cells against cancer. The whole concept came out of the overall understanding of the immune system mechanisms of recognition and destruction of pathogens, including malignant cells, in the process called immunosurveillance (87). However, immunosurveillance is only one aspect of the complex relationship between the immune system and cancer. It was shown that the immune system may also promote the emergence of primary tumors with reduced immunogenicity (88,89). The hypothesis of so-called cancer immunoediting explains the potential host-protective and tumor-sculpting functions of the immune system throughout tumor development. Cancer immunoediting is a dynamic process composed of three phases: elimination, equilibrium, and escape. Elimination represents the

classical concept of cancer immunosurveillance, equilibrium is the period of immune-mediated latency after incomplete tumor destruction in the elimination phase, and escape refers to the final outgrowth of tumors that have outstripped immunological restraints of the equilibrium phase (16). Cancer cells can utilize various mechanisms to escape from the immune system. Some factors are already known to play important roles in this evasion, such as loss of the MHC, loss of the antigen expression due to gene loss or mutation, secretion of immunosuppressive cytokines, and induction of immunosuppressive Tregs (87). Moreover, the immunosuppressive microenvironment within the solid tumor has special histopathological features such as high-density blood vessels, extensive vascular leakage, poor integrity of tissue structure, and others. These changes result in hypoxia, low pH, and the presence of immune suppressor cells (90). Study of different cancer infiltrating immune cell subsets including CD4+Foxp3+ regulatory T cells, antigen-presenting cells (APCs), myeloid-derived suppressor cells (MDSCs), effector T cell subsets, and recognition of immune signature networks have defined the principles of immune responses in the human cancer microenvironment. The obtained knowledge allowed for elucidation of the critical importance of reversing immune suppressive mechanisms (86).

1.4 Immune checkpoints in cancer

Cancer cells suppress the host's immune responses exploiting two major mechanisms: metabolic suppression and signaling suppression, and the latter is conditioned by T cell biology. Though TCR signaling is triggered by the specific recognition of antigenic peptides presented by MHC molecules, it is co-signaling receptors on T cells, either co-stimulatory or co-inhibitory, that determine their functional outcome (91). The first two signal model proposed in the 1970s was based on the observation, that besides antigen receptor signaling, the second co-stimulatory signal is required for the T cell activation as it provides additional information. The aim of the second signal is to ensure that the lymphocyte activation occurs only following the antigen presentation by APCs. In the next few decades, it was discovered that not only co-stimulatory pathways condition lymphocyte immune response, but also co-inhibitory receptors are involved in this process, serving as a counterbalance to activation signals (92). Thus, co-inhibitory

receptors also called “negative immune checkpoints”, play a central role in maintaining immune homeostasis by keeping the balance between the readiness of immune system to protect body from foreign pathogens and avoiding the reactivity towards self-components (93). Initially, self-reactive T cells are eliminated in the thymus during their development. However, if this process is incomplete, the autoreactive T cells that have escaped central tolerance are controlled by these peripheral mechanisms (94).

The first discovered co-stimulatory receptor CD28 is constitutively expressed in naïve T cells. The expression of its ligands, B7 family of cell surface molecules, must be upregulated for the co-stimulatory signal to be delivered. The lack of co-stimulation after TCR recognition of the MHC-antigenic peptides complex results in the development of peripheral immune tolerance. Additionally, once the T cell is activated, cytotoxic T lymphocyte-associated antigen 4 (CTLA4 or CD152) expression is induced. CTLA4 molecule has a higher affinity to B7 molecules as compared to CD28, and its binding to the ligands downregulates the process of T cell activation. Thus, CTLA4 appears as a co-inhibitory receptor (94,95). The second antigen-independent co-stimulatory signal for T lymphocyte activation includes CD40/CD40L, CD28/CD80(CD86), OX40/OX40L, and CD27/CD70 interactions. The second antigen-independent co-inhibitory signal that protects against excessive immune response includes PD-1/PD-L1(PD-L2), CTLA-4/CD80(CD86), CD80/PD-L1, TIM-3/GAL-9, BTLA-4/HVEM, and LAG-3/MHC (96). Signaling suppression by tumor cells is possible due to their ability to upregulate the expression of ligands for co-inhibitory receptors on their surface while downregulating the activity of co-stimulatory receptors on the effector cells (97). Thus, the negative immune checkpoints often become mediators of T cell dysfunction during cancer progression, serving as unwanted protection for cancer cells and preventing the anti-tumor immunity (98). Consequently, several immune checkpoints are currently seen as attractive targets for cancer immunotherapy: CTLA-4, T-cell immunoglobulin and ITIM domain (TIGIT), T-cell immunoglobulin-3 (TIM-3), lymphocyte activation gene 3 (LAG-3), and in particular programmed cell death protein-1 (PD-1) (99).

1.4.1 PD-1/PD-L1 interaction in cancer

In 1992, Ishida et al. isolated cDNA of PD-1 from IL-3-deprived LyD9 (murine hematopoietic progenitor) and 2B4-11 (murine T-cell hybridoma) cell lines. The activation of this molecule, also referred to as CD279, was suggested to be involved in apoptosis, a classical programmed cell death (100).

PD-1 expression changes dynamically depending on the immunological conditions. Developing thymocytes and resting naïve T cells constitutively express PD-1 at low levels, which is seen as one of the mechanisms of immune tolerance. Following the immune stimulation, PD-1 expression is induced on both CD4 and CD8 T cells. In the situation of rapid antigen exposure, PD-1 expression gradually decreases with time following the dynamics of the antigen removal. During chronic immune stimulation, PD-1 remains highly expressed, often leading to T cell exhaustion. The molecule can also appear on B cells, macrophages, and dendritic cells upon induction (101). Expression of PD-1 on NK cells used to be controversial due to the lack of studies consistency (102). However, recently low yet consistent basal expression of functional PD-1 was found on resting human NK cells in healthy donors. Moreover, it was observed that PD-1 expression increases on these cells after allogeneic hematopoietic stem cell transplantation (allo-HSCT). The PD-1 molecule on NK cells was shown to be involved in the suppression of their response following the exposure to programmed death-ligand 1 (PD-L1) molecule on target cancer cells (103).

PD-1 ligands are two transmembrane glycoproteins, PD-L1 and programmed cell death 1 ligand 2 (PD-L2). The different expression patterns of PD-L1 and PD-L2 specify their different functions.

The expression of PD-L2 (also known as B7-DC and CD273) is much more restricted than PD-L1 expression. PD-L2 can be expressed on macrophages, on cultured bone marrow-derived mast cells, on intestinal stromal cells, and approximately 50% of peritoneal B1 lymphocytes. Additionally, PD-L2 expression may be induced on dendritic cells by IL-4 and GM-CSF (104). It may be as well up-regulated on the surface of other lymphoid cells, such as activated T cells and B cells (96). Conversely, PD-L1 (also called B7-H1 and CD274) is expressed constitutively on many cell types including non-

hematopoietic cells. The protein was found to be present on vascular endothelial cells, epithelial cells, muscle cells, hepatocytes, pancreatic islet cells, and astrocytes in the brain. Thus this molecule is expressed in organs such as the heart, skeletal muscle, lung, liver, spleen, thymus and additionally is detected at sites of immune privilege, including the placenta and eye (96,105).

The expression of PD-L1 on non-lymphoid tissues suggests that PD-L1 may directly regulate self-reactive T cells or B cells and inflammatory responses in these tissues as well as in lymphoid organs (105). Among lymphoid cells, PD-L1 was reported to be expressed constitutively on APCs, T cells, B cells, monocytes, and epithelial cells, and to be upregulated in a number of cell types after the activation in response to proinflammatory cytokines (106).

Therefore, PD-L1 plays a role in maintaining peripheral tolerance, and PD-L2 plays a role in the immune response of lymph nodes (96). The axis formed by PD-1 and both of its ligands is exploited to deliver inhibitory signals balancing T cell activation (Figure 6), tolerance, and immunopathology (107).

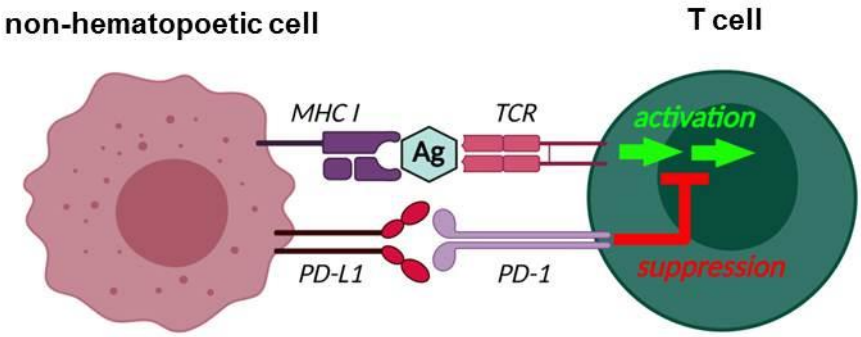

Figure 6 Mechanism of action of PD-1/PD-L1 immune checkpoint. Based on* (108). *Created with BioRender.com

As mentioned above, PD-1 is constitutively expressed by chronically stimulated CD4 and CD8 T cells following T-cell activation. Both the frequency and the level of PD-1 expression are increased on CD4 and CD8 T cells isolated from the TME tumor microenvironment as compared to T cells present in normal tissues and peripheral blood of the same patients (109). Similarly to the receptor, its ligands are commonly upregulated on the cancer cells obtained from various tumors. At first, the increased levels of PD-L1 in melanoma, ovarian, and lung cancer samples have been detected, and

currently, many other human cancers are on this list. Additionally, PD-L1 is often overexpressed on myeloid cells in the TME (110). High levels of PD-L1 protein expression have been observed in human tumor-associated APCs including tumor environmental dendritic cells (DCs), tumor-draining lymph node DCs, macrophages, fibroblasts, and T cells. The association between tumor-infiltrating T cells, IFN-γ signaling genes, and PD-L1 expression suggest that effector T cell-derived IFN-γ contributes to high levels of PD-L1 expression in the TME (86). Immune attack, via IFN-γ release, leads to inducible upregulation of PD-L1 creating an "immune shield" to protect against autoimmune attack in the setting of chronic inflammation or infection. Upregulated PD-L1 on these cells binds PD-1 on T cells, contributing to the development of T-cell exhaustion. Tumor cells have co-opted this PD-1/PD-L1 regulatory mechanism, designed to protect normal tissues from autoimmune attack, and instead overexpress PD-L1 to avoid immunologic surveillance to facilitate cancer growth (111).

1.4.2 Antibody-mediated PD-1/PD-L1 blockade in cancer treatment

Blocking the binding of PD-1 to PD-L1 was shown to restore T-cell activity and enhance the anti-tumor immune response, which makes PD-1/PD-L1 inhibitors successful therapeutics in numerous therapeutic applications (Figure 7).

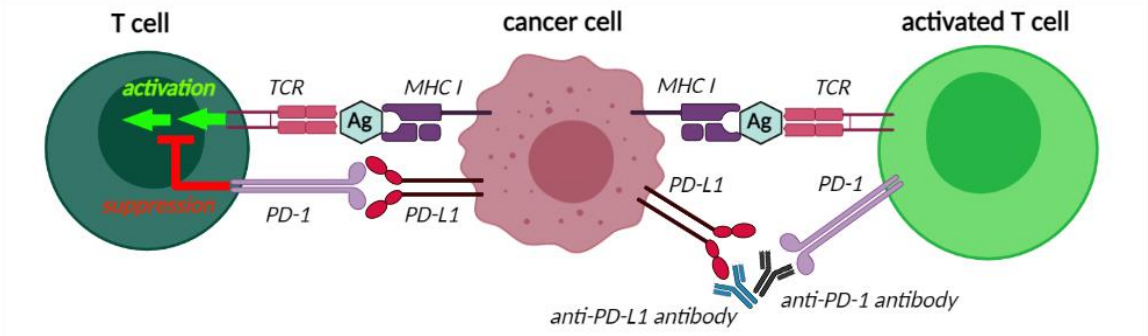

Figure 7 Mechanism of targeting inhibitory immune checkpoints with monoclonal antibodies. Based on* (112). *Created with BioRender.com.

Until now, PD-1 inhibitors (nivolumab, pembrolizumab, and cemiplimab) and PD-L1 inhibitors (atezolizumab, avelumab, and durvalumab) were approved by the FDA for the treatment of a wide spectrum of tumors (summarized in Table 2). In addition, a number of newly engineered PD-1/PD-L1 inhibitors are undergoing clinical trials in the hope of achieving improved clinical outcomes (113).

***Table 2 The list of FDA-approved monoclonal antibodies acting as inhibitors of negative checkpoints in human cancer. Based on* (112).**

Checkpoint inhibitor	Antibody format	Examples of Types of Cancers with FDA-Approved Use	Year of First Approval
Ipilimumab	Human anti-CTLA4 IgG1	Melanoma, renal cell carcinoma, metastatic colorectal cancer	2011
Pembrolizumab	Humanized anti-PD-1 IgG4	Melanoma, non-small-cell lung cancer, renal cell carcinoma, urothelial bladder cancer, Hodgkin lymphoma, head and neck cancer, Merkel cell carcinoma, microsatellite instability-high cancer, gastric cancer, hepatocellular carcinoma, cervical cancer, primary mediastinal large B-cell lymphoma	2014
Nivolumab	Human anti-PD-1 IgG4	Melanoma, non-small-cell lung cancer, renal cell carcinoma, urothelial bladder cancer, Hodgkin lymphoma, head and neck cancer, colorectal cancer, hepatocellular carcinoma, small cell lung cancer	2014
Atezolizumab	Humanized anti-PD-L1 IgG1	Non-small-cell lung cancer, urothelial bladder cancer, small cell lung cancer, breast cancer	2016
Avelumab	Human anti-PD-L1 IgG1	Merkel cell carcinoma, urothelial bladder cancer	2017
Durvalumab	Human anti-PD-L1 IgG1	Non-small-cell lung cancer, urothelial bladder cancer	2017
Cemiplimab	Human anti-PD-1 IgG4	Cutaneous squamous-cell carcinoma	2018

However, these antibodies only block the functions of the PD1/PD-L1 pathway and do not directly eliminate the PD-L1-positive cells, which gives cancer a chance to develop the evasion mechanisms (114). As mentioned earlier, the expression of PD-L1 can also be detected in normal cells of the vital organs, such as the heart, lungs, or skeletal muscle, where it serves to protect these tissues from autoimmunity. Additionally, the PD-L1 expression is a characteristic of activated B cells, dendritic cells, and monocytes. Therefore, most anti-PD-L1 antibodies tested in clinical settings were not designed to have the ability to trigger cytotoxic effects against the target cells. Although, recently there have been attempts to apply anti-PD-L1 antibodies inducing cytotoxic mechanisms. An example is an antibody avelumab, which is capable of inducing antibody-dependent cell-mediated cytotoxicity (ADCC) (115). However, in addition to increased anti-tumor immunity, the mechanism of action of immune checkpoint inhibitors (ICIs) revealed a new toxicity profile called immune-related adverse events (irAEs). The underlying mechanism of ICI immunotoxicity is related to the inflammation of healthy tissues due to a loss of self-tolerance. All organs can be affected by these new toxicities, although the most frequently affected organs include the skin,

digestive, and endocrine organs. The majority of toxicities caused by ICIs are low in severity, but some are more serious and require multidisciplinary management of side effects (116), especially considering patients' deaths that occurred due to fulminant myocarditis caused by the treatment (117). Therefore, there is a pressing need for the development of more tumor-specific approaches to targeting checkpoint molecules in cancer. One of the ways to overcome ICI limitations is to combine them with CAR-T therapy.

1.4.3 PD-1/PD-L1 inhibitors in combination with CD19-CAR-T therapy

Numerous clinical trials demonstrated that 70–90% complete remission (CR) can be achieved in pediatric and adult patients treated with CD19-targeting CAR-T-cells. However, up to 60% of patients relapse after the CAR treatment, and among those, 80-90% are CD19-positive relapses, which means that CD19 molecule is still present on the surface of cancer cells and can be detected by flow cytometry (118). Poor T cell expansion and short-term T cell persistence remain one of the main causes for lack of response and relapse following CAR-T therapy.

In classical Hodgkin lymphoma (cHL), the host antitumor immune response is known to be ineffective at least partially due to overexpression of PD-1 ligands and associated T-cell exhaustion (119). Genetic alterations of chromosome locus 9p24.1, containing the loci for PD-L1, PD-L2, and JAK2, contribute significantly to the upregulation of PD-L1 and PD-L2 in cHL. The mutations not only directly increase protein expression of PD-1 ligands, but also induce JAK2 overexpression, which leads to activation of the JAK/STAT signaling pathway, known to enhance the expression of PD-L1 and PD-L2 (120). The study conducted on biopsy samples from patients with newly diagnosed cHL revealed, that 97% of all analyzed samples had genetic alterations of the PD-L1 and PD-L2 loci, linked to the increased PD-L1 protein expression (121). PD-L1 is also expressed in NHL including diffuse large B-cell lymphoma (DLBCL). It is known to inhibit the activity of tumor-associated T cells in this disorder, even though PD-L1 expression rate in DLBCL is generally much lower as compared to cHL, with only 10–24% of DLBCL cases being positive for PD-L1 (122). However, DLBC represents 30-40% of all NHLs, and PD-L1 expression was found in both tumor cells and cells from the

microenvironment, mainly macrophages (123). Additionally, NF-κB transcription factor, which is constitutively activated in aggressive DLBCL with an activated phenotype (ABC-DLBCL) and in indolent B-cell lymphomas, is also able to increase tumor cell expression of PD-L1 either directly or indirectly (124). In particular, PD-L1 protein expression is associated with activated B-cell-like or non-germinal center B cell-like phenotypes of DLBCL, which are poor prognostic subgroups (125). In bone marrow aspirates (BMAs) from B-ALL patients, PD-1 expression on T-cell subsets is increased at diagnosis, and to a greater extent, at relapse (126). PD-1-positive/CD8-positive T cells were even more frequent in BMAs from patients who had multiply relapsed acute myeloid leukemia (AML) than in BMAs from those who had first relapsed AML (127). In a similar manner to a solid tumor, IFN-γ-induced PD-L1 expression on AML cells protected them from cytotoxic T cell lysis (128).

Similarly to host effector cells, CAR-T cells also acquire a differentiated and exhausted phenotype associated with increased expression of PD-1 (125). Following the infusion of CD19-specific CAR-T cells, 8 of 11 lymphoma patients had at least three-fold increased PD-1 expression on CD4+ CAR-positive cells from the time of infusion to the time of peak blood levels (129). In another study, patients with B-cell malignancies that relapsed after allogeneic stem cell transplantation were treated with CD19-targeting CAR-T cells. It was observed, that both CD8+ and CD4+ CAR-T cells significantly increased PD-1 expression between the time of infusion and post-adoptive cell transfer analysis. PD-1 expression was also higher on CAR-T cells than on unmodified T cells (130). An extensive transcriptomic analysis was performed to compare T cells from chronic lymphocytic leukemia (CLL) responders and non-responders post CD19 CAR-T therapy. The studies revealed that CAR-T cells from non-responders showed upregulated pathways involved in exhaustion and apoptosis. In particular, the PD-L1/PD-1 pathway was able to directly inactivate CD28 signaling in CAR-T using CD28 as a co-stimulatory domain, therefore inhibiting CAR-T cell function (120).

Numerous groups have demonstrated in preclinical models and subsets of patients with ALL or DLBCL the increased efficacy of CAR-T cell therapy with the co-administration of antibodies that inhibit the PD-1 pathway (62). PD-L1 blockade was shown to normalize CD4:CD8 ratios and restore CD8+ T cell cytotoxicity and immune

synapse formation *ex vivo* and *in vivo* (131). Furthermore, PD-1-deficient CAR-T cells showed improved anti-tumor efficacy *in vitro* and *in vivo* (120). Thus, the blockade of PD-1/PD-L1 immune checkpoint in combination with CAR-T cells could help to limit T cell exhaustion and restore their functions (132).

1.4.4 PD-1/PD-L1 inhibitors in combination with CAR-T in solid tumors

The combination of CAR-T therapy with PD-1/PD-L1 blockade is even more relevant in solid tumors treatment due to the specific challenges faced during the therapy of these cancers. Many cells in the TME can induce PD-L1 expression due to several factors, including IFN-γ, TNF-α, cell growth factors, hypoxia, and exosomes influence (80). These cells consist of the immunosuppressive tumor-associated macrophages (TAMs), MDSCs, and Treg cells (133). The effector functions of CAR-T cells that have reached the tumor site are thus being directly inhibited due to the PD-L1 overexpression on the surrounding cells (134).

As mentioned above, combining CAR-T cell therapy and checkpoint blocking antibodies may produce a synergistic effect. CAR-T cells administration could “heat” the tumor, and PD-1/PD-L1 blockade can prolong CAR T-cell functional persistence in the suppressive microenvironment (83). In general, the hot tumors show higher response rates to immunotherapy, including PD-1/PD-L1 blockade (81). This hypothesis has been supported by several preclinical studies. For example, in a HER2 transgenic mouse model of breast carcinoma, the combination of HER2-CAR-T cell treatment with PD-1 blockade resulted in improved tumor control (135). Another research showed, that PD-L1 blocking mini-body synergized with HER2-CAR-T cells in the growth control of prostate cancer in mice (136).

However, the combination of CAR-T cell treatment with repetitive intravenous infusions of checkpoint blocking antibodies has several disadvantages, including an associated increase in treatment cost and lack of penetration of the antibody to the tumor site (137). Therefore, in this study, we propose an alternative approach by using a CAR construct directly targeting PD-L1 molecule.

2. AIMS OF THE STUDY

CAR T-cell immunotherapy is one of the examples of successful cancer treatment based on adoptive cell transfer. However, the success was almost exclusively achieved in the treatment of B-cell hematologic malignancies. CAR-T cell therapy for solid tumors remains mostly ineffective due to several reasons, and one of them is the immunosuppressive tumor microenvironment (138). Inhibitory immune-checkpoint receptors on immune cells and their ligands, which are often overexpressed in solid tumors, contribute to the induction of functional suppression of the immune response (90). In particular, the PD-1/PD-L1 axis is known to support immune resistance within the tumor microenvironment. PD-1 was shown to be expressed on a large proportion of tumor-infiltrating lymphocytes in varying tumor histologies. Moreover, tumor cells themselves often tend to overexpress PD-L1, allowing them to avoid immune detection (139). Additionally, PD-L1 can appear in cancer cells or tumor stromal cells in an inducible manner, as a result of the effects of IFN-γ secretion during the immune effector cells' response against the tumor (140). Several studies have reported that PD-1/PD-L1 blockade in solid tumors improves adoptive cell therapy by reinvigorating T cells effector functions. The enhanced antitumor response following PD-1/PD-L1 blockade was observed in the treatment of melanoma, non–small cell lung cancer (NSCLC), renal cell carcinoma, head and neck squamous cell carcinoma, urothelial carcinoma, and microsatellite instability-high colorectal cancer (141). Thus, numerous attempts are taken to combine anti-PD-1 or anti-PD-L1 antibodies administration with CAR-T cell-based therapy. However, the systemic infusion of blocking PD-1 or PD-L1 antibodies may lead to non-specific T cell activation, low concentrations of antibodies in tumors, and elevated clinical costs (142). Therefore, there is a need for more tumor-specific methods for targeting PD-1/PD-L1 interactions in cancer.

In the current project, two modern therapeutic concepts were combined: the immune effector cells were armed with a newly designed PD-L1-CAR, to invoke a direct effect of killing the cells with high expression of PD-L1 – either cancer cells or tumor stromal cells. The research hypothesis was that the physical elimination of PD-L1-expressing cells within the tumor mass (both cancer cells and/or stromal cells of the

tumor) would translate into a direct local anti-cancer effect, and also, into disinhibition of the natural systemic anticancer immune response.

The approach was tested on breast cancer cell lines. Worldwide, breast cancer comprises 10.4% of all cancer incidences among women, making it the second most common type of non-skin cancer (after lung cancer), and the fifth most common cause of cancer death (143). The triple-negative breast cancer (TNBC) type constitutes 10–20% of all breast tumors and is characterized as a high-grade, aggressive malignancy with a high rate of distant metastasis and poorer disease-specific survival than other breast cancer subtypes. Approximately 20% of TNBC were also reported to exhibit constitutively high expression of PD-L1 (144,145).

The main aims of this project were to establish and optimize the technology of CAR-T cells generation in our laboratory and to provide proof-of-concept evidence of the PD-L1-CAR-T cells' effectiveness in the cancer cells elimination *in vitro*. The long-term objective of the research was a contribution to the safe use of PD-L1-CAR-expressing cytotoxic cells in anticancer therapy.

To accomplish the main objectives above the following specific aims were set:

- To screen a range of breast cancer cell lines regarding PD-L1 expression;
- To optimize the methods for the PD-L1-CAR expression on the surface of T cells;
- To evaluate the cytotoxic potential of PD-L1-CAR-T cells against cancer cells harboring various levels of PD-L1;
- To assess the safety of PD-L1-CAR-T cells against non-malignant cells.

3. MATERIALS AND METHODS

3.1 Cell culture

3.1.1 Culture of established adherent cell lines

The study was performed using human cell lines listed in Table 3.

Table 3 Cell lines used in the study.

Name of cell line	Primary tissue	Source (Institution)	Address
HEK293T	non-malignant embryonic kidney	ATCC	Manassas, VA, USA
MDA-MB-231	triple-negative breast cancer	ECACC	Wiltshire, UK
HCC-1806	triple-negative breast cancer	ECACC	Wiltshire, UK
MCF-7	ER-positive breast cancer	ECACC	Wiltshire, UK
ZR-75-1	ER-positive breast cancer	ECACC	Wiltshire, UK
T47D	ER-positive breast cancer	ECACC	Wiltshire, UK
SkBr3	HER2-positive breast cancer	ECACC	Wiltshire, UK
MCF-10A	non-malignant mammary epitelium	ECACC	Wiltshire, UK
HMEC	non-malignant mammary epitelium	Life Technologies	Carlsbad, CA, USA

HEK293T, ZR-75-1, and T47D cells were maintained in DMEM medium (Sigma-Aldrich). MDA-MB-231, HCC 1806, MCF-7, and SkBr3 cells were maintained in RPMI 1640 medium (Sigma-Aldrich). Both culture media were supplemented with 10% fetal bovine serum (FBS) (Sigma-Aldrich), 2 mM glutamine (Sigma-Aldrich), and 1% penicillin-streptomycin solution (Sigma-Aldrich). Additionally, ZR-75-1 and T47D culture media were supplemented with 1nM β-estradiol (Sigma Aldrich). MCF-10A cells were maintained in mammary epithelial basal media (MEBM, Lonza) containing 0.4% bovine pituitary extract (BPE), 10 ng/ml human epidermal growth factor (hEGF), 5 µg/ml human insulin, 0.5 µg/ml hydrocortisone, 30 µg/ml gentamicin and 15 µg/ml amphotericin, and 100 ng/ml cholera toxin (Sigma Aldrich). HMEC cells were cultured in HuMEC medium supplemented with epidermal growth factor, hydrocortisone, isoproterenol, transferrin, and insulin, and 50 µg/ml bovine pituitary extract, according to manufacturer protocol (Life Technologies).

All cells were grown and maintained at 37°C in cell culture incubators in a humidified atmosphere with 5% CO_2. The manipulations carried out on cultured cells were performed in the aseptic environment in a laminar flow cabinet to avoid

contamination with microorganisms. Cell lines were subcultured every 2-3 days when 65–80% confluent. The cell line cultures were routinely tested for Mycoplasma spp. Contamination by PCR technique.

3.1.2 Subculturing of cell lines

For adherent cell cultures, the medium was aspirated, and the flask was washed twice with 10 ml phosphate-buffered saline (PBS) w/o calcium chloride and magnesium chloride (Sigma-Aldrich). Cells were detached using 2 ml of 0.25% trypsin-EDTA solution (Sigma-Aldrich). Next, trypsin was neutralized with 8 ml of warm complete culture medium, respective to each cell line, and the cells were collected by centrifugation for 4 minutes at 300 × *g*. The cell pellet was resuspended in fresh media. Usually, the split ratio was 1:5 or 1:10, depending on confluency, growth tempo, and experimental plans.

3.1.3 Primary cells

Primary human T cells were isolated from human peripheral blood mononuclear cells (PBMCs) obtained from healthy donors. The buffy coats from healthy donors were purchased in the Regional Blood Center in Warsaw and the PBMCs were isolated in the aseptic environment in a laminar flow cabinet. The procedure was approved by the Local Bioethics Committee (approval number: AKBE/184/2018).

3.1.4 Isolation of PBMC

The PBMC suspension was prepared from buffy coats using a density gradient centrifugation. For this purpose, 50 ml of buffy coats were diluted with room temperature (25°C) PBS w/o calcium chloride and magnesium chloride (Sigma-Aldrich) up to 140 ml. Then, 35 ml of the mixture was layered over 15 ml of the Lymphoprep solution (Stemcell) in a 50 ml sterile tube following the centrifugation for 30 min at 700 × *g* at 25°C without brake. The cell suspension was separated into various layers after centrifugation, as presented in Figure 8.

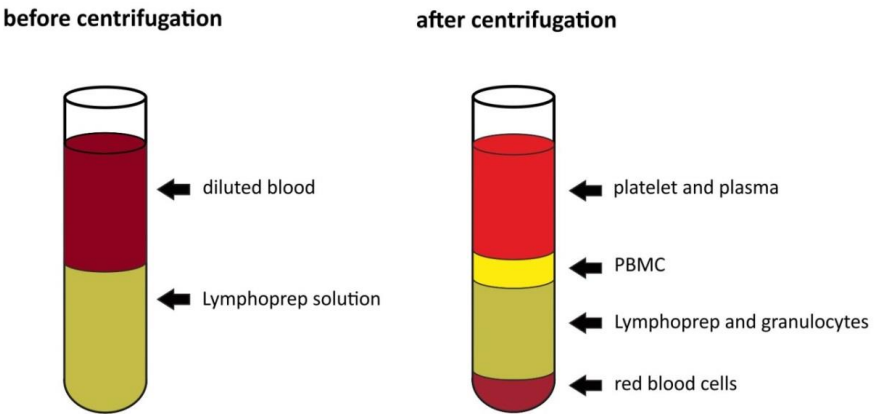

Figure 8 Preparation of PBMC suspension from buffy coats using a density gradient centrifugation. The band containing PBMCs at the interphase was collected.

The band containing PBMCs at the interphase was collected, transferred to a new sterile tube, washed twice with 40 ml of PBS, and centrifuged for 10 minutes at 750 × *g* at 25°C. To remove platelets, the cell pellet was washed with EasySep buffer (PBS supplemented with 2% FBS and 1 mM EDTA solution) and centrifuged for 10 minutes at 120 × *g* at 25°C. Next, the cell pellet was resuspended in EasySep buffer, the cells were counted, and the suspension was diluted with EasySep to the density of 5×10^7 cells per ml.

3.1.5 Isolation of T cells from PBMC

The T cells were isolated from fresh or previously frozen PBMCs by immunomagnetic negative selection using EasySep™ Human T Cell Isolation Kit (Stemcell). The procedure was performed according to the manufacturer's instructions. Magnetic-Activated Cell Sorting (MACS) is a passive separation technique to isolate different types of cells depending on their cluster of differentiation with a purity > 90% purification. The negative separation technique is based on using a cocktail of antibodies conjugated to magnetic beads to coat the cells other than those of interest and then remove the coated cells from a mixed population. For this purpose, the cell suspension is placed in an external magnetic field, the magnetic beads activate, and the labeled cells polarize while the cells of interest (unlabeled) are washed out.

The PBMCs, resuspended in the density of 5×10^7 cells per ml in EasySep buffer, were placed at polystyrene round-bottom tubes (5 ml or 14 ml) volume of 0.25 – 2 ml or 1 – 8.5 ml, respectively. The number of isolated T cells was dependent on experimental

plans. Next, 50 µL of Isolation Cocktail was added per each ml of the sample. The samples were mixed and incubated for 5 minutes at 25°C. The magnetic particles (RapidSpheres™) were mixed thoroughly for 30 seconds and then added to the samples (40 µl per ml). The samples were topped up with EasySep buffer either to 2.5 ml (if 5 ml tubes were used) or to 10 ml (if 14 ml tubes were used) and mixed gently by pipetting. The tubes were then placed into the magnet and incubated for 3 minutes at 25°C. After this time, the magnet with the tube was inverted in one continuous motion, pouring the enriched cell suspension containing T cells into a new sterile tube. The isolated T cells were counted and resuspended in the appropriate culture medium.

3.1.6 Subculturing of primary T cells

Primary human T cells were cultured in RPMI 1640 medium (Thermo Fisher Scientific) supplemented with 10% FBS (Sigma-Aldrich), 2 mM glutamine (Sigma-Aldrich), and 1% penicillin-streptomycin solution (Sigma-Aldrich). Medium containing 200 U/ml recombinant human IL-2 (PeproTech) was added to freshly cultured cells. T cells were activated and expanded by adding Dynabeads Human T-Activator CD3/CD28 (Thermo Fisher Scientific) at a bead-to-cell ratio of 1:1. For that purpose, T cells were centrifuged for 4 minutes at 300 × *g* and resuspended in EasySep buffer, transferred to a polystyrene round-bottom tube, and placed on a magnet for 1-2 minutes until the Dynabeads moved to the side of the tube. The supernatant containing the cells was transferred to a new tube and centrifuged for 4 minutes at 300 × *g*. The cell pellet was then resuspended in fresh medium supplemented with 200 U/ml IL-2 at a density of 0.5-1 × 10^6 cells/ml, and a new portion of CD3/CD28 Dynabeads was added.

3.1.7 Cell counting and viability measurement

Cells were counted using a hemacytometer. Cells were centrifuged for 4 minutes at 300 × *g,* and the pellet was resuspended in 1-5 ml of culture medium, respective to each cell line. Next, 20 µL of cell suspension was mixed with 20 µL of 0.4% trypan blue. The mixture was incubated at 25°C for approximately 3 minutes. A drop of the trypan blue/cell mixture was applied to a hemacytometer (KOVA® Glasstic Slide 10 With Counting Grids), and cells were counted under a light microscope. The unstained (viable)

and stained (dead) cells were counted separately in the hemacytometer. To calculate the total number of cells per ml, the total number of viable cells counted from 9 squares was multiplied by two (dilution of the trypan blue) and then by 10^4.

3.1.8 Cryopreservation and thawing of cells

The cells in the logarithmic phase of growth were used for cryopreservation. For this purpose, the 65-80% confluent cells were removed from the cell culture flask using the method for passaging adherent or suspension cells described above. The cells were counted, and then the portion of cells to be stored was resuspended in freezing medium (90% FBS and 10% DMSO) at density 2-3 × 10^6 cells/ml. Next, the cell suspension was transferred into sterile cryovials. The cryovials were placed in a chamber containing room temperature 100% isopropanol and stored at -80°C for a minimum of 24 h. After this time, for long-term storage, the cryovials with cells were moved to the tanks with liquid nitrogen.

For thawing the cells, the cryovials were removed from the tanks with liquid nitrogen and immediately placed in a 37°C water bath. Next, 1 ml of freezing medium with the cells was transferred to a sterile tube with 4 ml of cell growth media and gently mixed by pipetting. The cell suspension was then centrifuged for 4 minutes at 300 × *g*, and the cell pellet was resuspended in a fresh complete culture medium, respective to each cell line, and transferred into the culture flask. The medium was changed for the fresh one the next day in order to remove the rest of the cryoprotectant and eventually the dead cells.

3.2 Flow cytometry

Flow cytometry is a laser-based technology used for the analysis of single cells or particles as they flow in suspension through the focused beam of a laser in a measuring device. The interaction with the light is measured as light scatter and fluorescence intensity, which are independent parameters. Visible light scatter is measured in the forward direction (Forward Scatter or FSC), which indicates the relative size of the cell, and at 90° (Side Scatter or SSC), which indicates the internal complexity or granularity of the cell. The samples are prepared for fluorescent measurement through transfection

and expression of fluorescent proteins, staining with fluorescent dyes, or staining with fluorescently conjugated antibodies. After the laser light activates the fluorophore at the excitation wavelength, detectors process the emitted fluorescence. The intensity of the emitted light represents the antigen density or the characteristics of the cell being measured (146–148).

3.2.1 Fluorescence-activated cell sorting (FACS)

In a sorting cytometer, cell parameters such as scatter and fluorescence are analyzed in ways similar to those in non-sorting cytometers. A heterogeneous population of cells is suspended and passed across laser interrogation points, where the light signals emitted from the particles are collected, amplified, and analyzed. They then continue to flow downstream, where, in a sorting cytometer, the sheath stream is vibrated so that it breaks up into drops and the cells become enclosed in individual drops. If a cell in the analysis point has been determined to be a cell of interest according to the sort regions, the drop containing that cell will be charged positively or negatively so that it will be deflected to the proper collecting tube (149,150).

The cells can be sorted based on their morphology characteristics or surface and intracellular protein expression. The proteins are labeled with fluorescent antibodies.

In this study, target cancer cells MDA-MB-231 and MCF-7 were sorted after the modification with pLenti7.3-redluc lentiviral plasmid; the plasmid contains the sequence encoding GFP molecule. The cells were washed twice with PBS and then suspended in PBS at a density of 10-20 × 10^6 cells per ml. The suspension was next analyzed and sorted using FACSAria III (BD Bioscience).

3.2.2 Evaluation of degranulation and cytokine production

To evaluate T cell functions upon interaction with tumor cells, including degranulation capacity and cytokine production, flow cytometry-based assays were applied.

T cells are known to release the content of their cytotoxic granules, such as perforin and granzymes, into the immune synapse to kill their target. Lysosomes containing cytotoxic granules move to the cell surface and fuse with the plasma

membrane to release their contents upon specific receptor engagement between a target cell and a cytotoxic cell. This lysosomal fusion results in lysosomal-associated membrane glycoproteins (LAMPs), including CD107a, to be presented on the cell surface. Thus, staining for cell surface expression of CD107a is a leading method for measuring degranulation by flow cytometry.

Upon target cell interaction, T cells also produce and secrete cytokines, such as IFN-γ and TNF-α. To keep produced cytokines inside the immune cells, protein transport inhibitors BD GolgiStop™ (BD Biosciences) and BD GolgiPlug™ (BD Biosciences) were used. BD GolgiStop™ contains monensin, and BD GolgiPlug™ contains brefeldin A, both agents cause the accumulation of cytokines and/or proteins in the Golgi complex, which enhances the detectability of cytokine-producing cells with flow cytometric analysis. Moreover, to access intracellular IFN-γ and TNF-α, the cells were fixed and permeabilized before flow cytometry analysis.

T cells and CAR-T cells degranulation and cytokine release were evaluated against MCF-7 and MDA-MB-231 target cells (either parental or genetically modified).

Target cells were detached from culture flasks, resuspended in the complete culture medium, and pipetted into a U-bottom 96-well plate at a density of 1×10^5 cells per well. Effector cells were added to each well at density of 2×10^5, at the 2:1 E:T ratio. Next, 0.8 µl per well Golgi stop and 1 µl per well Golgi plug was added to inhibit protein transport, as well as 5 µl per well of a fluorescently labeled anti-CD107a antibody. The final volume of the sample in each well was 200 µl. The plate was centrifuged for 3 minutes at 250 × *g* to spin down the cells for their direct contact and then incubated for 4 or 8 hours at 37°C in a humidified atmosphere with 5% CO_2. Next, the plate was centrifuged for 4 minutes at 300 × *g*, the supernatant was removed, and the pellet was washed twice in 200 µl of EasySep buffer. After that, the anti-CD3 antibody, a marker for extracellular staining of T cells, together with viability dye were added to the cells both in 1:100 dilution in EasySep buffer. The plate was incubated for 20 minutes at 25°C, then centrifuged for 4 min at 300 × *g*. The supernatant was removed, and the pellet was washed once in 200 µl of EasySep buffer.

For the intracellular staining, the cells were resuspended in 100 µl of Fixation/Permeabilization Solution (BD Biosciences) and incubated for 15 minutes at 4°C. Then, the plate was centrifuged for 4 minutes at 300 × *g*, the supernatant was removed, and the pellet was washed once with 200 µl of Perm/Wash™ Buffer (BD Biosciences) containing saponin for better cell permeabilization. Next, anti-TNF-α and anti-IFN-γ antibodies were diluted 1:10 in Perm/Wash™ Buffer and added to the cell pellet in 25 µl followed the incubation for 20 minutes at 4°C. Finally, the cells were washed twice with 200 µl of Perm/Wash™ Buffer, resuspended in 200 µl of EasySep buffer, and analyzed by BD FACSCanto II (BD Biosciences) flow cytometer. The antibodies and viability dye used in the experiment are listed in Table 4.

Table 4 The list of antibodies and viability stain used in the evaluation of degranulation and cytokine production.

target	fluorochrome	producer
CD107a	PE	BD Bioscience
CD3	PerCP	BD Bioscience
TNFα	PE-Cy7	BD Bioscience
IFNγ	APC	BD Bioscience
viability stain	FVS-V510	Thermo Fisher Scientific

3.2.3 Compensation

When two or more fluorochromes are used in a single experiment, every fluorescent molecule emits light within an individual spectrum. The emission light is split according to wavelength and distributed to the detectors with proper filters that eliminate the light that is out of the spectrum characteristic for each molecule. However, the emission spectra may partly overlap, falling within the detector of another fluorochrome, and this signal is termed spillover. Compensation is the process by which the fluorescence spillover between detectors is calculated and mathematically corrected. For this purpose, single-color control samples are run with an experiment, and the signal from each fluorochrome that is detected in each of the other channels is measured. Based on these measurements, the compensation needed for signal removal is calculated (151,152).

In this study, both cells and polystyrene microparticles were used as single-color controls. In the case of using cells, they were stained with a single fluorescent dye as

described in the methods above. For performing compensation controls with polystyrene microparticles, BD™ CompBeads anti-mouse Ig, κ set (BD Bioscience) was used. The set contains both positive and negative beads, a drop of each was added to the mix with 100 µl of PBS, and the antibody was conjugated with fluorochrome in the same dilution as used in the experiment. The mix was incubated for 20 minutes at 4°C, then 500 µl of EasySep buffer was added, and the tube was centrifuged for 4 minutes at 300 × *g*. After removing the supernatant, the pellet was resuspended in 100 µl of EasySep buffer and analyzed by BD FACSCanto II (BD Biosciences) flow cytometer.

3.3 Western blotting

Western blotting is a semiquantitative biochemical technique used for the immunodetection of proteins following separation by gel electrophoresis. The mixture of separated proteins is transferred to a membrane, where an immobilized specific antigen is detected by a primary antibody. The unbound antibody is washed off, and next, the membrane is reacted with a secondary antibody labeled with an enzyme, which activity is used to visualize the target protein by a chemiluminescent or chromogenic method. The procedure allows for the identification of specific proteins from a complex mixture of proteins extracted from cells. Additionally, the amount of the present proteins may be evaluated, as it correlates with the band thickness and can be compared to the standard such as housekeeping proteins of a stable expression level (153,154).

3.3.1 Sample preparation and cell lysis

Medium from the cells with 80% confluency was removed, the cells were washed three times with ice-cold PBS, detached, pelleted by centrifugation, and resuspended in ice-cold lysis buffer (150 mM NaCl, 1% Triton X-100, 50 mM Tris-HCl pH 8.0) containing protease inhibitors (Roche). The lysates were centrifuged for 10 minutes at 12000 x *g* at 4°C, the supernatant was transferred to new tubes, and total protein concentration was quantified using a bicinchoninic acid (BCA) assay. Protein lysates were stored at -20°C or kept on ice.

3.3.2 Determining lysate protein concentration by BCA assay

The protein concentration was assessed by BCA assay (Pierce™ BCA Protein Assay Kit (Thermo Scientific). Bovine serum albumin (BSA) standard curves (between 0–1 000 µg/ml) were prepared in water. The samples were diluted ten times in water. A 10 µl of the standards and the samples were added to the plate in duplicates. Next, 200 µl of the BCA solution containing BCA protein assay carbonate buffer (Reagent A) and BCA protein assay cupric sulfate solution (Reagent B) in 1:50 ratio. Next, the plate was incubated for 30 min at 37°C with shacking. The absorbance was measured at 562 nm using Asys UVM340 microplate reader (Biochrom). The total protein concentration in each sample was then calculated based on the BSA standard curve.

3.3.3 Sample preparation

20-40 µg of the protein lysate was mixed with 5-times concentrated loading buffer (62 mM Tris-HCl pH 6.8; 5% β-mercaptoethanol; 10% glycerol; 2.5% SDS; 0.004% bromophenol blue) to the final 1 µg/µl concentration of the protein, then samples were boiled for 5 minutes at 95-100˚C in order to remove secondary and tertiary structures, thereby dissociating large protein complexes. B-mercaptoethanol served as a reducing agent.

3.3.4 Gel preparation

To perform sodium dodecyl sulfate-polyacrylamide gel electrophoresis (SDS-PAGE), the 1.5 mm polyacrylamide gels were prepared using BioRad Laboratories equipment. The resolving gel solution (12 or 15%) was prepared using the volumes presented in Table 5 depending on the percentage of gel required. The stacking gel solution was prepared according to the recipe presented in Table 5 and overlayed the resolving gel.

Table 5 The reagents and volumes used for the preparation of polyacrylamide gels.

Resolving gel						
Gel %	**Water (mL)**	**30% acrylamide (mL)**	**1.5 M Tris-HCl, pH 8.8 (mL)**	**10% SDS (µL)**	**10% APS (µL)**	**TEMED (µL)**
12%	3.2	4.0	2.6	100	100	10
15%	2.2	5.0	2.6	100	100	10
Stacking gel						
Gel %	**Water (mL)**	**30% acrylamide (mL)**	**1.5 M Tris-HCl, pH 8.8 (mL)**	**10% SDS (µL)**	**10% APS (µL)**	**TEMED (µL)**
4%	5.86	1.34	2.6	100	100	10
SDS: Sodium dodecyl sulfate; APS: Ammonium Persulfate; TEMED: Tetramethylethylenediamine.						

3.3.5 Sample electrophoresis (SDS-PAGE)

The samples containing equal amounts of protein (15-20 µg per lane) were loaded onto denaturing SDS-PAGE. The electrophoresis was carried out in the ProteanPlus™ Tetra Cell (BioRad Laboratories) apparatus in a running buffer containing 192 mM glycine, 0.1% SDS, and 25 mM Tris-HCl with an output of 30 mA while the samples were in the stacking gel, and then 40 mA when the samples reached the resolving gel.

3.3.6 Electrotransfer

After electrophoresis, the wet transfer was performed. The gel was transferred onto the Protran® nitrocellulose membrane (Schleicher and Schuell BioScience), and protein transfer was carried out in the transfer buffer (192 mM glycine, 25 mM Tris, 10% methanol) at a constant current of 80 mA for 16h or 200 mA for 2 h at 4°C using BioRad Laboratories equipment.

To verify the transfer effectiveness, the membrane was stained with Ponceau solution (Abcam). Ponceau is a reversible and negatively charged stain that binds to the positively charged amino groups of proteins and non-covalently to non-polar protein regions. The membranes were incubated with Ponceau for 5 min with rocking and then washed with TBST buffer (50 mM Tris-HCl pH 7,4; 150 mM NaCl and 0,1% Tween 20) until the protein bands were visible. The membranes were next washed with TBST buffer until they were completely destained.

3.3.7 Western blotting and protein detection

After the transfer, the membranes were washed in TBST buffer (50 mM Tris-HCl pH 7,4; 150 mM NaCl and 0,1% Tween 20) and incubated in blocking solution (10% w/v nonfat dry milk in TBST buffer) overnight at 4˚C with gentle agitation. The membranes were incubated in anti-PD-L1 (E1L3N®) XP® Rabbit mAb (Cell Signaling) primary antibody solution at dilution 1:1000 (in TBST with 5% w/v nonfat dry milk) overnight at 4˚C with constant rocking, then washed three times with TBST for 10 min each with rocking. Next, the secondary mouse anti-rabbit antibody (Jackson ImmunoResearch) conjugated with horseradish peroxidase (HRP) (diluted 1:10000 in TBST with 5% w/v nonfat dry milk) was added onto the membranes, which were then incubated for 2 h at 25°C with constant rocking. After the incubation, the membranes were washed three times with 1× TBST for 10 minutes each with rocking. The signal for HRP was detected using Super Signal West Pico Chemiluminescent Substrate (Thermo Fisher Scientific) kit. The reagents from the kit were mixed in 1:1 ratio and applied on the membrane for 2 min, then the chemiluminescence was detected by ChemiDoc (Bio-Rad) apparatus. As a loading control for Western blotting, the HRP-conjugated antibody recognizing β-actin was used at dilution 1:40000 in 1× TBST with 5% w/v nonfat dry milk. The membrane was incubated with the antibody for 30 minutes at 25°C, then washed three times with 1× TBST for 10 minutes each with rocking. The signal for HRP was detected as described above. The densitometry analysis was performed using Image Lab (Bio-Rad) software.

3.4 Agarose gel electrophoresis

Agarose gel electrophoresis is used to separate DNA fragments based on their molecular weight. The DNA phosphates are negatively charged; therefore, when placed in an electric field, the fragments migrate to the positive pole. The separation occurs due to the DNA samples' loading into the agarose gel, which agarose subunits associate non-covalently during gelation, forming a network. Depending on pore size, DNA fragments of different molecular weights migrate in the gel at a different speed. The DNA fragments are detected by staining the gel with the intercalating dye, ethidium bromide (EtBr), which allows the following visualization under UV light. Ethidium bromide stains DNA in a concentration-dependent manner, so it is possible to estimate the quantity of

DNA present in a band by comparing the band of known DNA amount. The size of the fragments can be determined by using known size standards and comparing the distance the unknown fragment has migrated (155,156).

To prepare 1% agarose gel, 1 mg of agarose was dissolved in 100 ml of 1× TAE buffer (40 mM Tris-acetate, 1 mM EDTA). Next, ethidium bromide (Promega) was added to the final concentration of 0.5 μg/ml, and the mix was poured into the gel tray with an appropriate well comb. After the solidification of the gel, the comb was removed, and the gel was transferred to the electrophoresis unit (BioRad) and filled with 1× TAE buffer until the gel was covered. Next, the samples for the electrophoresis were prepared, 200-500 ng of the diluted in water DNA was mixed with 5× concentrated loading dye (Thermo Fisher Scientific). The samples and the appropriate Perfect Plus 1 kb DNA Ladder (EURx), as a molecular weight standard for sizing the analyzed DNA fragments, were loaded into the gel wells. The electrophoresis was run at a constant voltage of 90-100 V, and the gel was then analyzed using ChemiDoc imager (BioRad).

3.5 Preparation of calcium competent *Escherichia coli* bacteria

Bacterial transformation is a process of non-viral horizontal gene transfer by which a recipient bacterial cell takes up exogenous DNA from the environment. The expression of the proteins involved in this mechanism is not constant; however, it can be induced under specific conditions in most transformable bacteria. The cell membranes then become permeable to DNA, and the bacteria develop competence for genetic transformation.

The most commonly used laboratory bacterial strain is *Escherichia coli*, which can be modified under artificial conditions. In this study, two strains of *E. coli* were used: a commercially available chemically competent bacteria DH5-alpha (NEB) and chemically prepared in our laboratory Stbl3 cells (157,158).

The Stbl3 cells were made competent by treating them with calcium chloride ($CaCl_2$). The addition of calcium chloride to the cell suspension allows plasmid DNA binding to lipopolysaccharide (LPS) receptor molecules on the bacterial cell surface. To prepare chemically competent Stbl3 cells, the bacteria were first cultured for 18 h at

37°C with shaking in the lysogeny broth (LB, Merck Millipore) medium. Next, 1 ml of the overnight culture was used to inoculate 100 ml of fresh LB in order to use the cells in their rapid growth later (log phase). The culture was grown with 220 RPM shaking at 37°C until it reached the density of approximately 5 x 10^7 cells per ml. After the verification of optical density of the bacterial culture at 600 nm (OD_{600}) using a spectrophotometer, a 5 ml aliquot of the cell suspension was transferred to a new sterile tube and cooled on ice for 10 minutes. Next, the cells were centrifuged at 5000 × *g* for 5 minutes at 4°C. The pellet was then resuspended in 25 ml of ice-cold 0.1 M $CaCl_2$ and incubated on ice for 20 minutes. After the incubation, the cells were again centrifuged at 5000 × *g* for 5 minutes at 4°C, and the pellet was resuspended in 5 ml of ice-cold 0.1 M $CaCl_2$ with 15% glycerol. The cell suspension was aliquoted into 50 µl portions and stored at -80°C until being used for transformation.

3.6 Bacterial transformation

The DNA introduced into a competent strain of bacteria usually is in the form of the plasmid. Plasmids are circular, double-stranded DNA molecules that are physically separated from the cell's chromosomal DNA and can replicate independently. Plasmid DNA occurs naturally in bacteria and contains genes that provide some benefit to the host cell, such as drug resistance. Like chromosomal DNA, plasmid DNA is duplicated before every cell division, which assures continued propagation of the plasmid through the following generations of the cell. The plasmids used in recombinant DNA technology replicate in *E. coli* and are engineered to optimize their use as vectors in DNA cloning. Their length is reduced as compared to naturally occurring, and the sequence is modified to contain a replication origin, a region in which exogenous DNA fragments can be inserted, and an antibiotic resistance gene – the transformed cells then can be selected from the untransformed cells by the inclusion of an antibiotic (159).

Transformation of plasmid DNA into *E. coli* in this study was performed using the heat shock method to insert a foreign plasmid or ligation product into bacteria. Chemically competent bacteria (either DH5-alpha or Stbl3) were quickly thawed on ice and then mixed with the DNA diluted in nuclease-free water. Typically, 1-10 ng of DNA resuspended in no more than 5 µl of water were added to a 50 µl aliquot of competent

cells. After 30 minutes of incubation on ice, the mixture of bacteria and DNA was placed at 42°C for 30-45 seconds (heat shock) and then cooled on ice for 2 minutes. Next, 500 µl of super optimal catabolite repression medium (SOC, NEB) was added to the tube, and the bacteria were incubated for 1 h at 37°C with shaking. After the incubation, the cells were centrifuged at 5000 × *g* for 5 minutes. The pellet was resuspended in 100 µl of the remaining SOC medium and plated out on LB agar plates containing the appropriate antibiotic.

3.7 Plasmid DNA preparation

All the manipulations were carried out in the aseptic environment in a laminar cabinet. Depending on the purpose, either 5 or 100 ml of LB medium was mixed with an appropriate antibiotic to the final concentration of 100 µg/mL of ampicillin or 50 µg/mL kanamycin. The culture was then inoculated with bacteria from a single colony at the LB agar plate and incubated for 18 h at 37°C with shaking. The next day, the DNA was isolated and purified using either QIAprep Spin Miniprep Kit (Qiagen) for 5 ml cultures or NucleoBond Xtra Midi kit (Macherey-Nagel) for 100 ml cultures according to the manufacturer's protocol. Both kits are based on the alkaline lysis of the bacterial cells.

3.8 Polymerase chain reaction

Polymerase chain reaction (PCR) is a technique that allows amplifying a specific DNA region *in vitro.* The process is carried out in a thermal cycler as different temperature is required at each reaction step. The double-stranded DNA (dsDNA) is denaturized by heating to around 95°C; then, primers bind onto the single DNA strands at approximately 60-65°C in the annealing process. Next, the polymerase binds to the primers and extends the primers by adding new nucleotides to the 3' end, using the single-stranded DNA as a template (160). Phusion DNA polymerase (Thermo Fisher Scientific), used in this study, operates at around 72°C. The steps, including annealing and extension, are repeated between 25 and 35 times, and, in the end, the reaction mixture is cooled down in order to obtain dsDNA as a product of the reaction.

In this study, the PCR was performed using Phusion High-Fidelity PCR Kit (Thermo Fisher Scientific) according to the manufacturer's instruction and ran in T100™ Thermal

Cycler (BioRad). Between 10 and 50 ng of the DNA sample was used as the template. Deoxyribonucleoside triphosphates mix (dNTP, Sigma) was used as a substrate to synthesize new DNA strands. Two primers (forward and reverse) were designed to amplify the region of interest and diluted to prepare 100 mM concentration stock. DMSO was added to disrupt secondary structure formation in the DNA template. The reaction mix was prepared as described in Table 6.

Table 6 The components of the reaction mix prepared for the amplification of the region of interest by PCR reaction.

Component	50 µl reaction	Final concentration
water	add to 50 µl	
5X Phusion™ HF Buffer	10 µl	1X
10 mM dNTP	1 µl	200 µM each
forward primer	2.5 µl	0.5 µM
reversed primer	2.5 µl	0.5 µM
template DNA	X µl	
DMSO	1.5 µl	3%
Phusion™ High–Fidelity DNA Polymerase	0.5 µl	0.02 U/µL

3.9 Chimeric Antigen Receptor

3.9.1 PD-L1-CAR construct

Second-generation PD-L1-targeting CAR was designed and its synthesis was ordered in Creative Biolabs (Shirley, NY 11967, USA). The construct consists of atezolizumab-based scFv combined with the CAR backbone with IgG4 hinge, CD28 (including the transmembrane region, TM), and CD3ζ signaling domains (Figure 9).

Figure 9 The modular structure of PD-L1-CAR construct (see details in text).

3.10 Molecular cloning

3.10.1 DNA Assembly

DNA assembly is a method of physically joining multiple DNA fragments to create a synthetically designed DNA sequence. The advantage of the DNA assembly cloning

method compared to restriction enzyme-based cloning is that it allows the insertion of one or more DNA fragments into any position of the linearized vector and does not rely on the presence of restriction sites within a particular sequence to be synthesized or cloned. At the moment, there are multiple methods of DNA assembly available, including NEBuilder® HiFi DNA Assembly (NEB), that was used in this study.

The technique was applied to cloning the PD-L1-CAR into a pSEW-GFP lentiviral vector (161) gifted by Prof. Torsten Tonn, Medical Faculty Carl Gustav Carus, Technical University in DresdenThe obtained vector was later used for modification of T cells. The new construct was cloned in collaboration with Dr. Malgorzata Bajor (Figure 10).

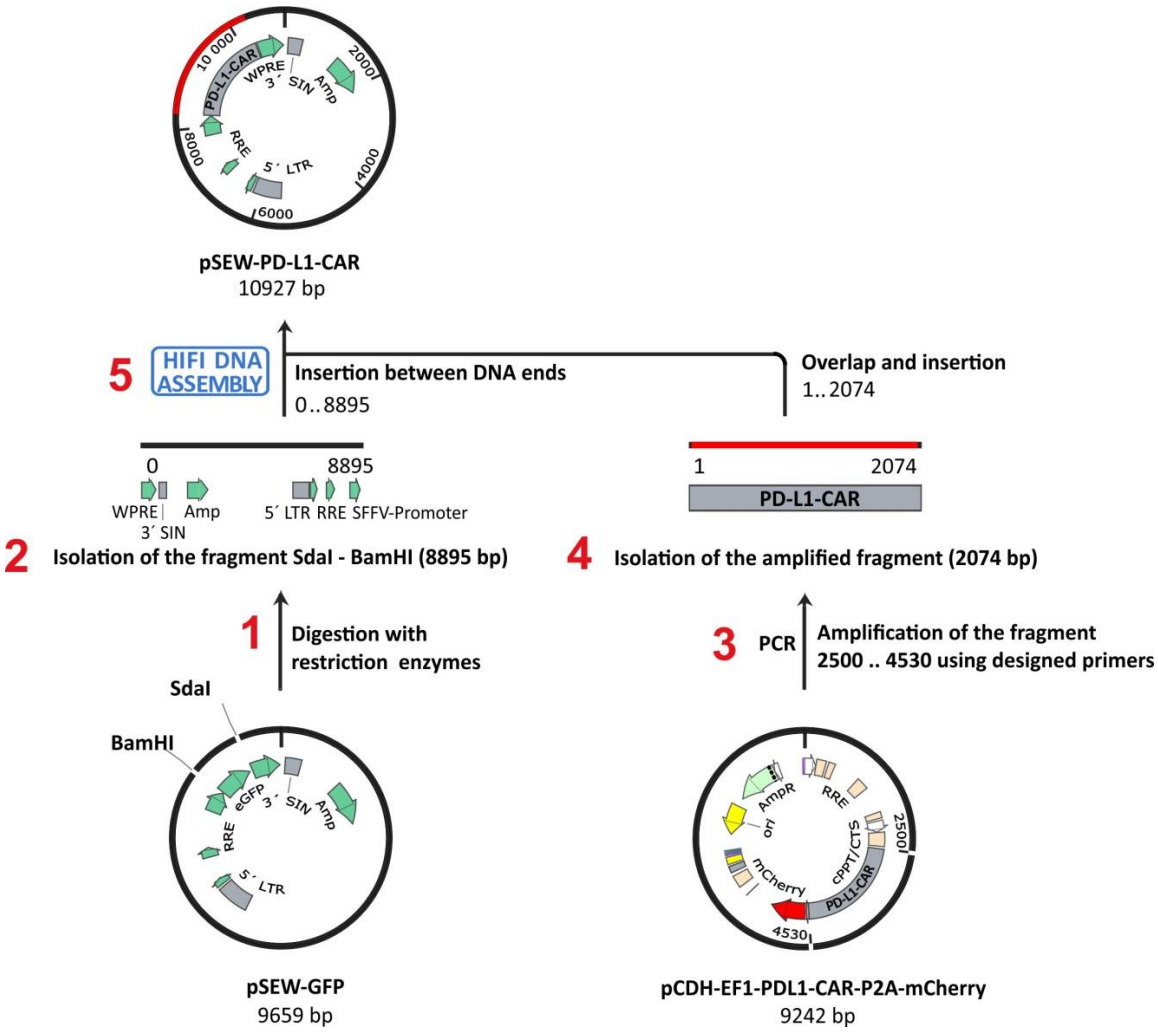

Figure 10 The scheme of PD-L1-CAR construct subcloning into the lentiviral vector pSEW (see details in the text). The map was generated using SnapGene software.

For this purpose, a pSEW-GFP vector was sequentially digested using Fast Digest BamHI and SdaI restriction enzymes (Thermo Fisher Scientific) for 15 minutes at 37°C.

Then, the reaction mix was run on 1% agarose gel in order to separate two DNA fragments and isolate an 8892 bp long vector without the GFP-encoding sequence. The vector was cut from the gel and cleaned up using Wizard® SV Gel and PCR Clean-Up Start-Up Kit (Promega). The DNA concentration was measured by Nanodrop (Thermo Fisher Scientific). Next, the insert containing the PD-L1-CAR-encoding sequence was prepared for the assembly. Using SnapGene software (GSL Biotech LLC), the primers for PCR amplification of the insert were designed so that the amplified DNA fragment would contain additional homologous to the vector overlapping ends. The PCR reaction was set using Phusion High-Fidelity PCR Kit (Thermo Fisher Scientific) and ran in T100™ Thermal Cycler (BioRad). The obtained PCR product was run on 1% agarose gel. The amplified fragment of desired 2074 bp length was isolated, cleaned up using Wizard® SV Gel and PCR Clean-Up Start-Up Kit (Promega). DNA concentration was measured by Nanodrop (Thermo Fisher Scientific). Next, the DNA assembly reaction mix was prepared using NEBuilder® HiFi DNA Assembly (NEB) according to the manufacturer's protocol. A total of 0.03–0.2 pmol of DNA fragments was used, NEBuilder HiFi DNA Assembly Master Mix was added, and the reaction mix was incubated for 15 minutes at 50°C. NEB 5-alpha Competent *E. coli* cells (provided in the cloning kit) were transformed with 2 µl of the assembled product, and bacteria were selected using ampicillin. The obtained colonies were cultured in LB medium supplemented with 100 µg/mL ampicillin, and plasmid DNA was isolated using QIAprep Spin Miniprep Kit (Qiagen). The constructs obtained from different clones were first verified by digestion with Fast Digest BamHI and SdaI restriction enzymes (Thermo Fisher Scientific) and run on 1% agarose gel. The results of the cloning were confirmed by DNA sequencing of the inserts.

3.10.2 sgRNA cloning

Lentiviral plasmid lentiCRISPR v2 containing both the *Streptococcus pyogenes* Cas9 nuclease and the single guide RNA (sgRNA) scaffold was a gift from Feng Zhang (Addgene, #52961). The plasmid map is presented in Figure 11.

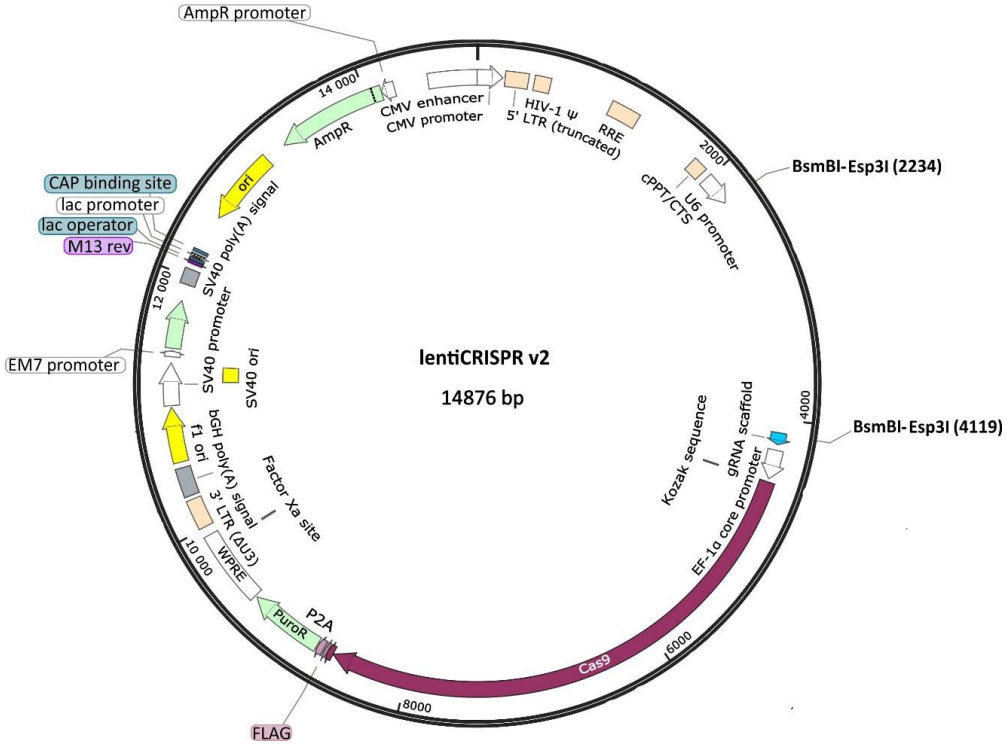

Figure 11 Lentiviral plasmid lentiCRISPR v2. The map was generated using SnapGene software.

The sequences of sgRNA targeting human PD-L1 were selected from Human CRISPR Knockout Pooled Library Brunello, and pairs of oligonucleotides (primers) for cloning these sequences into lentiCRISPR v2 vector were designed (Table 7). Oligonucleotides were purchased from the Oligo.pl service (Institute of Biochemistry and Biophysics of the Polish Academy of Sciences).

Table 7 The sequences of the sgRNA targeting PD-L1 subcloned into lentiCRISPR v2 vector.

	crRNA sequence	Pairs of primers for cloning
sgPD-L1_1	ACATGTCAGTTCATGTTCAG	Forward 5'-CACCGACATGTCAGTTCATGTTCAG-3' Reverse 5'-AAACCTGAACATGAACTGACATGTC-3'
sgPD-L1_2	ACTGCTTGTCCAGATGACTT	Forward 5'-CACCGACTGCTTGTCCAGATGACTT-3' Reverse 5'-AAACAAGTCATCTGGACAAGCAGTC-3'
sgPD-L1_3	CACCACCAATTCCAAGAGAG	Forward 5'-CACCGCACCACCAATTCCAAGAGAG-3' Reverse 5'-AAACCTCTCTTGGAATTGGTGGTGC-3'
sgPD-L1_4	GGTTCCCAAGGACCTATATG	Forward 5'-CACCGGGTTCCCAAGGACCTATATG-3' Reverse 5'-AAACCATATAGGTCCTTGGGAACCC-3'
sgPD-L1_5	TGAACATGAACTGACATGTC	Forward 5'-CACCGTGAACATGAACTGACATGTC-3' Reverse 5'-AAACGACATGTCAGTTCATGTTCAC-3'

First, lentiCRISPR v2 vector was linearized by digestion with Fast Digest BsmBI restriction enzyme (Thermo Fisher Scientific) for 15 minutes at 50°C. Afterward, the reaction mix was run on 1% agarose gel. The plasmid was purified using Wizard® SV Gel and PCR Clean-Up Start-Up Kit (Promega), and the DNA concentration was measured by Nanodrop (Thermo Fisher Scientific). The oligonucleotides were diluted in nuclease-free water to the final concentration of 100 µM. The mix of oligonucleotides with T4 ligase buffer (NEB) and T4 Polynucleotide Kinase (PNK, NEB) was prepared (Table 8).

Table 8 The components of the mix prepared for the phosphorylation and annealing of the oligonucleotides.

Component	Amount
forward primer	1 µl
reverse primer	1 µl
T4 PNK	1 µl
10X T4 Ligase buffer	5 µl
ddH_2O	42 µl

The reaction of phosphorylation and annealing of oligonucleotides was carried out in the thermocycler (BioRad) in the following conditions: incubation for 30 min at 37°C, then heating to 95°C for 2 min and cooling down to 25°C at 0.1°C per second. Annealed and phosphorylated oligonucleotides were diluted 1:100 in nuclease-free water and 2 µl of the mix was used to set up the reaction of ligation with linearized lentiCRISPR v2 vector (Table 9).

Table 9 The components of the mix prepared for the ligation of the sgRNA sequences and lentiCRISPR v2 vector.

Component	Amount
digested vector DNA	100 ng
annealed oligos	2 µl
T4 ligase	1 µl
10X T4 Ligase buffer	2 µl
ddH_2O	up to 20µl

The mix was incubated for 18 h at 16°C. The next day, 5 µl of the ligation mix was used to transform Stbl3 competent *E. coli* cells, and the bacteria were selected using 100 µg/mL ampicillin. The obtained colonies were cultured in LB medium with ampicillin, and plasmid DNA was isolated using QIAprep Spin Miniprep Kit (Qiagen). The constructs

obtained from different clones were first verified by digestion with Fast Digest BsmBI restriction enzyme (Thermo Fisher Scientific) and run on 1% agarose gel. The cloning results were confirmed by DNA sequencing of the inserts at the Oligo.pl service (Institute of Biochemistry and Biophysics of the Polish Academy of Sciences).

3.11 Modification of the target cell lines by lentiviral transduction

Constructs (plasmids) used for lentiviral modification of target cell lines:

- Lentiviral plasmid lentiCRISPR v2 (Addgene, #52961) containing both the *Streptococcus pyogenes* Cas9 nuclease and the sgRNA scaffold with subcloned crRNA sequences for human PD-L1 (described above) expressed together with a puromycin resistance marker (Figure 11);
- Lentiviral vector for bicistronic expression of a gene consisting of a subcloned sequence of human PD-L1 gene and a puromycin resistance marker (pLVX-IRES-Puro, Takara Bio) was a gift from Dr. Angelika Muchowicz, Department of Immunology, Medical University of Warsaw (Figure 12);

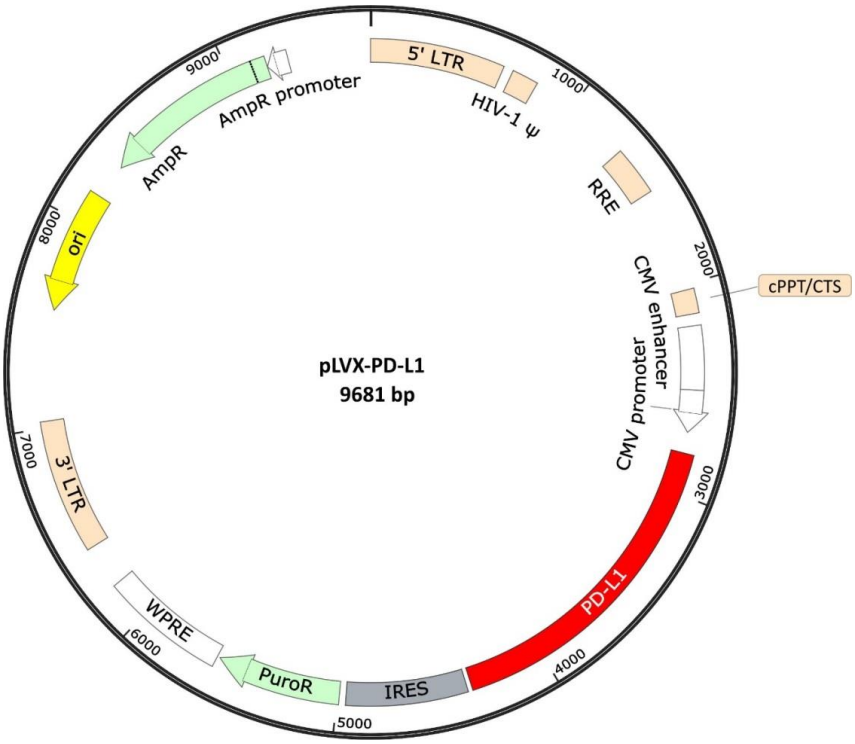

Figure 12 Lentiviral vector pLVX-PD-L1. The map was generated using SnapGene software.

- Lentiviral plasmid pLenti7.3-redluc (Thermo Fisher Scientific) containing a GFP marker was a gift from Dr. Angelika Muchowicz, Department of Immunology, Medical University of Warsaw (Figure 13);

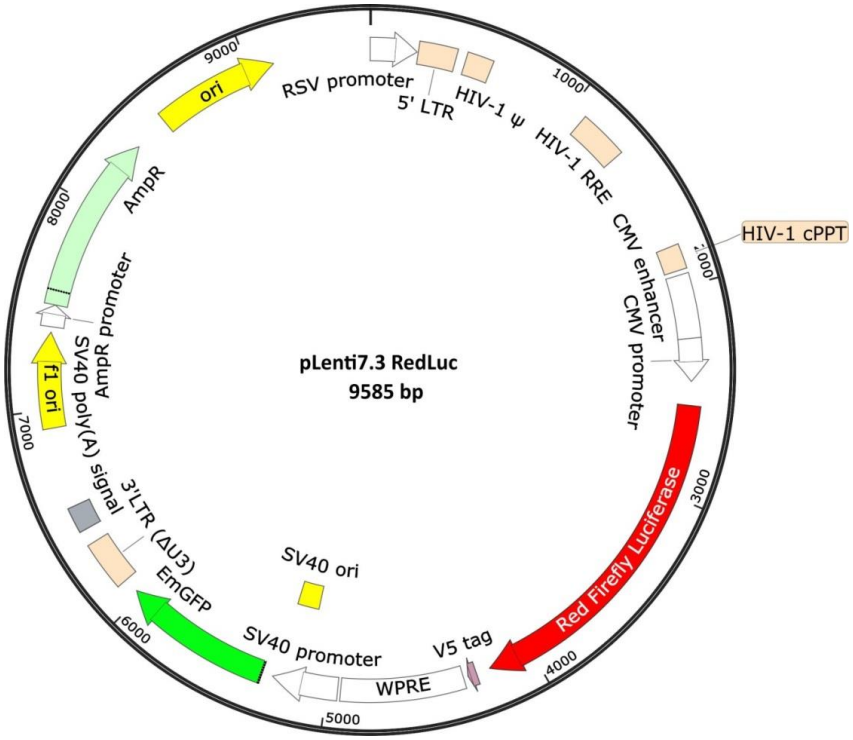

Figure 13 Lentiviral vector pLenti7.3-redluc. The map was generated using SnapGene software.

3.11.1 Lentiviral transduction of target cell lines

Lentiviruses express reverse transcriptase, which converts the viral RNA to double-stranded DNA, and integrase, which inserts this viral DNA into the host DNA. Once the viral DNA is integrated into the host DNA, it divides along with the host cell, allowing to obtain stable expression of the introduced gene of interest. In this study, MCF-7 and MDA-MB-231 cell lines were modified first with pLenti7.3-redluc to express luciferase. Then, MDA-MB-231 cell lines or luciferase reporter MDA-MB-231 stable cell lines were transduced with lentiCRISPR v2 sgPD-L1 to knock out PD-L1 encoding gene or with lentiCRISPR v2 sgNTC (non-targeted control) as a control (Figure 14).

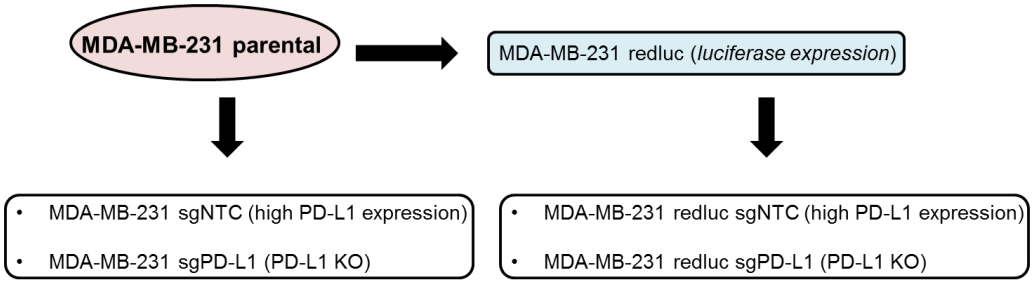

Figure 14 The sequential lentiviral modifications of MDA-MB-231 cells. First, the cells were modified to express luciferase, next the modification with sgNTC or sgPD-L1 was performed.

MCF-7 cell lines or luciferase reporter MCF-7 stable cell lines were transduced with pLVX-IRES-PD-L1 plasmid to overexpress PD-L1 molecule or with pLVX-IRES-Puro plasmid as a control. Moreover, the MCF-7 cell lines transduced with lentiCRISPR v2 sgPD-L1 to knock out PD-L1 encoding gene, or with lentiCRISPR v2 sgNTC as control were also modified (Figure 15).

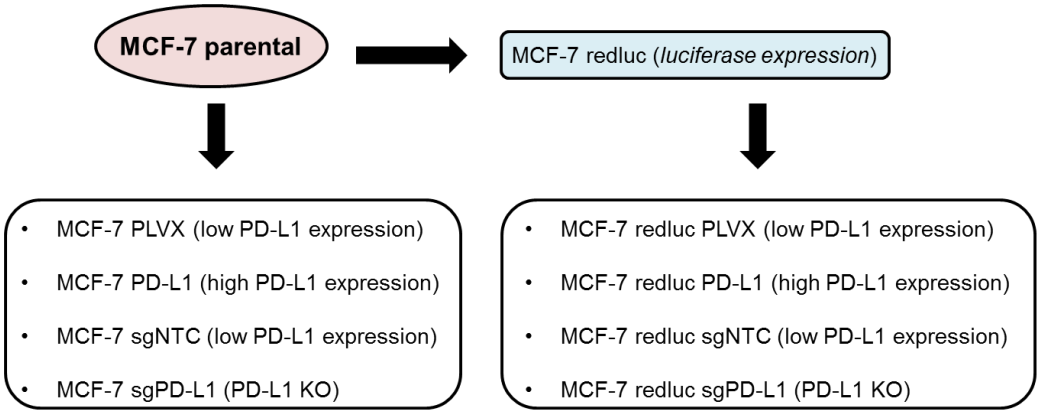

Figure 15 The sequential lentiviral modifications of MCF-7 cells. First, the cells were modified to express luciferase, next the modification with empty PLVX vector or PD-L1 overexpression was performed.

HEK293T packaging cell line was used for the lentivirus production. Briefly, the HEK293T were transfected using a polyethyleneimine (PEI) transfection protocol to deliver simultaneously a transfer plasmid with gene of interest, VSV-G envelope expressing plasmid pMD2.G (Addgene, #12259) and lentiviral packaging plasmid psPAX2 (Addgene, #12260). For this purpose, HEK293T cells were seeded at a density of 2.8 × 10^6 cells per 10 cm plate in a complete culture medium a day before transfection. After 24 h, the culture medium was replaced with 9 ml of Reduced-Serum Medium (Opti-MEM, Gibco) supplemented with 5% FBS. A mixture of three transfection plasmids was prepared in 500 µl of Opti-MEM:

- 1.3 pmol of psPAX2;
- 0.72 pmol of pMD2.G;
- 1.64 pmol of transfer plasmid.

A control transfer plasmid with fluorescent protein (e.g., GFP) expression was used to confirm the transfection efficiency using a fluorescent microscope.

PEI (Sigma) was diluted with 500 µl of Opti-MEM and mixed with DNA in a 3:1 ratio (µg PEI: µg DNA). Next, the tube was mixed thoroughly and incubated for 15 minutes at room temperature. Afterward, the transfection mix was transferred dropwise onto a 10 cm tissue culture plate with HEK293T cells. The cells were incubated for 18 h, and then the medium was replaced with 10 ml of complete culture medium. The virus was harvested 48 h after transfection. The culture medium containing the lentiviral particles was aspirated from the plates, filtered through a 0.45 µm syringe filter, and centrifuged at 3000 × *g* for 18 h at 4°C. Approximately 600 µl of concentrated viral supernatant at the bottom of the centrifuged tube were used for further steps of lentiviral transduction or stored at -80°C.

For lentiviral transduction, target cells were seeded at the 6-well culture plate at a density of 2 × 10^5 cells per well in a complete culture medium. The next day, the medium was replaced with 600 µl of concentrated viral supernatant mixed with 400 µl of complete culture medium and 4 µg/ml polybrene (Sigma-Aldrich). The plate with the cells was centrifuged at 300 × *g* for 1 h at 25°C and then incubated for 24 h. On the next day, the medium was replaced with a fresh appropriate culture medium.

3.11.2 Puromycin selection

Mammalian antibiotic resistance to puromycin delivered by pLVX-IRES-Puro and lentiCRISPR v2 vectors enabled the selection of a stable cell culture by eliminating unmodified cells. As a result, a more homogenous cell population was obtained. Puromycin selection was performed 48 h after transfection. Puromycin stock of 2 mg/ml concentration was diluted 1:1000 in a complete culture medium, and the mix was used to replace medium in the cell cultures without detaching the cells. After 24 h, the medium was again replaced with a fresh medium containing 2 µg/ml of puromycin to remove dead cells from the culture. After 5 days of puromycin treatment, the cells were

recovered in a complete culture medium and used for further experiments. After transduction with pLenti7.3-redluc, cells with the highest GFP expression were sorted using BD FACSAria III flow cytometer (described in the Materials and Methods section, paragraph № 3.4.1).

3.12 Modification of T cells by mRNA electroporation

3.12.1 Plasmid pCIpA102 expressing CAR for in vitro mRNA synthesis

Plasmid vector pCIpA102 (162) for mRNA expression (Figure 16) was a gift from Dr. Stein Sæbøe-Larssen from Oslo University Hospital, Norway. The sequence recognized by MfeI restriction enzyme is incorporated directly after the polyA tail of the insert and linearization of the plasmid with the enzyme recognizing this restriction site serves as a stop signal for RNA polymerase.

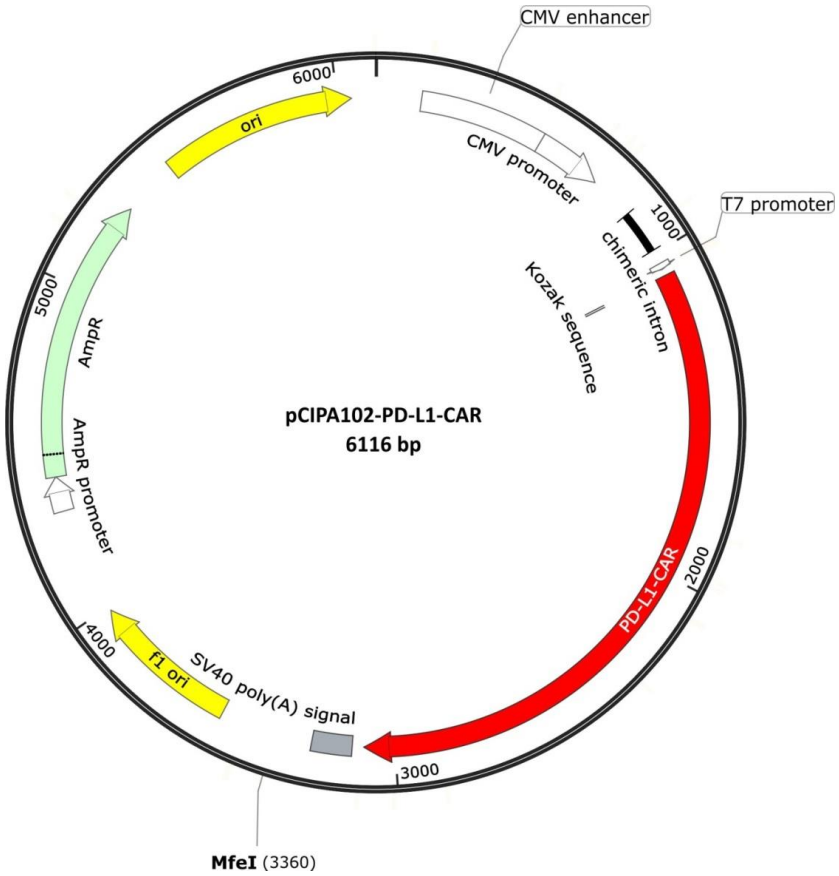

Figure 16 Vector pCIpA102 for PD-L1-CAR mRNA expression. The map was generated using SnapGene software.

The sequence encoding PD-L1-CAR was subcloned into pCIpA102 vector by Dr. Agnieszka Graczyk-Jarzynka.

3.12.2 *In vitro* mRNA synthesis

mRNA for PD-L1-CAR was produced *in vitro* using RiboMAX™ Large Scale RNA Production System (Promega). The primary *in vitro* transcription produces uncapped, 5'-triphosphorylated RNA. Meanwhile, the 5'-cap is a hallmark of eukaryotic mRNA and its presence is necessary for numerous cellular interactions. The preparation of correctly capped RNAs is essential to assess the proper functioning of mRNAs, as it also increases mRNA stability and translational efficiency (163). In order to obtain capped CAR encoding mRNA, the anti-reverse cap analog (ARCA) methylated at the 3'-OH of the N7-methylguanosine ribose was directly added to the reaction during *in vitro* transcription. As the limitation of a co-transcriptional capping is a competition of the cap analog with GTP as initiator nucleotide, the synthesis protocol was optimized by lowering the GTP concentration. According to the manufacturer's suggestion, a 4:1 mixture of a cap analog to GTP was used in transcription reactions.

During the mRNA synthesis process, all the manipulations were carried out in a laminar hood to avoid RNA nucleases contamination. First, 40 µg of pCIpA102 plasmid with an appropriate insert were linearized by digestion with MfeI (New England BioLabs) restriction enzyme for 18 h at 37°C. Next, the plasmid in the reaction mix was purified using QIAquick PCR Purification Kit (Qiagen). The DNA concentration was measured using Nanodrop (Thermo Scientific), and the restriction digest was confirmed by 1% agarose gel. The linearized plasmid was used as a template in the reaction of mRNA synthesis. The reaction mix included: nuclease-free water, ribonucleotide triphosphates, an anti-reverse cap analog (ARCA, Trilink), a T7 transcription buffer, a T7 enzyme mix, and a DNA template (Table 10).

Table 10 The components of the mix prepared for in vitro mRNA synthesis.

Component	100 µl reaction
water	add to 100 µl
rATP (100 mM)	7.5 µl
rCTP (100 mM)	7.5 µl
rUTP (100 mM)	7.5 µl
rGTP (100 mM)	2.25 µl
ARCA (100 mM)	9 µl
5X T7 transcriprion buffer	20 µl
T7 enzyme mix	10 µl
DNA template	**10 µg**

The mix was incubated for 4 h at 37°C, then 10 U of DNA nuclease were added to digest the DNA template for 15 min. Next, the synthesized mRNA was precipitated by adding an equal volume of lithium chloride (LiCl, Thermo Fisher Scientific) to the probe, which was then incubated for 20 minutes at -20°C. Precipitated mRNA was collected by centrifugation at 12 000 × *g* for 30 minutes at 4°C, the supernatant was removed, and the pellet was resuspended in 500 µl of 70% ethanol. Next, the mixture was centrifuged at 12 000 × *g* for 10 minutes at 4°C, the supernatant was discarded, and the pellet was centrifuged again at 12 000 × *g* for 1 minute at 4°C to remove the remaining supernatant. The pellet was left to dry for 20 minutes at 25°C, suspended in 50 µl of nuclease-free water, and left to dissolve for 18 h at 4°C. The concentration of completely dissolved mRNA concentration was measured by Nanodrop. The obtained mRNA was aliquoted in 20-40 µl portions (in concentration 1 µg/µl) and stored at -80° for further experiments.

3.12.3 T cells electroporation

Human T cells were counted, resuspended at a density of 1 × 10^6 cells per ml in a culture medium, and activated by adding Dynabeads Human T-Activator CD3/CD28 (Thermo Fisher Scientific) and IL-2 as described previously. On the fourth day of stimulation, the cells were electroporated with PD-L1-CAR mRNA. The procedure was performed using Gene Pulser Xcell Electroporation Systems (BioRad) and Gene Pulser/Micropulser electroporation cuvettes (BioRad).

T cells were centrifuged at 300 × *g* for 4 minutes and then resuspended in EasySep buffer. Dynabeads Human T-Activator CD3/CD28 (Thermo Fisher Scientific)

were removed using a magnet. Then T cells were centrifuged again at 300 × *g* for 4 minutes, and the supernatant was removed. Electroporation buffer was mixed with mRNA, and the T cells were resuspended in the mix. Electroporation conditions were optimized in this study. The cell number, buffer volume, and amount of mRNA were adjusted to the configuration of used cuvettes (Table 11).

Table 11 Optimized conditions for T cell electroporation.

Cuvette size	Number of T cells	Buffer volume	mRNA amount	Conditions
1 mm	1 mln	50 µl	10 µg	100 V 5 ms
2 mm	2 mln	100 µl	10 µg	200 V 5 ms
4 mm	4 mln	400 µl	20 µg	550 V 5 ms

The T cells were then transferred to electroporation cuvettes, electroporated, and quickly transferred using Pasteur's pipette to a 6-well culture plate with 2 ml per well of prewarmed complete medium supplemented with 200 U/ml IL-2. The cells were incubated for 18 h at 37°C in a cell incubator in a humidified atmosphere with 5% CO_2, and then the PD-L1-CAR expression was evaluated by flow cytometry.

3.13 Modification of T cells by lentiviral transduction

A pSEW plasmid expressing PD-L1-CAR was used for T cell modification. The lentiviral particles were produced in HEK293T cells as described in the Materials and Methods section (paragraph № 3.12.1). As a control, the original pSEW-GFP plasmid was used.

Before the transduction, freshly isolated or thawed human PBMCs were seeded onto a 6-well culture plate at a density of 1 × 10^6 cells per well in 3 ml of RPMI complete culture medium. PBMC's were stimulated with 2.4 µg/ml of phytohemagglutinin-L (PHA-L, Sigma Aldrich) for three days. On the fourth day, the plate was centrifuged at 300 × *g* for 4 minutes, approximately 2.5 ml of the medium were gently aspirated and replaced with 600 µl of concentrated viral supernatant, and 4 µg/ml of polybrene (Sigma-Aldrich) was added. The plate was centrifuged at 1000 × *g* for 1 h at 32°C followed by incubation for 18 h at 37°C in a humidified atmosphere with 5% CO_2. On the next day, the cells were centrifuged at 300 × *g* for 4 minutes and then resuspended in 4 ml of complete culture medium supplemented with 200 U/ml IL-2 (PeproTech) and Dynabeads Human T-Activator CD3/CD28 (Thermo Fisher Scientific) at a bead-to-cell ratio of 1:1. The CAR

expression on the surface of the T cells was evaluated by flow cytometry 48 h after transduction.

3.14 Evaluation of CAR expression on the surface of T cells

CAR expression on the surface of modified T cells was evaluated by flow cytometry, using anti-Fc antibody or protein L. Anti-Fc antibody binds to the Fc portion of an immunoglobulin, whereas protein L binds to the kappa light chain of immunoglobulin.

For the Fc staining, the T cells were centrifuged at 300 × *g* for 4 minutes and washed with EasySep buffer. After washing, the supernatant was removed, and the T cells were stained in 50 µl of anti-Fc antibody using goat anti-human IgG, Fcγ fragment specific antibody conjugated with Alexa Fluor 647 (Jackson ImmunoResearch) detecting a CH2-CH3 hinge region of the CAR. The antibody was diluted at 1:200 in EasySep buffer. The staining of CAR-T cells was performed for 20 minutes at 4°C in darkness. Next, the T cells were washed once with 200 µl of EasySep buffer, resuspended in 200 µl of EasySep buffer, and analyzed by BD FACSCanto II (BD Biosciences) flow cytometer.

For the protein L staining, the T cells were centrifuged at 300 × *g* for 4 minutes and washed with EasySep buffer. After washing, the supernatant was removed, and the T cells were resuspended in 200 µl of EasySep buffer. Biotinylated protein L (GenScript) was reconstituted in PBS at 1 mg/ml, and then 1 µg was added to the T cells. After 45 minutes of incubation at 4°C, the cells were washed twice with 200 µl of EasySep and then incubated with diluted 1:100 APC-conjugated streptavidin (BD Bioscience) for 20 minutes at 4°C in darkness. Next, the T cells were washed once with 200 µl of EasySep buffer, resuspended in 200 µl of EasySep buffer, and analyzed by BD FACSCanto II (BD Biosciences) flow cytometer.

3.15 Luciferase assay

Luciferases make up a class of oxidative enzymes found in several species that enable the organisms that express them to emit light, and this ability is called bioluminescence. The enzyme catalyzes the oxidation of firefly luciferin, requiring oxygen and ATP (Figure 17).

Figure 17 Luciferase-based assay principle (see details in text).

Mammalian cells transduced with the gene encoding firefly luciferase also possess the ability of bioluminescence, which can be used to monitor cell viability and proliferation because of the requirement of ATP. As a cell population proliferates, the amount of available ATP increases, resulting in a concomitant increase in the bioluminescent signal of the population. Conversely, a dying cell will stop emitting light once its remaining intracellular ATP has been used up (164,165).

In this study, luciferase-based assays were used to evaluate the cytotoxicity of PD-L1-CAR expressing T cells against target cancer cell lines. For this purpose, MCF-7 and MDA-MB-231 cell lines (both parental and modified) were stably transduced to express luciferase as described in the Materials and Methods section (paragraph № 3.13.1). For the assay, MCF-7 redluc or MDA-MB-231 redluc target cells were seeded onto the 96-well black plates with a clear bottom (PerkinElmer) at a density of 2.5×10^4 cells per well in 100 µl of complete culture medium in triplicates and left to attach for 18 h at 37°C in a humidified atmosphere with 5% CO_2. The T cells from the cell culture were centrifuged at 300 × *g* for 4 min and then resuspended in EasySep buffer to remove Dynabeads Human T-Activator CD3/CD28 (Thermo Fisher Scientific) using a magnet as described previously. Next, the T cells were centrifuged at 300 × *g* for 4 minutes again, and the cell pellet was resuspended in RPMI complete culture medium. Next, the culture medium from tested target cell lines was removed and replaced with 100 µl of T cells in an appropriate effector-to-target (E:T) ratio. The plate was then centrifuged at 200 × *g* for 3 minutes and incubated for 18 h at 37°C in a humidified atmosphere with 5% CO_2.

For a bioluminescence readout, a Bright-Glo™ Luciferase Assay System (Promega) was used. Directly before the readout, 100 µl of the mix of Bright-Glo™ Luciferase Assay Buffer with the Bright-Glo™ Luciferase Assay Substrate was added to each well of the plate with co-cultured cells. The plate was incubated for 5 minutes in darkness at 25°C, and then the luminescent signal was detected using Victor Plate Reader (PerkinElmer).

3.16 RTCA assay

The xCELLigence RTCA system (ACEA Biosciences) was used to monitor the viability of the target tumor cells during the co-incubation with the effectors. The microtiter plates, dedicated to the xCELLigence instrument, possess gold microelectrodes fused to their bottom surface. In the presence of an electrically conductive solution, such as a culture medium, the electron flow is freely transmitted between the electrodes. Once the cells seeded onto the plate start to adhere, the interaction between the electrodes and the solution is disrupted (Figure 18). The assay is based on measuring the changes in the electron flow impedance and this cellular resistance to alternating current is used to monitor the viability of surface-attached cancer cell targets continuously from the moment the cells begin to attach to the substrate. The impedance signal is measured automatically at the desired frequency and is expressed as arbitrary units called cell index. The software suite allows for normalizing the readout and converting the impedance parameter to % cytolysis and other kinetic relevant parameters. The immune effector cells are non-adherent and do not directly affect the impedance signal. However, the reduction of the attached target cancer cells number allows monitoring the effector cells' cytotoxic activity in real-time (166,167).

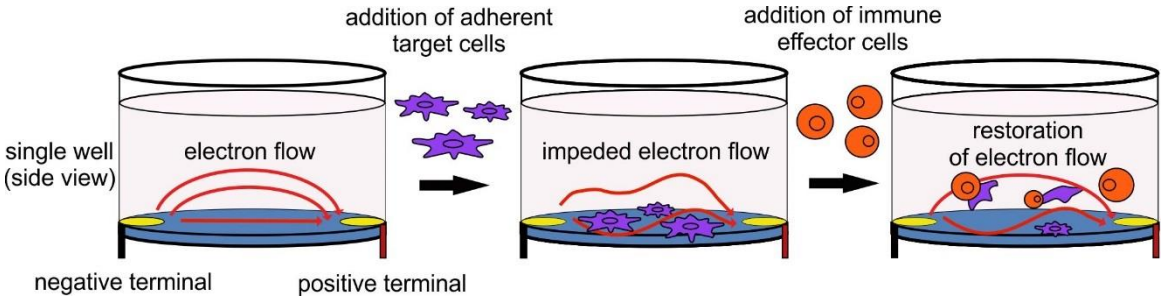

Figure 18 RTCA assay principle (see details in text).

All xCELLigence RTCA system-based experiments were conducted at 37°C (5% CO_2, 95% humidity). First, adherent target cells were detached from the culture plates, counted, and seeded onto 16-well E-Plates (ACEA Biosciences) at a density of 3×10^4 cells per well in 100 µl of the appropriate medium. The plates were incubated for 30 minutes at 25°C, then placed into the xCELLigence RTCA system and the cell proliferation was monitored for 24 h with the impedance measured every 15 minutes. Before each RTCA experiment, the Dynabeads Human T-Activator CD3/CD28 (Thermo Fisher

Scientific) were magnetically removed from the T cells. Next, the T cells were centrifuged at 300 × *g* for 4 minutes, and the T cell pellet was resuspended in RPMI complete culture medium. The medium from the 16-well E-Plates with target cancer cells was removed and replaced with 100 µl of T cells in an appropriate E to T ratio. For the indicated experiments, 0.4 mg/ml atezolizumab (ATZ, Roche) was added. The E-Plates with targets and effectors were incubated for 30 minutes at 25°C, then placed back into the xCELLigence RTCA system, and the cancer cells viability was monitored for 12-24 h with the impedance measured every 5-15 minutes. The analysis of the results was performed using RTCA Software Pro (ACEA Biosciences) and GraphPad Prism 8 (GraphPad Software). The impedance changes were normalized to the time of effector cell addition and plotted over time as normalized cell index.

3.17 Preparation of the supernatants from target-induced T cells or PD-L1-CAR T cells

MDA-MB-231 breast cancer cells were seeded onto a 6-well plate at a density of 1×10^6 per well in 2 ml of RPMI complete culture medium and incubated 24 h at 37°C in a humidified atmosphere with 5% CO_2. Next, the medium was removed and replaced with the unmodified or PD-L1-CAR T cells at the 1:1 E:T ratio. Target and effector cells were co-incubated for the next 24 h at 37°C in a humidified atmosphere with 5% CO_2. Afterward, the supernatants were collected, centrifuged at 2 000 × *g* for 5 minutes, and left for further experiments at -20°C.

3.18 Cytokine array

Human Cytokine Array, Panel A (R&D Systems) was used to determine the relative levels of 36 different human cytokines, chemokines, and acute-phase proteins in the supernatants collected from co-incubated for 24 h cancer and effector cells. The array includes nitrocellulose membranes with the capture antibodies spotted in duplicates and a cocktail of biotinylated detection antibodies, that make complexes with the cytokines which can be later bound by its cognate immobilized capture antibody on the membrane. Streptavidin-Horseradish Peroxidase and chemiluminescent detection reagents included in the kit were used to detect chemiluminescence.

The procedure was performed according to the manufacturer's protocol. All reagents were brought to 25°C before use. The supernatants from the T cells were collected as described in Materials and Methods paragraph № 3.17, and 1 ml was used for the array. The signals on the developed membranes were visualized by chemiluminescence detection using ChemiDoc Imaging System (Bio-Rad Laboratories). The exposure times were 4 and 8 minutes. The densitometric analysis was performed using Image Lab software (Bio-Rad Laboratories) and GraphPad Prism 8 (GraphPad Software).

3.19 Incubation of target cell lines with cytokines or supernatants

Cytokines TNF-α (Peprotech) and IFN-γ (Gibco) were reconstituted in H_2O at 100 µg/ml and stored at -80°C. The supernatants from the T cells were collected as described in Materials and Methods paragraph № 3.17. One day before the experiment, MCF-7 or HEK293T cells were seeded onto a 12-well plate at a density of 2×10^5 cells per well in 1 ml of RPMI complete culture medium and left to adhere. The next day, the cytokines were added to the medium in 30 µg/ml concentration, either separately or in combination. For the treatment with the supernatants from activated T cells, the culture medium was replaced with 1 ml of the supernatants. The target cells were incubated with the treatment for 4, 8, or 24 h. Then the cells were detached with 0.25% trypsin-EDTA solution, transferred to a 96-well plate, washed twice with 200 µl of EasySep buffer, and stained with 1:100 diluted APC-conjugated anti-PD-L1 antibody (Thermo Fisher Scientific, clone MIH1) for 20 minutes at 25°C. After the incubation, the cells were washed once with 200 µl of EasySep buffer, resuspended in 200 µl of EasySep buffer, and analyzed by BD FACSCanto II (BD Biosciences) flow cytometer.

3.20 Analysis of the results

The results obtained by the flow cytometry technique were analyzed using FlowJo cell analysis software (FlowJo). Imaging software Image Lab (BioRad) was used to compare the signal generated by the bands detected on the Western blot and cytokine arrays. SnapGene software (GSL Biotech LLC) was used to analyze nucleic acid sequences. GraphPad Prism 8 statistics software was used for data analysis and visualization. The

data were analyzed with either T-test for unpaired samples, one-way, or two-way ANOVA with Tukey multiple comparison test. P values less than 0.05 were summarized with one asterisk, less than 0.01 with two, less than 0.001 with three, and less than 0.0001 with four asterisks. The experiments were carried out in at least two biological replicates, and one representative result of each of them was shown. The results were represented as an arithmetic average from the biological replicates. The figures were prepared using CorelDraw software (Corel Corporation) and BioRender.com.

4. RESULTS

4.1 PD-L1 protein expression in breast cancer cell lines

To evaluate PD-L1 protein expression in breast cancer cell lines the Western blotting and flow cytometry methods were applied. Six cell lines representing different subtypes of breast cancer: triple-negative (MDA-MB-231, HCC-1806), ER-positive (MCF-7, ZR-75-1, T47D), and HER2-positive (SkBr3) were analyzed by Western blotting (Figure 19A). Densitometric analysis of the blots showed that the triple-negative breast cancer cell line, MDA-MB-231, exhibited the highest level of PD-L1 protein as compared to other analyzed cell lines (Figure 19B).

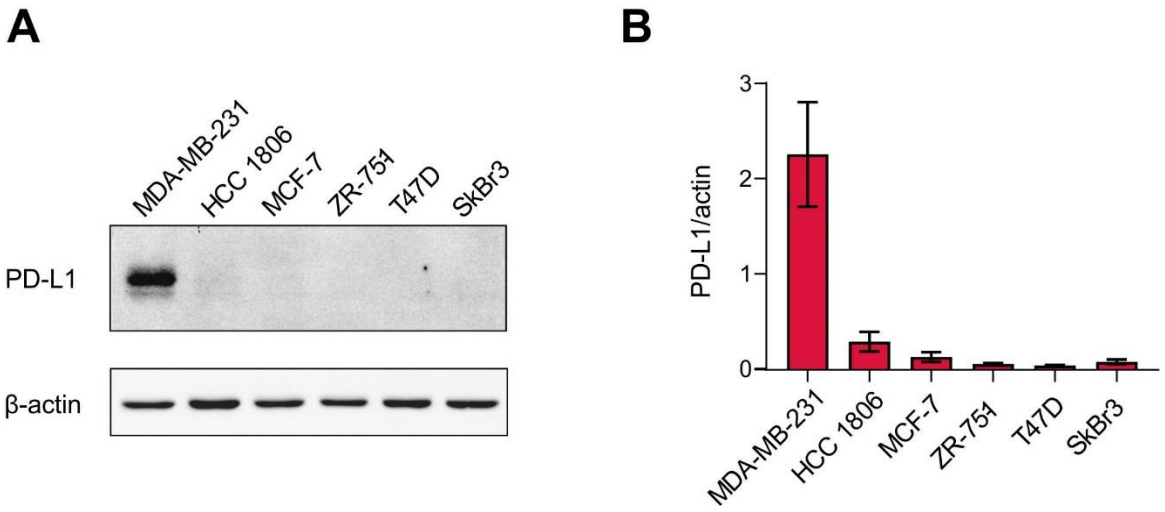

Figure 19 Comparison of PD-L1 protein expression in six breast cancer cell lines. (A) Representative Western blotting shows the amount of PD-L1 protein in 20 µg of total protein lysates loaded onto the SDS-polyacrylamide gel and separated by electrophoresis in reducing conditions. The experiment was repeated three times. (B) Bands were quantified by densitometry; the signal for the PD-L1 band was normalized to the corresponding actin. The data are presented as mean ± SEM from three experiments.

Next, the surface expression of PD-L1 on MDA-MB-231 cells (PD-L1^{high} according to Western blotting analysis) and MCF-7 cells (PD-L1$^{low/null}$ according to Western blotting analysis) was determined by flow cytometry using an anti-PD-L1 monoclonal antibody (MIH1 clone). The flow cytometry results confirmed the results obtained by Western blotting analysis, the PD-L1 protein was highly expressed on the surface of MDA-MB-231 cells (Figure 20A), while on MCF-7 cells its expression was undetectable (Figure 20B).

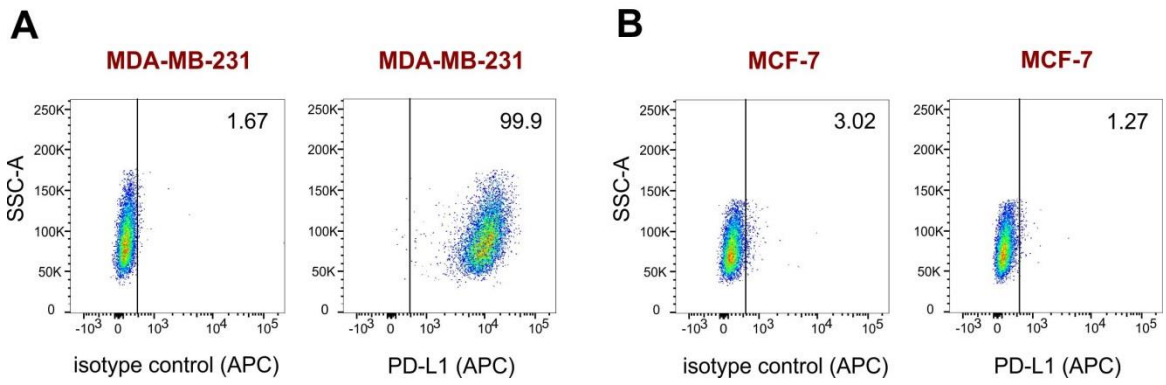

Figure 20 Evaluation of surface PD-L1 expression on selected cell lines. Representative dot plots show surface PD-L1 expression on (A) MDA-MB-231 and (B) MCF-7 cells evaluated by flow cytometry against a background from isotype control. The staining was performed using an anti-PD-L1 antibody (clone MIH1, dilution 1:100). Numbers on the plots indicate the percentage (%) of PD-L1 positive cells. The PD-L1 expression level in cells was verified prior to an experiment.

Based on the results obtained with two analytical methods, for further studies MDA-MB-231 cell line was selected as a model with the high level of target protein expression, and the MCF-7 cell line was primarily selected as a negative control, due to its low level of PD-L1 expression in steady state.

4.2 Generation of the models for the evaluation of PD-L1-CAR-T cells anticancer potential

4.2.1 Luciferase expressing target cell lines

The selected breast cancer cell lines (MDA-MB-231 and MCF-7) were modified by lentiviral transduction with pLenti7.3-redluc plasmid to express luciferase. The transduction efficiency was evaluated by flow cytometry based on GFP expression (Figure 21).

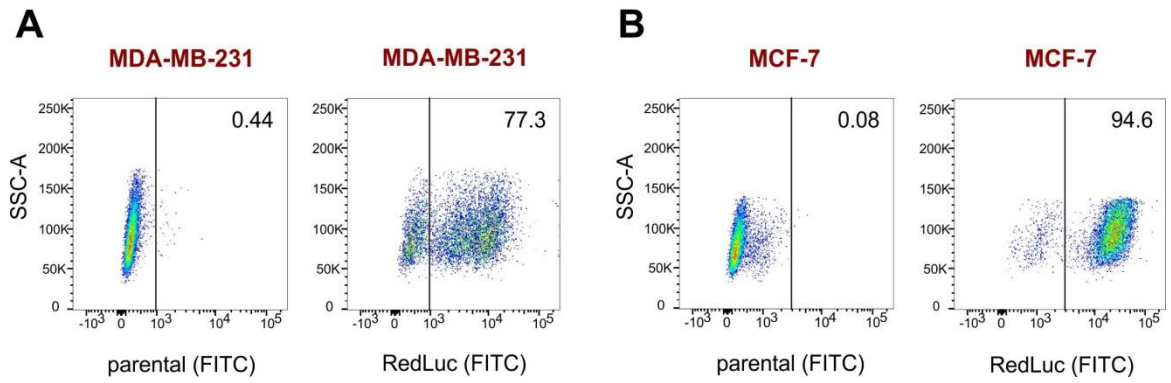

Figure 21 Evaluation of transduction efficiency with pLenti7.3-redluc plasmid. The GFP expression in target cell lines was evaluated by flow cytometry. Numbers on the plots indicate the percentage (%) of GFP positive (A) MDA-MB-231 cells and (B) MCF-7 cells transduced with pLenti7.3-redluc plasmid. RedLuc expression in transduced cells was monitored before luciferase-based assays performance. The RedLuc expression level in transduced cells was verified prior to an experiment.

MDA-MB-231 redluc and MCF-7 redluc cell lines were further used as target cells in luciferase-based cytotoxic assays.

4.2.2 Generation of the PD-L1-knock-out (KO) derivative of MDA-MB-231 cell line

The PD-L1-knock-out derivative of MDA-MB-231 cell line (MDA-MB-231-sgPD-L1) was generated to verify the specificity of the newly generated PD-L1-CAR. The MDA-MB-231 cell line modified with lentiCRISPR v2 plasmid with control sgNTC sequence (MDA-MB-231-sgNTC) was used as a control. Surface PD-L1 expression on generated cell lines was analyzed by flow cytometry. The results confirmed the significant decrease of PD-L1 surface expression on MDA-MB-231 sgPD-L1 cells as compared to parental and MDA-MB-231 sgNTC cells (Figure 22A). The Western blotting analysis also revealed a decrease in PD-L1 expression in MDA-MB-231 sgPD-L1 cells, while the expression in sgNTC control was not affected by the genetic modification as compared to the parental MDA-MB-231 cell line (Figure 22B).

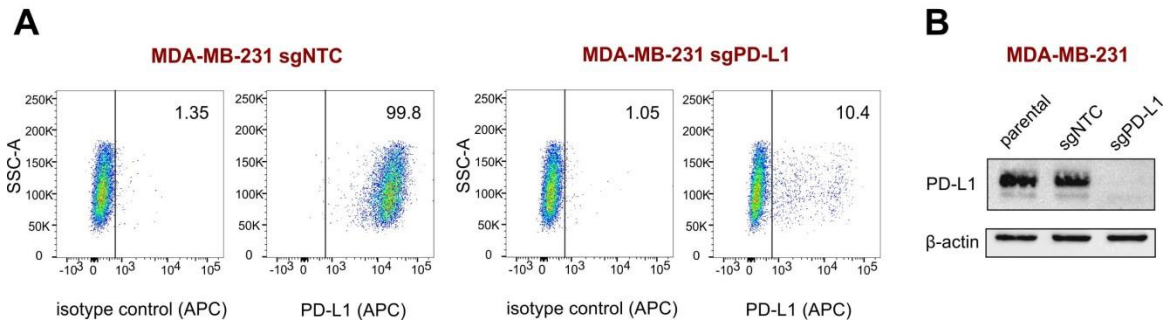

Figure 22 Evaluation of PD-L1 expression in PD-L1-knockout (KO) derivative of the MDA-MB-231 cell line. (A) Representative dot plots show surface PD-L1 expression evaluated by flow cytometry against a background from isotype control. The staining was performed using an anti-PD-L1 antibody (clone MIH1, dilution 1:100). Numbers on the plots indicate the percentage (%) of PD-L1 positive cells. The PD-L1 expression level in transduced cells was verified prior to an experiment. (B) Representative Western blotting shows the amount of PD-L1 protein in 20 µg of total protein lysates loaded onto the SDS-polyacrylamide gel and separated by electrophoresis in reducing conditions. The experiment was repeated three times.

4.2.3 Generation of the PD-L1-overexpressing derivative of MCF-7 cell line

The PD-L1-overexpressing derivative of the MCF-7 cell line (MCF-7 PD-L1) was also generated to verify the specificity of the newly generated PD-L1-CAR. The MCF-7 cell line transduced with an empty pLVX vector was used as a control (MCF-7 PLVX).

Surface PD-L1 expression on newly generated cell lines was analyzed by flow cytometry. The results confirmed the significant increase of PD-L1 protein expression on MCF-7 PD-L1 cells as compared to MCF-7 PLVX control (Figure 23A). Western blotting analysis as well showed a high increase in PD-L1 expression in MCF-7 PD-L1 cells, while the expression in PLVX control was not affected by the genetic modification as compared to the parental MCF-7 cell line (Figure 23B).

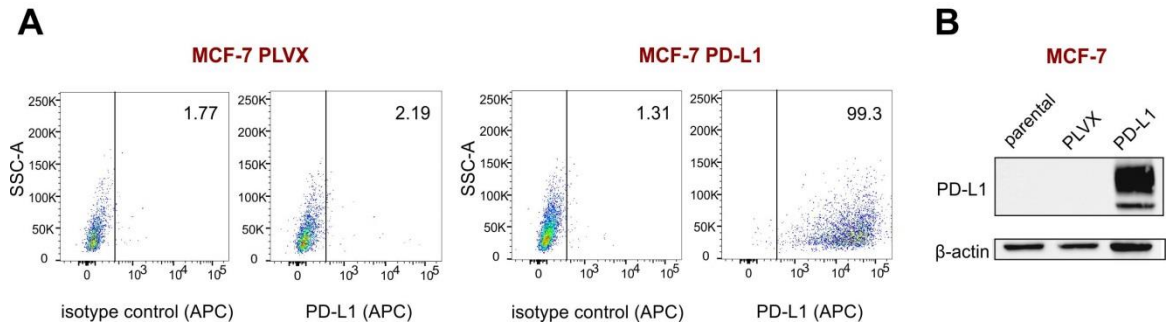

Figure 23 Evaluation of PD-L1 expression in PD-L1-overexpressing derivative of MCF-7 cell line. (A) Representative dot plots show surface PD-L1 expression evaluated by flow cytometry against a background from isotype control. The staining was performed using an anti-PD-L1 antibody (clone MIH1, dilution 1:100). Numbers on the plots indicate the percentage (%) of PD-L1 positive cells.The PD-L1 expression level in transduced cells was verified prior to an experiment. (B) Representative Western blotting shows the amount of PD-L1 protein in 20 µg of total protein lysates loaded onto the SDS-polyacrylamide gel and separated by electrophoresis in reducing conditions. The experiment was repeated three times.

4.3 Implementation of primary human T cells modification with PD-L1-CAR construct

The most commonly used method for primary human T cell modification with chimeric antigen receptors is viral delivery. Both lentiviruses and gammaretroviruses can transduce and integrate their transgenes into the host cell genome, thus allowing for stable CAR expression. However, gammaretroviruses are unable to effectively transduce non-dividing cells and also are considered to be more immunogenic and oncogenic than lentiviruses (168). In this study, the PD-L1-CAR construct was delivered in primary human T cells using the lentiviral vector pSEW.

Another strategy for CAR introduction into the effector cells is using non-viral vectors, which includes plasmid DNA or mRNA delivery with liposomes or electroporation. These methods are considered a safer approach as transient CAR expression limits the time T cells can exhibit their anti-tumor activity (169). Electroporation of mRNA was shown to result in higher modification efficiency and higher viability of the targeted cells (170), thus, the PD-L1-CAR-encoding mRNA was used to modify primary human T cells during this study.

4.3.1 Modification of the primary T cells with PD-L1-CAR construct via mRNA electroporation

The CAR-encoding mRNA was synthesized *in vitro* and introduced into primary human T cells using a square-wave electroporation system. The surface protein expression was analyzed by flow cytometry 18-24 h post-electroporation and monitored for the next 72 h.

It was observed, that 24 h post-electroporation, almost 100% of the effector cells expressed the PD-L1-CAR (Figure 24A). The analysis in the following days revealed, that albeit the percentage of PD-L1-CAR-T cells remained high 48 h post-electroporation, the geometric mean fluorescence intensity index (geomean) was already notably decreased (Figure 24B). Subsequently, 72 h post-electroporation almost 90% of the T cells did not express the CAR construct on their surface (Figure 24A and B).

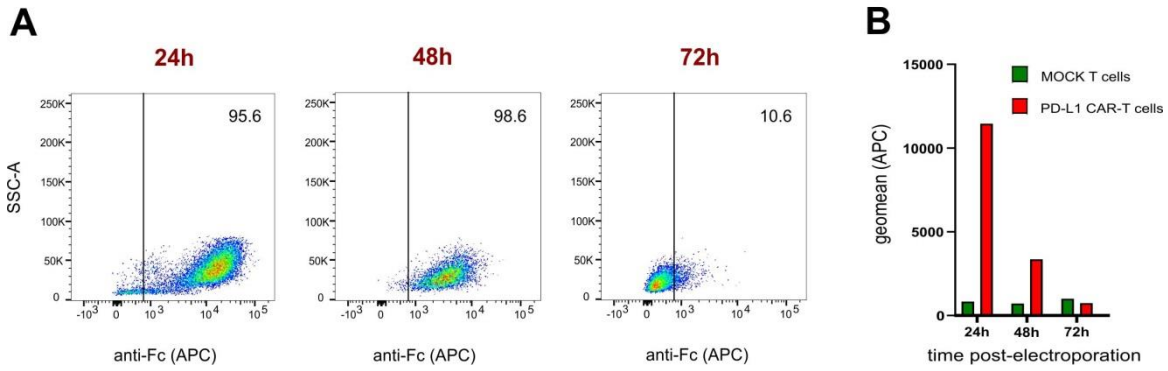

Figure 24 The expression of the PD-L1-CAR construct on the surface of T cells. (A) Representative dot plots show surface PD-L1-CAR expression evaluated by flow cytometry at indicated time points. The staining was performed using an anti-Fc antibody (dilution 1:100). Numbers on the plots indicate the percentage (%) of PD-L1-CAR positive cells. (B) The representative graph shows the analysis of geometric mean fluorescence intensity following PD-L1-CAR staining 24-72 h post electroporation. The experiment was repeated three times.

The protocol for T cell modification via mRNA electroporation was established and implemented. The obtained results indicated, that the PD-L1-CAR-encoding DNA is successfully translated, and the protein is expressed on the surface of modified effector cells. However, the short-termed PD-L1-CAR expression on the electroporated T cells is a limiting factor for the cytotoxicity evaluation. Thus, to achieve long-term CAR expression on the T cells, lentiviral modification was applied.

4.3.2 Modification of the primary T cells with PD-L1-CAR construct via lentiviral transduction

The PBMCs were stimulated with PHA-L for 3 days, and the obtained population composed mainly from CD3+ T cells was transduced with a lentiviral vector encoding PD-L1-CAR. The achieved efficiency of the modification was approximately 40% of the CAR-positive cells. Therefore, to increase the efficiency of transduction, the optimization of the transduction protocol, included the addition of efficiency enhancers. It was observed, that polybrene, which is a cationic polymer that neutralizes the charge repulsion between virions and the cell surface, improves the PD-L1-CAR construct transduction efficiency up to 70% (Figure 25).

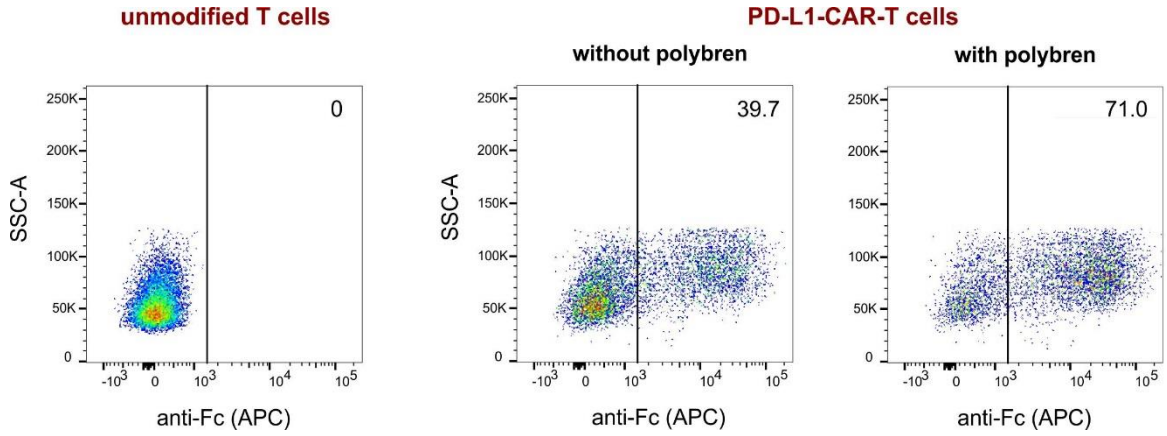

Figure 25 The efficiency of the T cells lentiviral transduction with PD-L1-CAR. Representative dot plots show surface PD-L1-CAR expression evaluated by flow cytometry 96 h post-transduction. The staining was performed using an anti-Fc antibody (dilution 1:100). Numbers on the plots indicate the percentage (%) of PD-L1-CAR positive cells. The experiment was repeated twice. Data from one donor is shown.

Next, CAR-modified T cells were monitored in order to determine the stability of PD-L1-CAR surface expression. The modified T cells maintained the surface PD-L1-CAR expression from day 4 post-transduction up to 3 weeks (Figure 26).

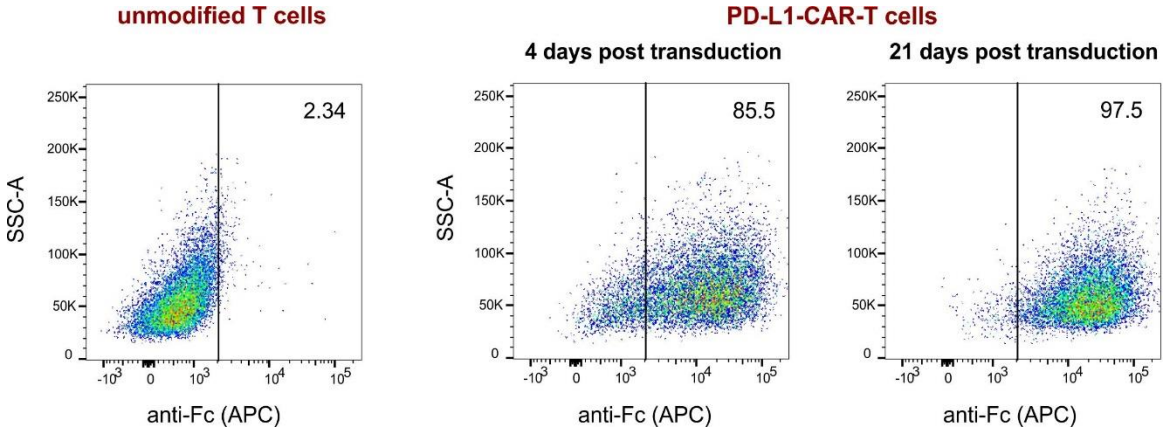

Figure 26 The expression of the PD-L1-CAR construct on the surface of transduced T cells. Representative dot plots show surface PD-L1-CAR expression evaluated by flow cytometry 4 and 21 days post-transduction. The staining was performed using an anti-Fc antibody (dilution 1:100). Numbers on the plots indicate the percentage (%) of PD-L1-CAR positive cells. The staining was performed following each T cell transduction to determine the modification efficiency. Data from one donor is shown.

Thus, for the further evaluation of the PD-L1-CAR anticancer efficacy, the T cells were modified by lentiviral transduction, which allows achieving a stable effector cell modification.

4.3.3 Evaluation of PD-L1-CAR expression

The presence of the PD-L1-CAR protein on the T cell surface was assessed by flow cytometry. As the extracellular domain of the CAR construct structurally consists of a single-chain antibody-like fragment, to evaluate the PD-L1-CAR expression on the effector cell surface the anti-Fc antibody conjugated with the fluorochrome or biotinylated protein L were used in the study. The results of the staining, indicating the efficacy of the T cell modifications, were similar regardless of the method of staining used (Figure 27).

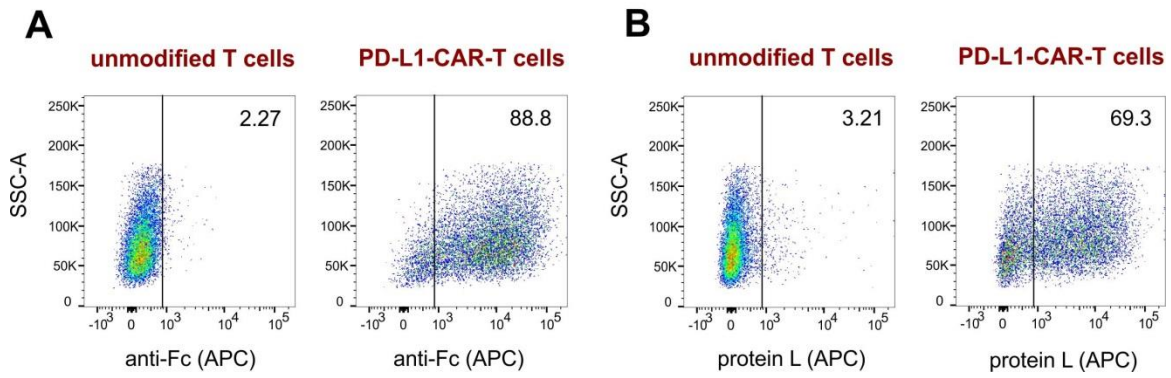

Figure 27 Evaluation of the PD-L1-CAR expression on the T cell surface. Representative dot plots show surface PD-L1-CAR expression evaluated by flow cytometry 4 days post-transduction. The staining was performed using (A) an anti-Fc antibody (dilution 1:100) or (B) biotinylated protein L (1 µg/sample) followed by APC-conjugated streptavidin (dilution 1:100). Numbers on the plots indicate the percentage (%) of PD-L1-CAR positive cells. The experiment was repeated twice. Data from one donor is shown.

However, as staining using anti-Fc antibody resulted in better separation of positive and negative populations, staining with protein L requires an additional step of the cell incubation with streptavidin-conjugated with a fluorochrome, as a method of choice in the following experiments, the staining with an anti-Fc antibody was performed.

4.3.4 PD-L1 is expressed on activated unmodified T cells, but not on activated PD-L1-CAR-T cells

As it is known, PD-L1 can be expressed not only by tumor cells but also by effector cells (171), thus, its expression was evaluated on primary T cells. It was observed that the stimulation of T cells with CD3/CD28 beads evoked the upregulation of the surface PD-L1 molecule on T cells within 24 h, with the expression reaching the peak on the day 3-4 post-stimulation and decreasing back to the basal level after Day 7 (Figure 28).

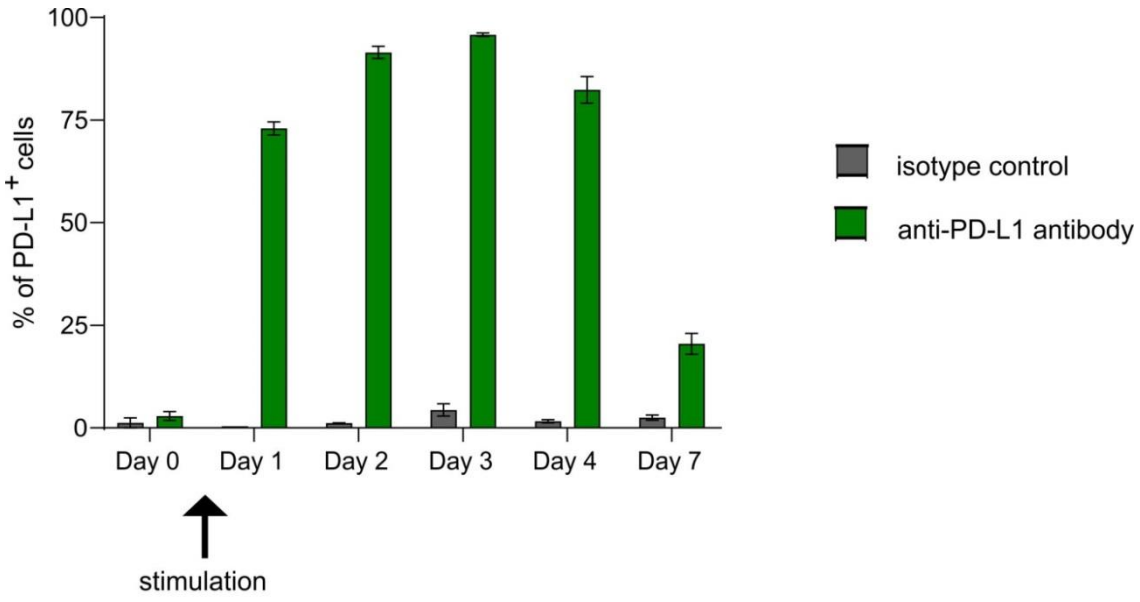

Figure 28 The PD-L1 expression on the primary T cells stimulated with CD3/CD28 beads. T cells were isolated from PBMC and cultured in the absence (Day 0) or presence of CD3/CD28 beads (Day 1-7). The cells were stained using an anti-PD-L1 antibody (clone MIH1, dilution 1:100) and the PD-L1 expression was evaluated by flow cytometry. The experiment was performed twice. Data from one donor are shown as means ± SD.

The observed effect may suggest a possible risk of fratricidal killing between the activated effector cells bearing the PD-L1-CAR construct. Thus, the dynamic of PD-L1 expression in PD-L1-CAR-T cells was compared to the PD-L1 expression in unmodified T cells. The transduction efficiency was evaluated 48 h after modification, the CAR expression was detected on 80-90% of the T cells (Figure 29).

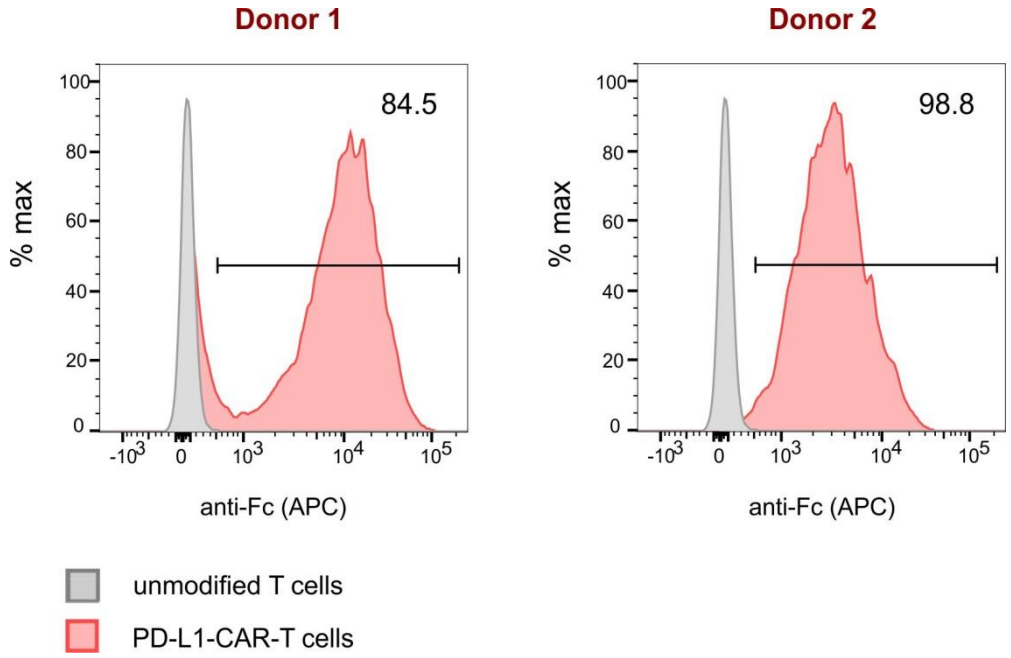

Figure 29 The PD-L1-CAR expression on the surface of T cells evaluated 48 h after the lentiviral transduction. Representative dot plots show surface PD-L1-CAR expression evaluated by flow cytometry. The staining was performed using an anti-Fc antibody (dilution 1:100). Numbers on the plots indicate the percentage (%) of PD-L1-CAR-positive cells. Data from two donors are shown and the experiment was repeated twice.

Simultaneously, the PD-L1 expression on unstimulated T cells was evaluated. The PD-L1 protein was detected on approximately 10% of unmodified T cells, while PD-L1-CAR-T cells were PD-L1-negative as compared to isotype control (Figure 30, Day 0). However, greater differences in PD-L1 surface expression between the groups were observed already 24 h after CD3/CD28 beads addition, as the expression on unmodified T cells notably increased in contrast to PD-L1-CAR-T cells which remained PD-L1-negative (Figure 30, Day 1). The analysis in the following days revealed, that while the dynamics of PD-L1 expression on unmodified T cells was similar to observed previously, the PD-L1 protein was undetectable on the surface of PD-L1-CAR-T cells (Figure 30, Day 4 and Day 7). Both groups were re-stimulated on Day 7, by adding the fresh portion of CD3/CD28 beads, and the PD-L1 staining 24 h afterward showed, that only unmodified T cells upregulated PD-L1 expression (Figure 30, Day 8).

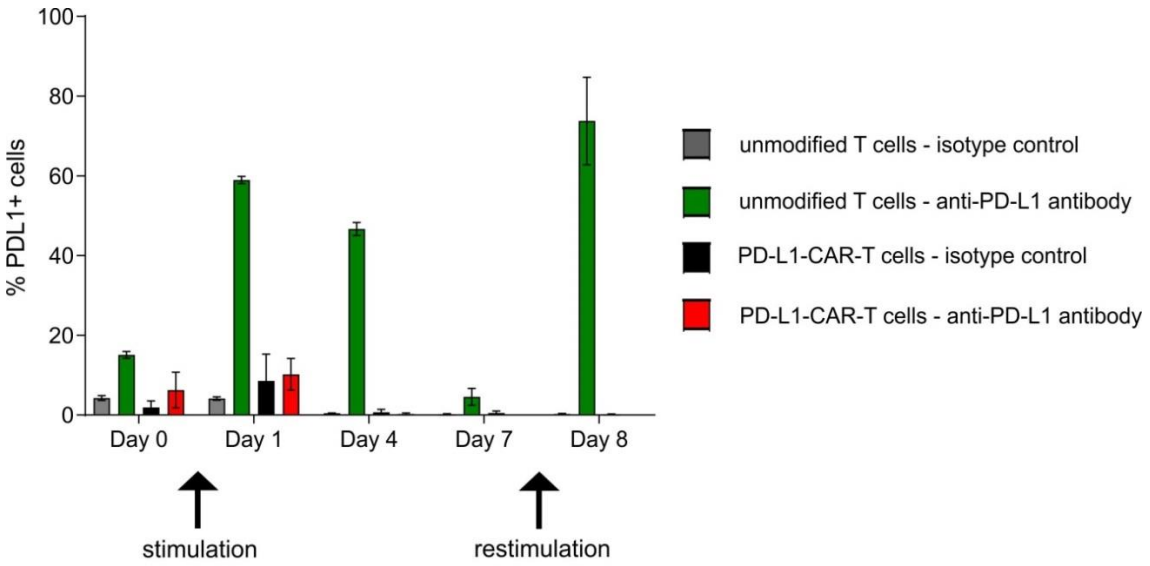

Figure 30 The PD-L1 expression on the PD-L1-CAR-T cells stimulated with CD3/CD28 beads. T cells were isolated from PBMC and transduced with the lentiviral vector encoding PD-L1-CAR. Unmodified T cells were used as control. Both groups of cells were stimulated with CD3/CD28 beads 48 h post-transduction (Day 0) and restimulated one week afterward (Day 7). The PD-L1 expression dynamics were monitored before and following the stimulation. The cells were stained using an anti-PD-L1 antibody (clone MIH1, dilution 1:100) and the PD-L1 expression was evaluated by flow cytometry. Data are shown as means ± SD from 2 donors and the experiment was repeated twice.

The results indicate that PD-L1-CAR-bearing effector cells may eliminate the T cells with the ability to upregulate PD-L1 expression, leaving in the culture only the population that did not have an inducible expression of the target molecule.

To verify whether the loss of PD-L1 expression occurred on the PD-L1-CAR-T cells surface only, the total PD-L1 expression in unmodified T cells and PD-L1-CAR-T cells was assessed by Western blotting analysis. It was confirmed, that the level of total PD-L1 protein was low in both unmodified and PD-L1-CAR-T cells before the addition of CD3/CD28 beads (Figure 31A, Day0). The increase in PD-L1 expression was observed following the stimulation, wherein the level of total PD-L1 protein was notably reduced in PD-L1-CAR-T cells as compared to unmodified T cells obtained from the same donor (Figure 31A, Day1, and Day4). On Day7, both unmodified T cells and PD-L1-CAR-T cells had low PD-L1 expression, which confirmed the results obtained previously using flow cytometry (Figure 31A, Day7). Both groups were re-stimulated with the fresh portion of CD3/CD28 beads on Day7, and in the cell lysates were collected 24 h later, a higher level of total PD-L1 protein was found in the samples from unmodified T cells than from PD-

L1-CAR-T cells (Figure 31A, Day8). The densitometry analysis was performed to quantify the antibody responses on Western blots (Figure 31B)

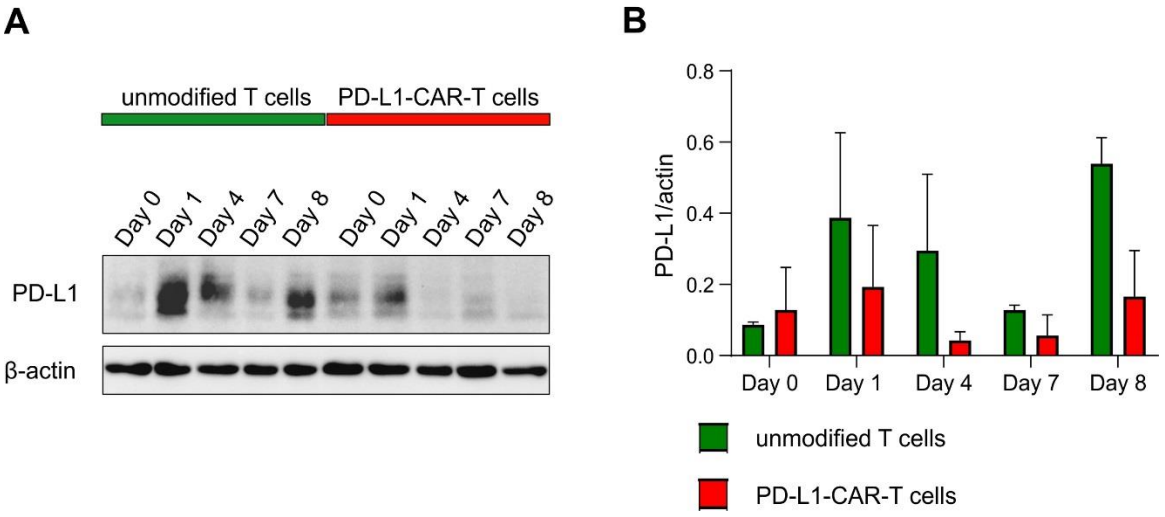

Figure 31 Evaluation of PD-L1 expression in unmodified T cells and PD-L1-CAR-T cells following the stimulation with CD3/CD28 beads. (A) Representative Western blotting shows the amount of PD-L1 protein in 20 µg of total protein lysates loaded onto the SDS-polyacrylamide gel and separated by electrophoresis in reducing conditions. The experiment was performed on T cells from two donors. (B) Bands were quantified by densitometry; the signal for the PD-L1 band was normalized to the corresponding actin. Data are shown as means ± SD.

The results of the Western Blotting analysis demonstrate, that the pattern of surface PD-L1 expression on both unmodified T cells and PD-L1-CAR-T cells correlates with the changes of total PD-L1 protein amounts in the cells following the stimulation with CD3/CD28 beads. Thus, the population of PD-L1-CAR-T cells appears to lack the ability to induce PD-L1 protein expression in response to stimulation.

4.4 Evaluation of the anticancer efficacy of PD-L1 CAR-T cells against cancer cells

4.4.1 PD-L1-CAR-T cells degranulate and produce cytokines in the presence of target cells with high PD-L1 expression specifically

In order to investigate the effector functions of generated PD-L1-CAR-T cells against the selected breast cancer cell lines with various PD-L1 expression levels, the degranulation of CAR-T cells was assessed by CD107a surface staining and the cytokine production was evaluated within intracellular TNF-α and IFN-γ staining.

First, PD-L1-CAR-T cells were targeted against parental MDA-MB-231 and MCF-7 cells. Within 4 h of the experiment, it was observed, that CD107a expression increased significantly on the surface of PD-L1-CAR-T cells following co-incubation with MDA-MB-231 cells (PD-L1^{high}), but not MCF-7 cells (PD-L1$^{low/null}$) (Figure 32A, red bars). Similarly, PD-L1-CAR-T cells targeted against MDA-MB-231 cells produced significantly more TNF-α and IFN-γ, than PD-L1-CAR-T cells targeted against MCF-7 cells (Figure 32B and C, red bars).

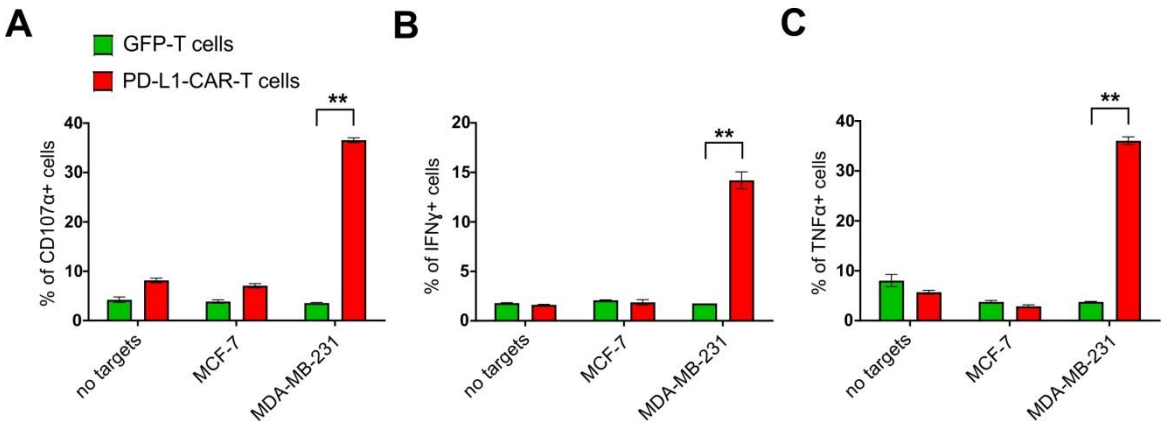

Figure 32 Degranulation and cytokine production by PD-L1-CAR-T cells and control GFP-T cells following co-incubation with parental breast cancer cells. Effector and target cells were co-incubated for 4 h at a 2:1 E:T ratio. The assay results were evaluated by flow cytometry. (A) Expression of CD107a, a marker of degranulation, in PD-L1-CAR T cells and control GFP-T cells targeted against MDA-MB-231 and MCF-7 cells. (B, C) Cytokine production by PD-L1-CAR T cells and GFP-T cells against MDA-MB-231 and MCF-7 cells, as measured by intracellular expression of IFN-γ and TNF-α. The assay was repeated three times and the results shown are representative of one experiment. Data are shown as means ± SD. The statistical analysis was performed by the use of an unpaired T-test. **p<0.001.

Next, the PD-L1-CAR-T cells were co-incubated with the PD-L1-knockout (KO) derivative of MDA-MB-231 cell line (MDA-MB-231-sgPD-L1), and the PD-L1-overexpressing derivative of MCF-7 cell line (MCF-7-PD-L1). The expression of CD107a on PD-L1-CAR-T cells incubated with MDA-MB-231-sgPD-L1 cells (PD-L1$^{low/null}$) was significantly lower than on the effectors incubated with MDA-MB-231-sgNTC (PD-L1^{high}). At the same time, MCF-7 cells that were genetically modified to overexpress PD-L1 (MCF-7 PD-L1) demonstrated the gained capability to induce degranulation of PD-L1-CAR-T cells, which was significantly higher than in the case of the effector cells incubated with control MCF-7 PLVX cells. The results are depicted in Figure 33A. The results of the intracellular cytokine staining (Figure 33 B and C) revealed, that once the PD-L1 gene

was knocked out in the MDA-MB-231 cells, they were no longer capable of inducing the effector cells cytokine production, similarly to MCF-7 PLVX cells (PD-L1$^{low/null}$). The opposite effect was observed with MCF-7 PD-L1 cells, which provoked cytokines production in PD-L1 CAR-T cells similarly to MDA-MB-231 cells with naturally high PD-L1 expression.

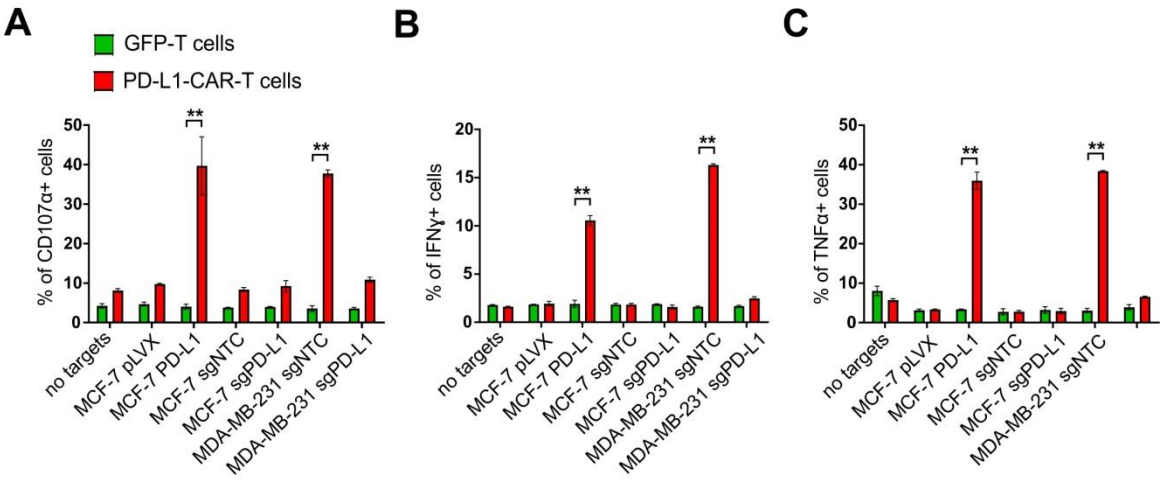

Figure 33 Degranulation and cytokine production by PD-L1-CAR-T cells and control GFP-T cells following co-incubation with modified breast cancer cells. Effector and target cells were co-incubated for 4 h at a 2:1 E:T ratio. The assay results were evaluated by flow cytometry. (A) Expression of CD107a, a marker of degranulation, in PD-L1-CAR-T cells and GFP-T cells targeted against MDA-MB-231 and MCF-7 derivative cell lines. (B, C) Cytokine production by PD-L1-CAR-T cells and GFP-T cells against modified MDA-MB-231 and MCF-7 cells, as measured by intracellular expression of TNF-α and IFN-γ. The assay was repeated three times using T cells from different donors and the results shown are representative of one experiment. Data are shown as means ± SD. Statistical analysis was performed by unpaired T-test. **p<0.001.

The results indicate the ability of the PD-L1-CAR construct to specifically recognize the target molecule on the surface of the cancer cells and confirm that PD-L1-CAR-T cells produce a functional response in the target presence.

4.4.2 PD-L1 CAR-T cells exhibit improved cytotoxicity against target MDA-MB-231 (PD-L1^{high}) cancer cells

In order to directly evaluate the killing ability of PD-L1-CAR-T cells against MDA-MB-231 cell lines, the effectors were incubated with luciferase-expressing targets for 18 h. The following luminescence measurements suggested that CAR-bearing effectors eliminate over 60% of MDA-MB-231 sgNTC cells with naturally high PD-L1 expression, while the

knockout of PD-L1 encoding gene in MDA-MB-231 cells strongly diminishes PD-L1-CAR-T cells killing ability (Figure 34, red bars).

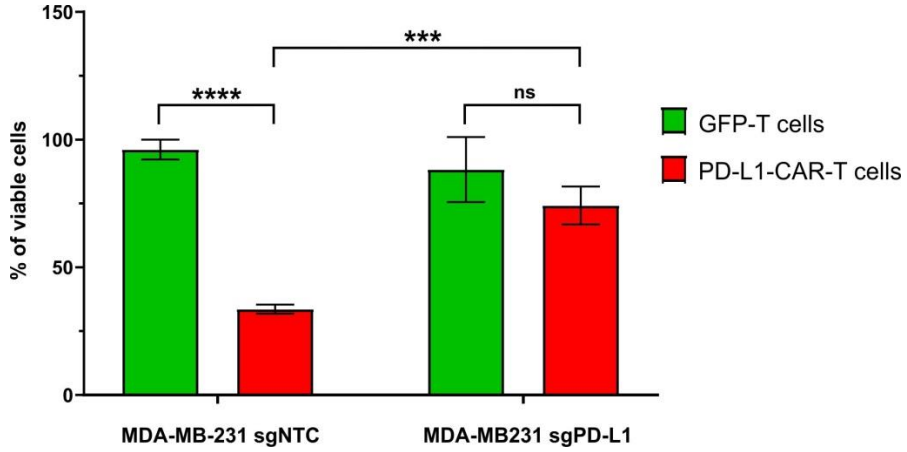

Figure 34 The killing potential of PD-L1-CAR-T cells and GFP-T cells against breast cancer cells MDA-MB-231 sgNTC (PD-L1^{high}) and MDA-MB-231 sgPD-L1 (PD-L1^{low}) determined by luciferase-based killing assay. Cancer cell lines were seeded onto the plate and left to adhere for 24 h. The next day, PD-L1-CAR-T cells and GFP-T cells were added to the target cells at a 2:1 E:T ratio. After 18 h of incubation, the cultures were lysed, and the percentage of viable target cells was measured based on luminescence analysis. The assay was repeated twice in triplicates and the results shown are representative of one experiment. The data are shown as means ± SD. Statistical analysis was performed by two-way ANOVA with Tukey's multiple comparisons test: ****p<0.0001, ***p<0.001, ns - statistically non-significant difference.

Additionally, to monitor PD-L1-CAR-T cell cytotoxic activity towards parental MDA-MB-231 cancer cell lines in a real-time manner, the RTCA system was utilized. Parental MDA-MB-231 cells (PD-L1^{high}) were efficiently eliminated by PD-L1-CAR-T cells, with close to no viable targets left after 12 h incubation with the effectors (Figure 35A, light red curve). Control GFP-T cells exhibited a modest natural cytotoxic effect against the cancer cells, however, much lower than of the T cells bearing the PD-L1-CAR construct (Figure 35A, light green curve). To confirm the PD-L1-CAR construct specificity, the PD-L1 targeting antibody atezolizumab was added to the experimental groups in order to competitively block the binding of PD-L1-CAR-T to its target. The blockade of the PD-L1 target on the surface of the MDA-MB-231 cells led to their improved survival when incubated with PD-L1-CAR-T cells (Figure 35A, dark red curve), and did not affect the basal natural cytotoxicity of GFP-T cells (Figure 35A, dark green curve). The comparison of viable target cell amount in each group after 12 h of killing assay was depicted in Figure 35B.

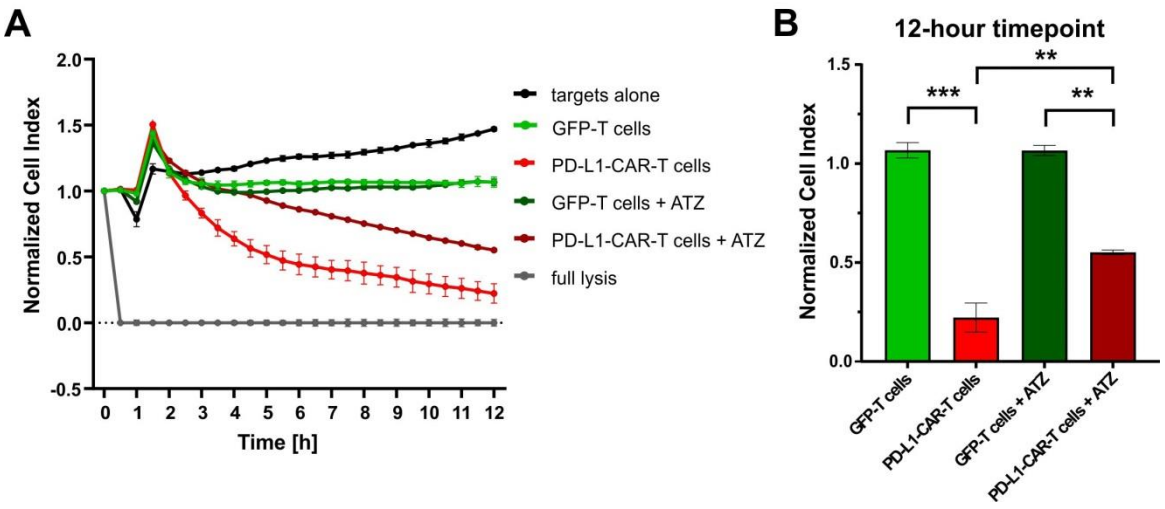

Figure 35 The killing potential of PD-L1-CAR-T cells and GFP-T cells against parental MDA-MB-231 cancer cells determined by impedance analysis. Cancer cell lines were seeded onto the plate and left to proliferate for 24 h. The next day, PD-L1-CAR-T cells or control GFP-T cells were added to the monolayers of target cancer cells at a 2:1 E:T ratio in the absence or presence of 0.4 mg/ml atezolizumab. The CAR-T cell-mediated killing was monitored for the next 12 hours. (A) Representative mean impedance curves from two wells are shown. (B) Normalized cell index for target cells in each group after 12 h co-incubation with the effectors. The experiment was repeated in duplicates two times and the results shown are representative of one experiment. The data are shown as means ± SD. Statistical analysis was performed by one-way ANOVA with Tukey's multiple comparisons test: ***p<0.001, **p<0.01.

Additionally, the RTCA assay was performed using MDA-MB-231-derived cell lines with different levels of PD-L1 expression. It was observed, that the cytotoxicity of PD-L1-CAR-T cells against the MDA-MB-231-sgPD-L1 cells was strongly diminished as compared to the MDA-MB-231-sgNTC controls (Figure 36A, red curves), while basal natural cytotoxicity of GFP-T cells was similar regardless of PD-L1 expression on targets (Figure 36A, green curves). The comparison of viable target cell amount in each group after 12 h of killing assay was depicted in Figure 36B.

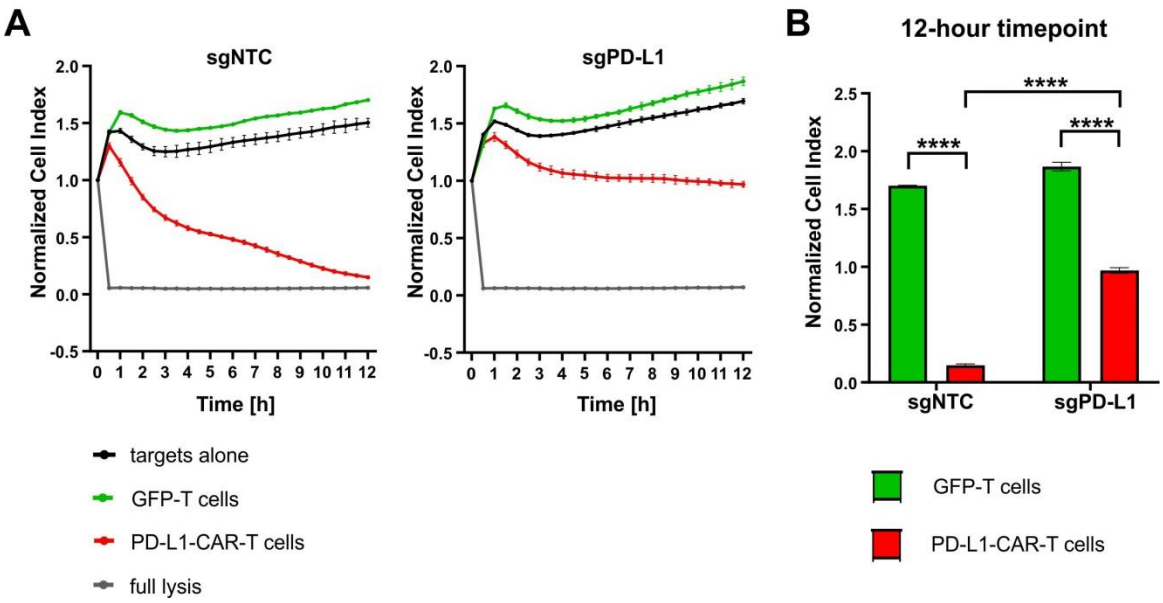

Figure 36 The killing potential of PD-L1-CAR-T cells against MDA-MB-231 sgNTC (PD-L1^{high}) and MDA-MB-231 sgPD-L1 (PD-L1^{low}) breast cancer cells determined by impedance analysis. Cancer cell lines were seeded onto the plate and left to proliferate for 24 h. The next day, PD-L1-CAR-T cells or control GFP T cells were added to the monolayers of target cancer cells at a 2:1 E:T ratio. The CAR-T cell-mediated killing was monitored for the next 12 hours. (A) Representative mean impedance curves from two wells are shown. (B) Normalized cell index for target cells in each group after 12 h co-incubation with the effectors. The experiment was repeated in duplicates two times and the results shown are representative of one experiment. The data are shown as means ± SD. Statistical analysis was performed by two-way ANOVA with Tukey's multiple comparisons test: ****p<0.0001.

Altogether, the obtained results suggest the ability of PD-L1-CAR-T cells to efficiently eliminate target MDA-MB-231 cells which have naturally high PD-L1 expression. Concomitantly, as it was observed that atezolizumab blockade of the PD-L1 protein or PD-L1 genetic knock-out inhibits PD-L1-CAR-T cells cytotoxic activity, the results confirm the ability of the modified effectors to recognize the target specifically.

4.4.3 PD-L1-CAR-T cells surprisingly exhibit cytotoxicity against target MCF-7 (PD-L1$^{low/null}$) cancer cells.

In order to directly evaluate the killing ability of PD-L1-CAR-T cells against MCF-7 cell lines, the effectors were incubated with luciferase-expressing targets for 18 h. Surprisingly, MCF-7 cells, which have initially low PD-L1 expression (MCF-7-PLVX and MCF-7-sgNTC), were killed with a similar potency as the MCF-7 cells engineered to

express exogenous PD-L1 molecule. Whereas, the killing of the MCF-7 cells with genetic PD-L1 knock-out was not observed (Figure 37, red bars).

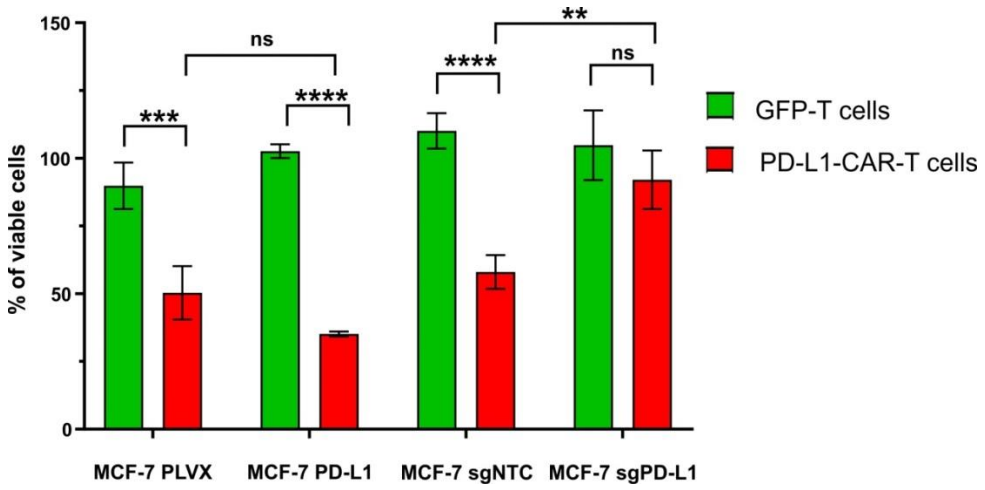

Figure 37 The killing potential of PD-L1-CAR-T cells and control GFP-modified T cells against breast cancer cells MCF-7-PLVX (PD-L1^{low}), MCF-7-PD-L1 (PD-L1^{high}), MCF-7-sgNTC (PD-L1^{low}), and MCF-7-sgPD-L1 (PD-L1^{null}) determined by luciferase-based killing assay. Cancer cell lines were seeded onto the plate and left to adhere. The next day, PD-L1-CAR-T cells and GFP-T cells were added to the target cells at a 2:1 E:T ratio. After 18 h of incubation, the cultures were lysed and the percentage of viable target cells was measured based on luminescence analysis. The assay was repeated twice in triplicates and the results shown are representative of one experiment. The data are shown as means ± SD. Statistical analysis was performed by two-way ANOVA with Tukey's multiple comparisons test: ****p<0.0001, ***p<0.001, **p<0.01, ns - statistically non-significant difference.

Additionally, to monitor PD-L1-CAR-T cell cytotoxic activity towards parental MCF-7 cancer cell lines in a real-time manner, the RTCA system was utilized. Control GFP-T cells exhibited negligible cytotoxicity against target MCF-7 cells (Figure 38A, light green curve). In contrast, parental MCF-7 cells (PD-L1$^{low/null}$ in steady-state, see Fig. 20B) were efficiently eliminated by PD-L1-CAR-T cells by the end of the 12 h co-incubation, however, a 4 – 6 h delay of the beginning of the killing was observed (Figure 38A, light red curve). The addition of atezolizumab, and therefore, the blockade of potential PD-L1 molecule on the target cell surface, resulted in impaired PD-L1-CAR-T cells cytotoxic activity towards MCF-7 cells (Figure 38A, dark red curve). The presence of atezolizumab did not affect the activity of the GFP-T cells towards cancer cells (Figure 38A, dark green curve). The comparison of viable target cell amount in each group after 12 h assay is depicted in Figure 38B.

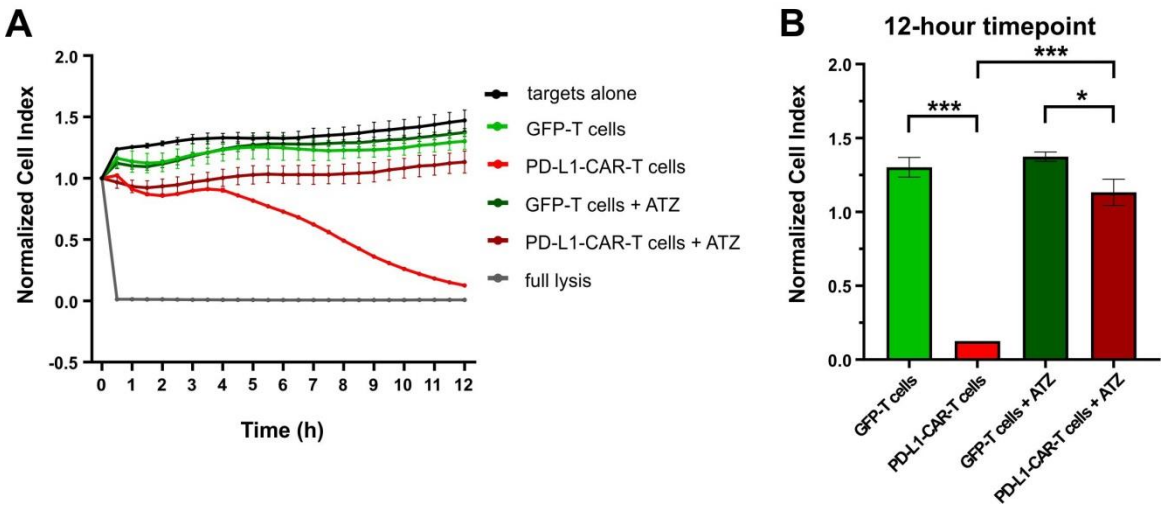

Figure 38 The killing potential of PD-L1-CAR-T cells against parental MCF-7 breast cancer cells measured by impedance analysis. The MCF-7 cancer cell line was seeded onto the plate and left to adhere. The next day, PD-L1-CAR-T cells or control GFP-T cells were added to the monolayers of MCF-7 cells at a 2:1 E:T ratio in the absence or presence of 0.4 mg/ml atezolizumab. The CAR-T cell-mediated killing was monitored for the next 12 hours. (A) Representative mean impedance curves from two wells are shown. (B) Normalized cell index for target cells in each group after 12 h co-incubation with the effectors. The experiment was repeated in duplicates two times results shown are representative of one experiment. The data are shown as means ± SD. Statistical analysis was performed by two-way ANOVA with Tukey's multiple comparisons test: ****p<0.0001, ***p<0.001, ns - statistically non-significant difference.

Next, the PD-L1-CAR-T cells were evaluated in RTCA assay against MCF-7-PD-L1 cells (PD-L1^{high}) versus MCF-7-PLVX control (PD-L1^{low}). It was observed, that PD-L1-CAR-T cells exhibit rapid and potent cytotoxic effect against MCF-7-PD-L1 cells, and also a delayed, but specific cytotoxicity against the MCF-7-PLVX controls (Figure 39A, red curves). The basal cytotoxicity of GFP-T cells exhibited a similar pattern regardless of initial PD-L1 expression level on targets (Figure 39A, green curves). The comparison of viable target cell amount in each group after 12 h of killing assay is depicted in Figure 39B.

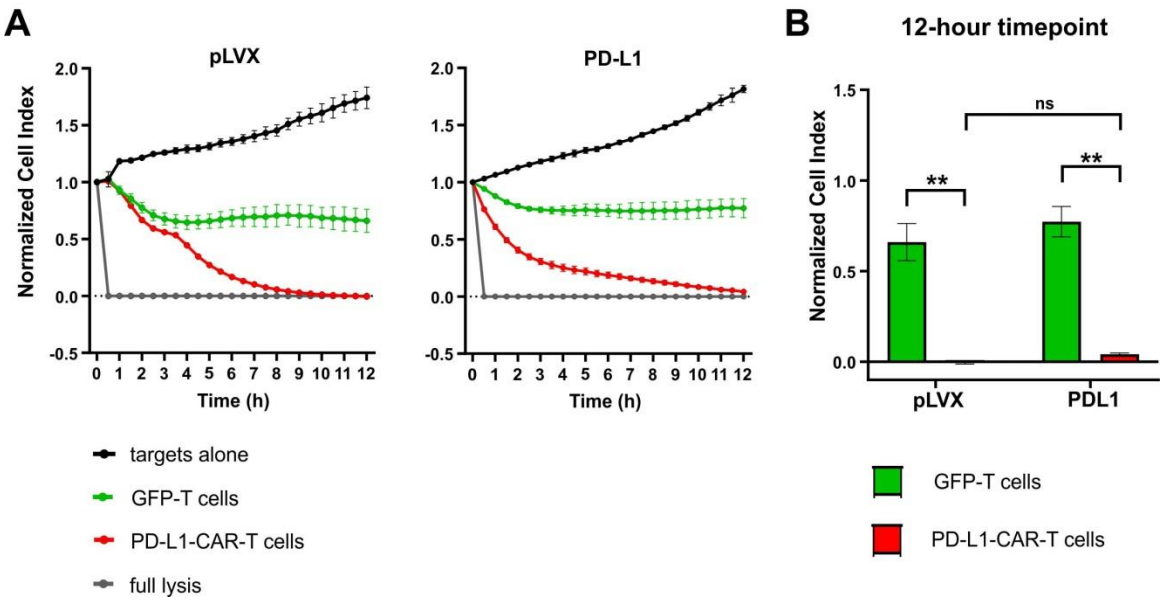

Figure 39 The killing potential of PD-L1-CAR-T cells against MCF-7-PLVX (PD-L1^{low}) and MCF-7 PD-L1 (PD-L1^{high}) breast cancer cells measured by impedance analysis. Cancer cell lines were seeded onto the plate and left to adhere. The next day, PD-L1-CAR-T cells or control GFP-T cells were added to the monolayers of target cancer cells at a 1:1 E:T ratio. The CAR-T cell-mediated killing was monitored for the next 12 hours. (A) Representative mean impedance curves from 2 wells are shown. (B) Normalized cell index for target cells in each group after 12 h coincubation with the effectors. The experiment was repeated in duplicates two times and the results shown are representative of one experiment. The data are shown as means ± SD. Statistical analysis was performed by two-way ANOVA with Tukey's multiple comparisons test: ****p<0.0001, ***p<0.001, ns - statistically non-significant difference.

The results confirm the specificity of the PD-L1-CAR construct, but suggest a possible induction of PD-L1 expression on the target MCF-7 cells during their longer incubation with the modified T cells, as this effect was not observed previously in the 4 h functional assay.

4.5 Investigation of the potential self-amplifying effect of the PD-L1-CAR

4.5.1 PD-L1-CAR-T cells may induce PD-L1 expression on MCF-7 cells by inflammatory cytokines secretion

To investigate, whether the PD-L1 protein can be upregulated on the surface of MCF-7 cells, the cells were treated with TNF-α and IFN-γ, as these cytokines were previously reported to influence the PD-L1 expression on several other cancer cells (172). It was observed, that IFN-γ alone induced PD-L1 expression on the surface of MCF-7 cells after

8 h of treatment (Figure 40, blue histograms), however, the effect was more potent and visible when IFN-γ was combined with TNF-α (Figure 40, orange histograms). The treatment with TNF-α alone did not affect the PD-L1 expression on the target cells regardless of the time of the treatment (Figure 40, green histograms).

Simultaneously, the potential ability of antigen-activated PD-L1-CAR-T to induce PD-L1 expression on the target cells was assessed. The conditioned supernatants collected from T cells and MDA-MB-231 co-cultures were transferred onto the MCF-7 cells. Once cells were incubated for 4 hours with the supernatant from activated PD-L1-CAR-T cells, the induction of the surface expression of PD-L1 on MCF-7 cells was observed. The percentage of PD-L1-positive cancer cells kept increasing with the prolongation of the treatment (Figure 40, red histograms). By contrast, the MCF-7 cells treated with the supernatants from unmodified T cells remained PD-L1-negative regardless of the incubation time (Figure 40, purple histograms).

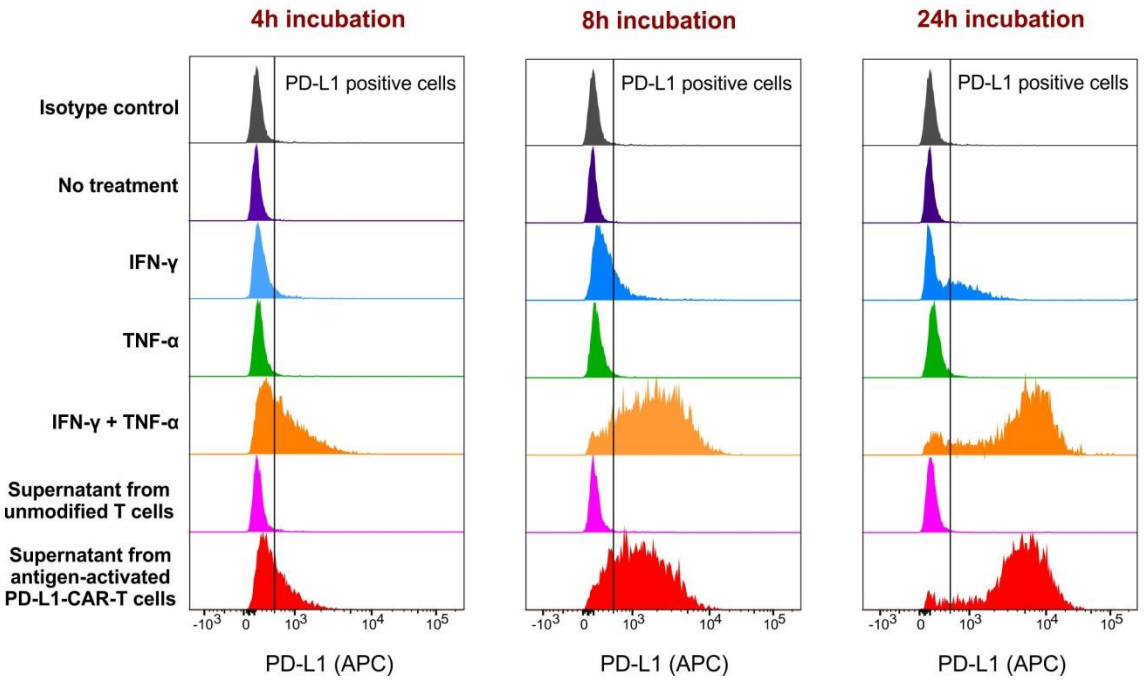

Figure 40 The PD-L1 expression on MCF-7 cells treated with either cytokines or the supernatant from activated PD-L1-CAR-T cells. MCF-7 cells were seeded onto culture plates and left to adhere for 24 h. Next, the cytokines were added to the culture medium, or the culture medium was exchanged for conditioned supernatants from the 24 h co-cultures of unmodified T cells or PD-L1-CAR-T cells with MDA-MB-231 cells. The PD-L1 expression was assessed by flow cytometry 4 h, 8 h, and 24 h after the incubation with either treatment. The staining was performed using an anti-PD-L1 antibody (clone MIH1, dilution 1:100). The experiment was repeated twice, and the representative data are shown.

Both the effect potency and the time-dependent dynamics of the PD-L1 expression induction were similar within the MCF-7 cells treated by either combination of TNF-α and IFN-γ cytokines or the supernatant from antigen-activated PD-L1-CAR-T cells. Thus, the results suggest, that the potential self-amplifying mechanism of PD-L1-CAR-T cells action may be conditioned by their cytokine production, which may have a stimulatory effect on the PD-L1 expression.

4.5.2 Antigen-activated PD-L1-CAR-T cells produced significantly increased amounts of cytokines and chemokines

In order to investigate, what other components contained in the supernatant from antigen-activated CAR-T cells may contribute to the PD-L1 induction in target cells, the supernatants from PD-L1-CAR-T cells were collected and analyzed following the incubation with MDA-MB-231 cells (PD-L1^{high}). The analysis was performed using an antibody array which allows to simultaneously detect the relative levels of several cytokines and chemokines. The results indicated that a set of proteins is produced by PD-L1-CAR-T cells in a higher amount than by unmodified T cells after 24 h co-culture with MDA-MB-231 cells (Figure 41A). The expression of 17 out of 36 analyzed proteins was significantly upregulated in PD-L1-CAR-T cells, with TNF-α and IFN-γ cytokines among them (Figure 41B).

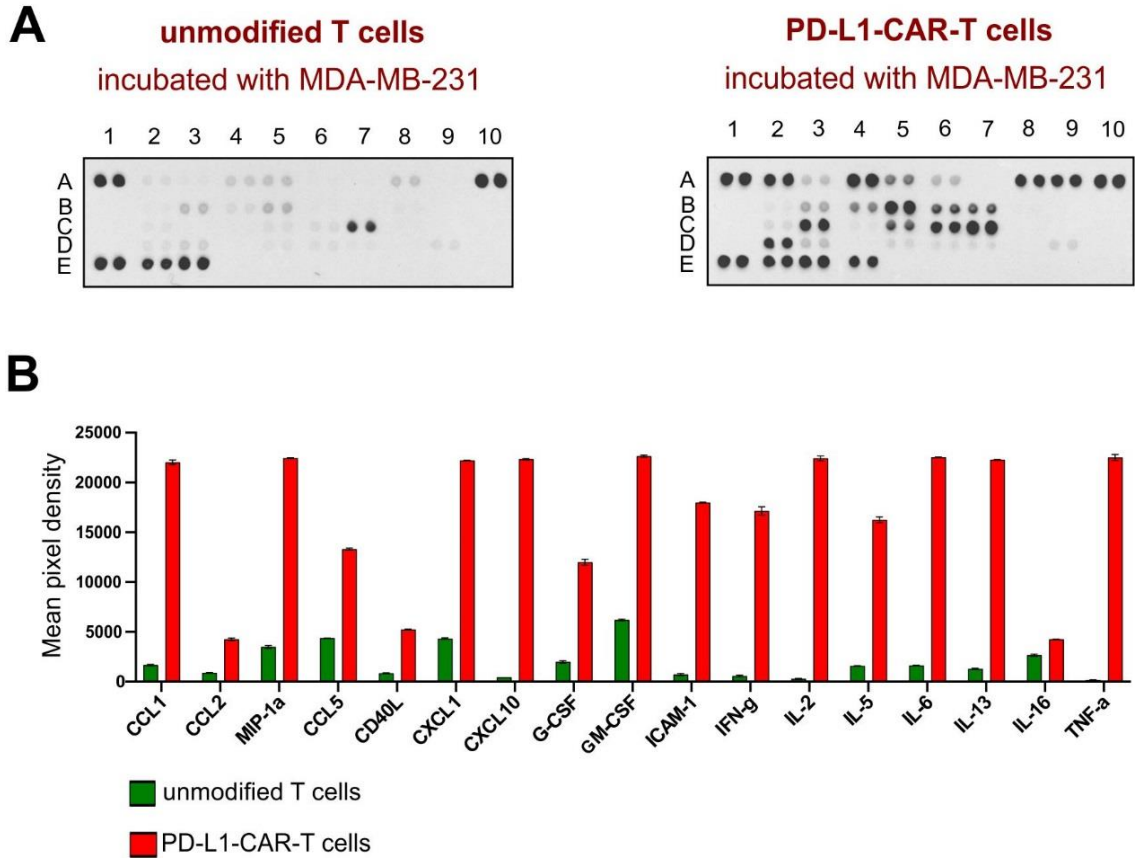

Figure 41 Evaluation of PD-L1-CAR-T cells cytokine production following antigen-mediated activation. The relative levels of human cytokines were assessed in supernatants collected from unmodified T cells or PD-L1-CAR-T cells co-cultured with MDA-MB-231 cells for 24 h at a 1:1 E:T ratio. (A) The cytokine array assay was performed (B) The significant changes of 17 out of 36 cytokines are presented. The experiment was repeated using T cells from two donors, each analyzed in duplicates. The representative data from one donor is shown. The data are shown as means ± SD.

Thus, the antigen-mediated activation of the T cells was followed by the increased cytokine production, which collectively may induce PD-L1 expression on cancer cells. Consequently, the initially PD-L1-negative target cells may become sensitive to the treatment with the PD-L1-CAR-T cells.

4.6 Evaluation of the PD-L1-CAR-T cells cytotoxicity against non-malignant cells

4.6.1 PD-L1-CAR-T cells exhibit cytotoxicity against non-malignant mammary cell lines which express PD-L1 protein

In order to assess the safety of the PD-L1-CAR in the breast cancer treatment, the T cells bearing the construct were targeted against non-malignant mammary cells: telomerase-

immortalized human mammary epithelial cells HMEC and spontaneously immortalized cell line MCF10A.

First, the PD-L1 expression in the HMEC and MCF10A cells was assessed. The flow cytometry analysis revealed that HMEC cells expressed a very low level of surface PD-L1, while approximately 40% of MCF10A cells were PD-L1-positive (Figure 42A). However, the Western blotting analysis has shown, that the PD-L1 protein was present in both mammary HMEC and MCF10A cells, but not in another non-malignant cell line HEK293T, which appeared to be PD-L1-negative and thus served as a negative control (Figure 42B).

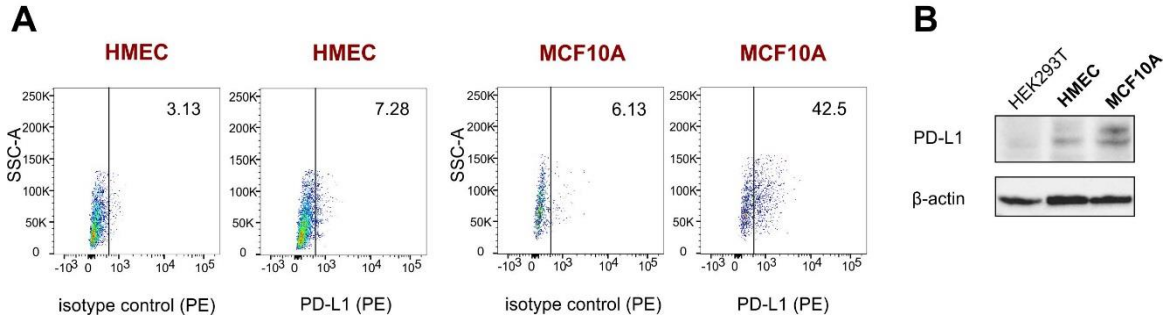

Figure 42 Evaluation of PD-L1 expression in non-malignant mammary cell lines. (A) Representative dot plots show surface PD-L1 expression evaluated by flow cytometry against a background from isotype control. The staining was performed using an anti-PD-L1 antibody (clone MIH1, dilution 1:100). Numbers on the plots indicate the percentage (%) of PD-L1 positive cells. The experiment was repeated three times. (B) Representative Western blotting shows the amount of PD-L1 protein in 20 µg of total protein lysates loaded onto the SDS-polyacrylamide gel and separated by electrophoresis in reducing conditions. The experiment was repeated three times.

The results suggest, that both non-malignant mammary cell lines exhibit PD-L1 expression, however, in the case of HMEC cells, the protein is located predominantly in the intracellular compartments.

Next, the RTCA assay was performed to directly assess the potential cytotoxicity of PD-L1-CAR-T cells against HMEC and MCF10A cells. The results showed, that both HMEC and MCF10A cells were eliminated by the CAR-T cells with a similar dynamic, regardless of their level of surface PD-L1 expression (Figure 43, light-red curves). Control GFP-T cells exhibited little to no cytotoxicity against both non-malignant mammary cells (Figure 43, light green curve). To confirm, that the PD-L1-CAR-T cells were specifically killing the target cells expressing the PD-L1 molecule, atezolizumab was added to block

the potential recognition of PD-L1 protein by the CAR scFv. The antibody presence resulted in the impaired cytotoxic activity of the CAR-T cells towards both HMEC and MCF10A cells (Figure 43, dark red curves). The presence of atezolizumab did not affect the activity of the GFP-T cells towards cancer cells (Figure 43, dark green curves).

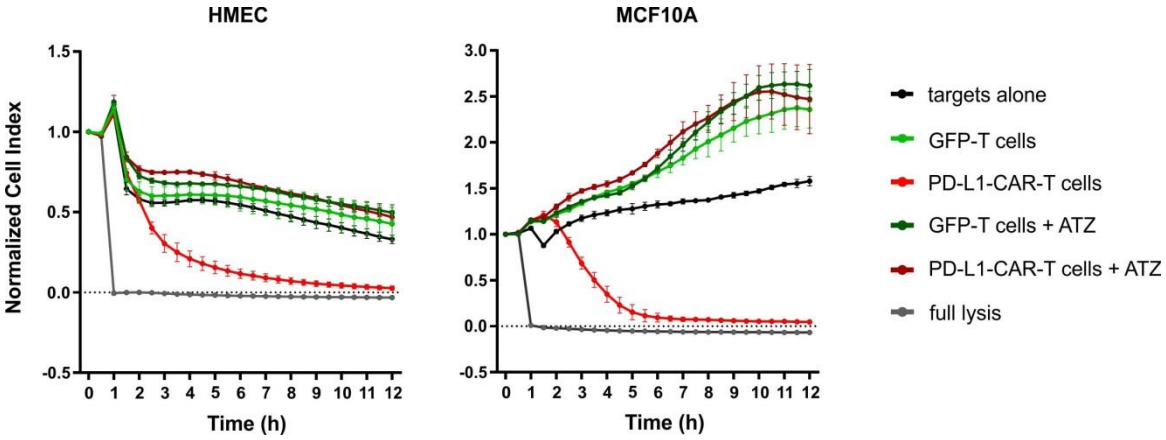

Figure 43 The killing potential of PD-L1-CAR-T cells against HMEC and MCF10A non-malignant breast cells measured by impedance analysis. Target cell lines were seeded onto the plate and left to proliferate for 24 h. The next day, PD-L1-CAR-T cells or control GFP-T cells were added to the monolayers of target cancer cells at a 2:1 E:T ratio. The CAR-T cell-mediated killing was monitored for the next 12 hours. Representative mean impedance curves from two wells are shown. The experiment was performed twice in duplicates and the results shown are representative of one experiment. The data are shown as means ± SD.

As the addition of atezolizumab and therefore PD-L1 blockade on target cells impaired PD-L1-CAR-T cells cytotoxicity towards HMEC cells, the results suggested that these non-malignant cells may upregulate the PD-L1 expression on their surface in response to the PD-L1-CAR self-amplification activity.

To further investigate, whether the PD-L1-CAR-T cell cytotoxicity towards HMEC cells may be conditioned by the self-amplifying effect of the effectors, both HMEC and MCF10A cells were incubated with the conditioned supernatants collected from T cells and MDA-MB-231 co-cultures. The PD-L1 expression on targets cells was analyzed by flow cytometry following 24 h treatment. It was observed, that not only HMEC cells upregulate the PD-L1 expression, but the percentage of PD-L1-positive MCF10A cells also increased in the presence of the supernatants from the antigen-activated PD-L1-CAR-T cells (Figure 44, red histograms). By contrast, the treatment with the supernatants from unmodified T cells had no impact on the PD-L1 steady-state expression level on both cell lines (Figure 44, purple histograms).

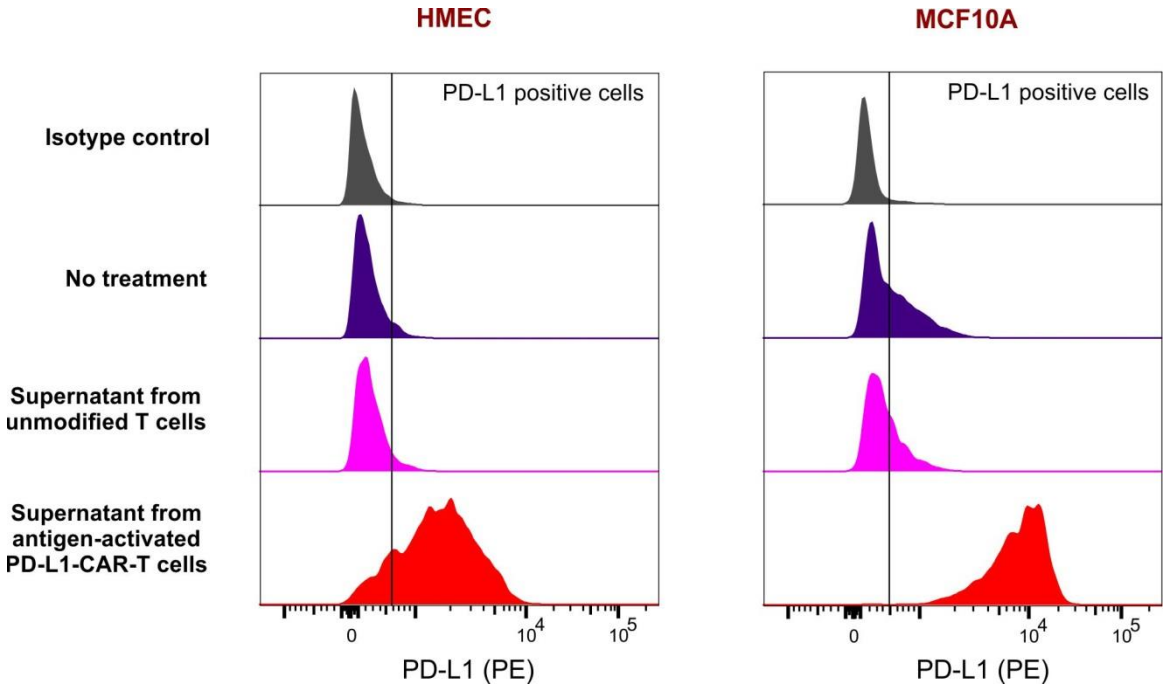

Figure 44 The PD-L1 expression on HMEC and MCF10A cells treated with the supernatant from activated PD-L1-CAR-T cells. HMEC and MCF10A cells were seeded onto culture plates and left to adhere for 24 h. Next, the culture medium was exchanged for conditioned supernatants from the 24 h co-cultures of either unmodified T cells or PD-L1-CAR-T cells with MDA-MB-231 cells. The PD-L1 expression was assessed by flow cytometry 24 h after the incubation with the treatment. The staining was performed using an anti-PD-L1 antibody (clone MIH1, dilution 1:100). The experiment was repeated twice and the representative data are shown.

The results support previous observation on MCF-7 cells, and therefore the hypothesis of the possible self-amplification mechanism of PD-L1-CAR-T cells. Notwithstanding, the results indicate the risk of a potential on-target/off-tumor cytotoxicity of PD-L1-CAR-T cells towards non-malignant mammary cells expressing PD-L1 either in steady-state or following the induction.

4.6.2 Non-malignant HEK293T cells do not upregulate PD-L1 expression and are resistant to treatment with PD-L1-CAR-T

The evaluation of PD-L1 expression in various non-malignant cell lines indicated that HEK293T cells express the protein neither on their surface (Figure 45), nor in the intracellular compartments (Figure 42B).

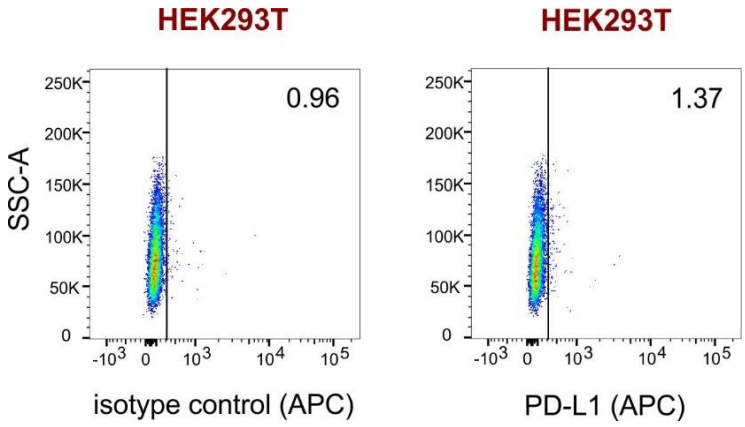

Figure 45 Evaluation of PD-L1 expression in non-malignant cell line HEK293T. Representative dot plots show surface PD-L1 expression evaluated by flow cytometry against a background from isotype control. The staining was performed using an anti-PD-L1 antibody (clone MIH1, dilution 1:100). Numbers on the plots indicate the percentage (%) of PD-L1 positive cells. The staining was repeated three times.

As it was previously observed, that initially PD-L1-negative MCF-7 cells can upregulate PD-L1 expression on their surface under certain conditions (Figure 39), the ability of HEK293T cells to express PD-L1 following the treatment with TNF-α and IFN-γ cytokines or the supernatant from antigen-activated PD-L1-CAR-T cells was also analyzed (Figure 46).

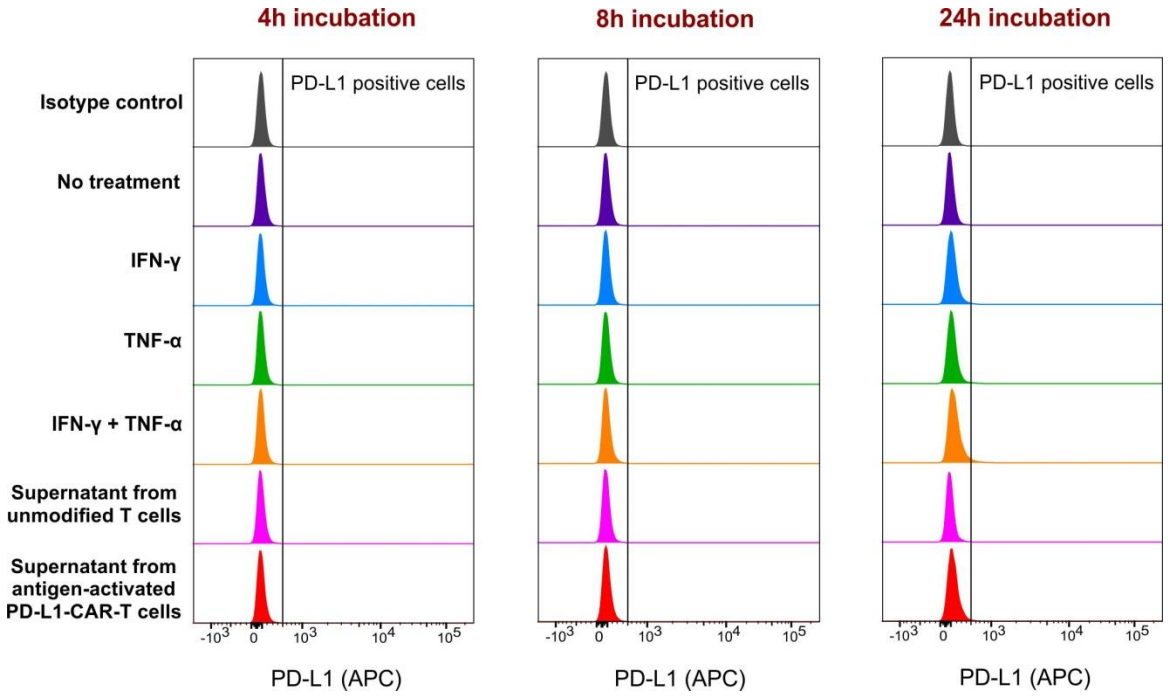

Figure 46 The PD-L1 expression on HEK293T cells treated with either cytokines or the supernatant from activated PD-L1-CAR-T cells. HEK293T cells were seeded onto culture plates and left to adhere for 24 h. Next, the cytokines were added to the culture medium, or the culture medium was exchanged for conditioned supernatants from the 24 h co-cultures of unmodified T cells or PD-L1-CAR-T cells with MDA-MB-231 cells. The PD-L1 expression was assessed by flow cytometry 4 h, 8 h, and 24 h after the incubation with either treatment. The staining was performed using an anti-PD-L1 antibody (clone MIH1, dilution 1:100). The experiment was repeated twice, and the representative data are shown.

The results show, that, unlike MCF-7 cells, the HEK293T cells remain PD-L1-negative regardless of the treatment conditions, making them potentially resistant to the PD-L1-CAR-T cells cytotoxicity.

In order to investigate, whether the non-malignant cells that lack PD-L1 expression, either steady-state or induced, may still be targeted by PD-L1-CAR-T cells, the HEK293T cells were used as target cells in the luciferase-based cytotoxicity assay. For this purpose, the HEK293T cells were modified by lentiviral transduction to express luciferase (Figure 47).

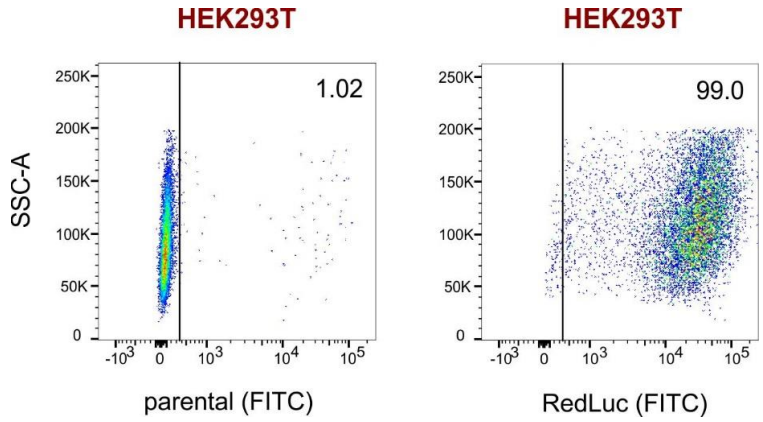

Figure 47 Evaluation of HEK293T transduction efficiency with pLenti7.3-redluc plasmid. The GFP expression in target cell lines was evaluated by flow cytometry. Numbers on the plots indicate the percentage (%) of GFP positive HEK293T cells transduced with pLenti7.3-redluc plasmid. The RedLuc expression level in transduced cells was verified prior to an experiment.

Next, the cytotoxic activity of PD-L1-CAR-T cells against HEK293T cells was evaluated in a luciferase-based killing assay. The results presented that HEK293T cells remained almost completely resistant to the treatment with PD-L1-CAR-T cells, even when E:T ratio was as high as 5:1 (Figure 48, red bars). Control GFP-T cells had similar to the CAR-T cell effect on the HEK293T cells viability in the assay (Figure 48, green bars).

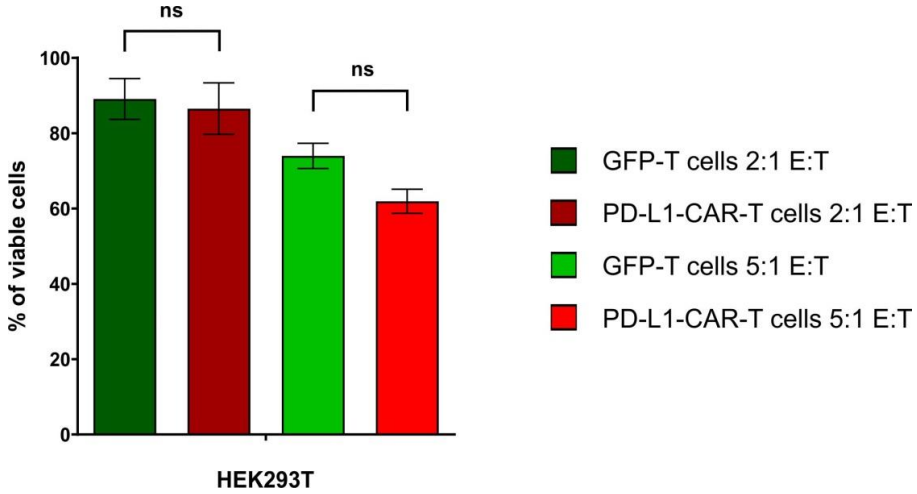

Figure 48 The killing potential of PD-L1-CAR-T cells and control GFP-modified T cells against HEK293T determined by luciferase-based killing assay. Target cell lines were seeded onto the plate and left to adhere. The next day, PD-L1-CAR-T cells and GFP-T cells were added to the target cells at a 2:1 and a 5:1 E:T ratios. After 18 h of incubation, the cultures were lysed, and the percentage of viable target cells was measured based on luminescence analysis. The assay was repeated twice in triplicates and the results shown are representative of one experiment. The data are shown as means ± SD. Statistical analysis was performed by unpaired T-test: ns - statistically non-significant difference.

In order to verify, whether HEK293T may be in general resistant to the T-cell mediated cytotoxicity, the luciferase-expressing cell line was additionally modified by lentiviral transduction to overexpress PD-L1 molecule (Figure 49).

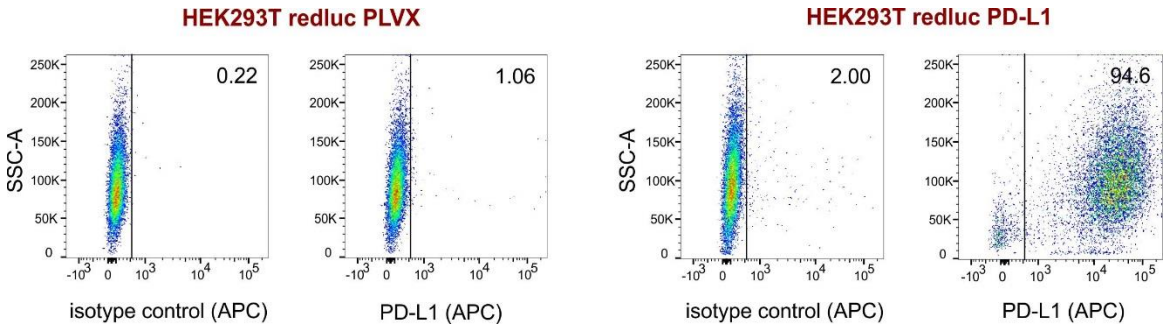

Figure 49 Evaluation of PD-L1 expression in PD-L1-overexpressing derivative of HEK293T cell line. Representative dot plots show surface PD-L1 expression evaluated by flow cytometry against a background from isotype control. The staining was performed using an anti-PD-L1 antibody (clone MIH1, dilution 1:100). Numbers on the plots indicate the percentage (%) of PD-L1 positive cells. The PD-L1 expression level in transduced cells was verified prior to an experiment.

Next, the cytotoxic activity of PD-L1-CAR-T cells against generated HEK293T PLVX and HEK293T PD-L1 cells was compared in a luciferase-based killing assay. It was observed, that artificially introduced PD-L1 into HEK293T cells resulted in their E:T ratio-dependent sensitivity to the PD-L1-CAR-T cells cytotoxicity (Figure 50, dark red and light red bars). Control GFP-T cells exhibited little to no effect on HEK293T cell viability, regardless of PD-L1 expression on the targets (Figure 50, dark green and light green bars).

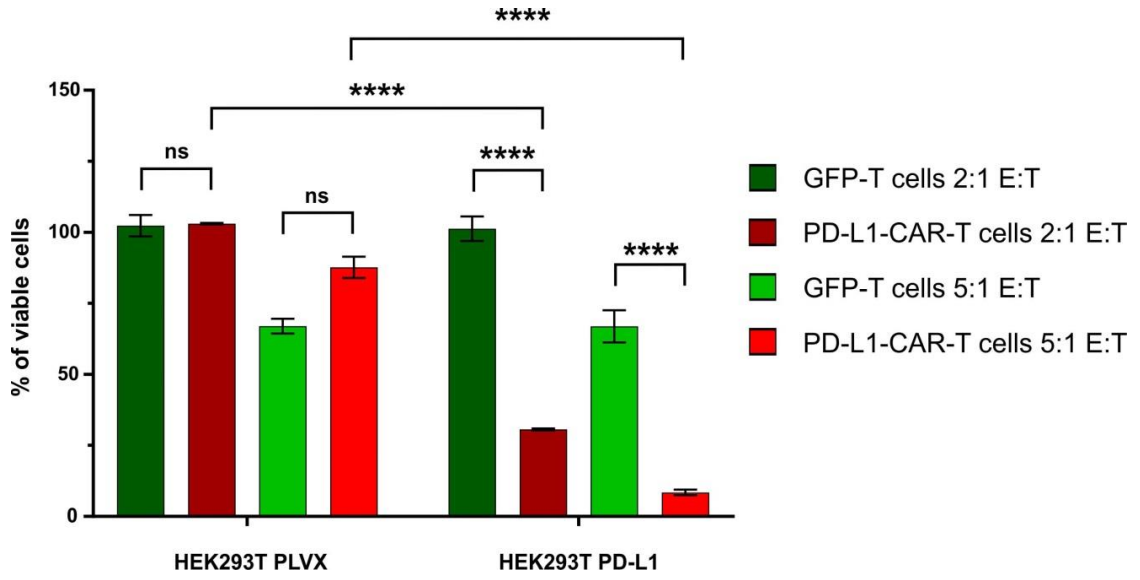

Figure 50 The killing potential of PD-L1-CAR-T cells and control GFP-modified T cells against HEK293T PLVX cells (PD-L1^{null}) and HEK293T PD-L1 (PD-L1^{high}) cells determined by luciferase-based killing assay. Target cell lines were seeded onto the plate and left to adhere. The next day, PD-L1-CAR-T cells and GFP-T cells were added to the target cells at a 2:1 and a 5:1 E:T ratios. After 18 h of incubation, the cultures were lysed, and the percentage of viable target cells was measured based on luminescence analysis. The assay was repeated twice in triplicates and the results shown are representative of one experiment. The data are shown as means ± SD. Statistical analysis was performed by two-way ANOVA with Tukey's multiple comparisons test: ****p<0.0001, ns - statistically non-significant difference.

The results suggested, that non-malignant cells HEK293T, which do not exhibit PD-L1 expression, neither steady-state nor induced, may be resistant to the treatment with PD-L1-CAR-T cells.

5. DISCUSSION

The CAR-T cell-based therapy has still limited success in solid tumor treatment due to several challenges. One of them is finding a suitable target molecule for the CAR construct. Unlike B cell-derived hematological cancers, in which the tumor cells almost universally express CD19 marker, solid tumors rarely express on their surface one tumor- or tissue-specific antigen. It is more common to find a tumor-associated antigen (TAA) that is overexpressed on tumors as compared to normal tissues (173). PD-L1 molecule can be considered such an antigen, as its increased expression is found, among others, in breast cancer, lung cancer, colorectal cancer, gastric cancer, bladder cancer, pancreatic cancer, prostate cancer, and DLBCL (174). Moreover, present in TME immune cells as well as cancer-associated fibroblasts (CAFs), which are an important component of the tumor stroma, also express PD-L1 (80). Additionally, increased PD-L1 expression on cancer cells leads to increased inhibition of T cell activity and subsequent tumor survival (175). Altogether, the listed characteristics of PD-L1 molecule make it an attractive target for CAR-based therapy and thus, this approach was evaluated within the presented project.

5.1 Targeting PD-L1 molecule in breast cancer treatment

Within this study, the anticancer efficacy of the PD-L1 targeting CAR was evaluated using breast cancer cells as a model. The analysis of PD-L1 mRNA expression in 45 breast cancer cell lines and 5,454 breast cancers showed, that the molecule was upregulated in 20% of 5,454 breast cancers and 38% of 1,205 basal tumors (176). The evaluation of PD-L1 protein expression in six breast cancer cell lines performed within this study demonstrated, that triple-negative MDA-MB-231 cells exhibited the highest PD-L1 protein level as compared to other analyzed cell lines (Figure 18). The results confirmed the earlier reported observations, in which, PD-L1 expression was found to be increased in 20% of breast tumors lacking expression of estrogen receptor, progesterone receptor and HER2/neu (HER2) indicating PD-L1 as a relevant therapeutic target in TNBC (144). TNBCs are generally aggressive tumors with a high rate of metastasis and poorer prognosis than other breast cancer subtypes. TNBC patients are usually treated with cytotoxic chemotherapy, as endocrine therapy or anti-HER2 antibody trastuzumab is

ineffective in their case. However, systemic treatment with chemotherapy often results in early relapse and metastasis. Moreover, a recent study has shown that treatment of human or murine TNBC cells with currently applied chemotherapeutic drugs affects the transcriptional induction of PD-L1 mRNA and protein expression, leading to a marked increase in the percentage of PD-L1+ breast cancer cells (177). The hypothesis of the unstable PD-L1 phenotype of these tumors was additionally supported by the studies that evaluated PD-L1 gene and protein expression in both cancer and immune cells in TNBC. It was found, that there was no correlation between the number of PD-L1 gene copy number and the level of PD-L1 protein expression, which suggests that PD-L1 expression on breast tumors is rather induced by exogenous factors, such as IFN-γ released by activated T- or NK cells entering the initially PD-L1-negative tumor site (178). Moreover, PD-L1 was found to be upregulated not only on breast cancer cells, but also on the TILs in the tumor microenvironment, and whilst the first phenotype is rather associated with unfavorable prognosis for the patient, the PD-L1 expression on the immune cells may be related to a better survival (179,180).

Thus, targeting PD-L1 molecule can be a reasonable alternative in TNBC treatment. The recently obtained results of the IMpassion130 trial support the feasibility of such an approach. The study, where nab-paclitaxel and anti-PD-L1 antibody atezolizumab were combined in the metastatic TNBC treatment, demonstrated the prolonged progression-free survival in patients, especially those with PD-L1-positive phenotype (181). Additionally, as numerous reports revealed that TNBCs are immunogenic and the presence of TILs is associated with better patients' clinical outcomes (182), CAR-T therapy, being a combination of the adoptive cells transfer and targeted therapy, is a promising tool in the treatment of TNBC specifically.

5.2 Targeting PD-L1 molecule using CAR-based approach

Following the modification, CAR-T cells are cultured and expanded *in vitro* prior to their reinfusion into a patient. It is known, that T cells are capable of fratricide killing, which in normal conditions serves as a mechanism to maintain T cell homeostasis (183). In the case of CAR-T cells production, this ability may be especially concerning in circumstances where the target antigen is constitutively or transiently expressed on a T cell (184). The

issue was addressed within this study, therefore, the PD-L1 protein expression was evaluated on primary human T cells. The results revealed that stimulation via CD3/CD28 receptors upregulates PD-L1 on the T cells, posing the risk of the fratricidal killing between the T cells bearing PD-L1-CAR construct (Figure 28). However, further analysis has shown, that even though the T cells expressing PD-L1 may be eliminated from the culture of PD-L1-CAR-T cells, the fratricide is transient and induces the disappearance of the antigen from the PD-L1-CAR-T cells in contrast to unmodified T cells (Figure 30). Additionally, the possibility of the PD-L1 antigen masking by the presence of PD-L1-CAR molecule was excluded by the evaluation of the total PD-L1 protein amount in the analyzed T cells (Figure 31). These results suggest, that the population of resistant PD-L1-negative T cells is selected, and these cells can be expanded *in vitro*. Notably, PD-L1 was previously reported to be expressed on cytotoxic T cells from melanoma patients, and the level of PD-L1+ CD8+ cells was strongly correlated with a number of markers associated with a negative impact on disease outcome, such as high levels of circulating MDSCs and decreased levels of plasmacytoid DCsPMID: 25592374 (185). Additionally, recent studies have demonstrated, that PD-L1 was upregulated on T cells in response to antigen-presentation in a model of pancreatic adenocarcinoma cancer, and PD-L1 ligation on T cells induces intracellular signaling that is equally suppressive to that of PD-1. Moreover, in a murine model, conditional deletion of PD-L1 in T cells improved their adaptive tumor immunity (186). Thus, the elimination of the PD-L1+ T cells in the process of PD-L1-CAR-T cells production may be beneficial for the anticancer efficacy of the modified effectors. In this study, the results obtained from functional and cytotoxicity assays confirm the unaffected ability of the PD-L1-negative PD-L1-CAR-T cells to degranulate, produce cytokines, and kill target cancer cells.

Importantly, the specificity of the PD-L1-CAR-T cells was also confirmed. The results have shown, that PD-L1-CAR-T cells degranulation in a 4 hour-long assay was strongly conditioned by the steady-state PD-L1 presence on the target cells, as PD-L1-CAR-T cells exhibited a response towards MDA-MB-231 cells (PD-L1^{high}), but not MCF-7 cells (PD-L1^{low}) (Figure 32). Additionally, the genetic knock-out of PD-L1 in MDA-MB-231 cells led to a loss of their ability to provoke degranulation of the effectors, which excludes the possibility of their sensitivity to PD-L1-CAR-T cells due to other factors.

Similarly, the natural resistance of MCF-7 cells was excluded, as their genetic modification to overexpress PD-L1 led to PD-L1-CAR-T cells response comparable to the response to MDA-MB-231 cells with naturally high target molecule expression (Figure 33). The results of the cytotoxicity assays performed using MDA-MB-231 cells also show the effectiveness and specificity of PD-L1-CAR-T cells in the elimination of cancer cells expressing PD-L1. It was observed, that both genetic PD-L1 knock-out (Figure 34, Figure 36) and PD-L1 blockade with atezolizumab (Figure 35) reversed otherwise potent PD-L1-CAR-T cells cytotoxicity against MDA-MB-231 cells.

Surprisingly, initially, PD-L1^{low} MCF-7 cells appeared to be sensitive to the treatment with PD-L1-CAR-T cells in a prolonged co-incubation of the targets with the effectors. The evidence of the decreased effector cytotoxicity observed following genetic PD-L1 knock-out in MCF-7 cells (Figure 37) or PD-L1 blockade on the targets with atezolizumab (Figure 38) suggested, that killing was conditioned by the presence of the target protein on MCF-7 cells or the induction of its expression. This hypothesis was supported by the observation of the killing dynamics in real-time, as the MCF-7 PLVX cells were eliminated by PD-L1-CAR-T cells with 4-6 h delay as compared to MCF-7 PD-L1 cells (Figure 39). It has been earlier reported, that PD-L1 expression can be regulated in cancer cells by signaling pathways, transcriptional factors, and epigenetic factors (187). Several proinflammatory agents, including IFN-γ, were shown to upregulate PD-L1 on various cancer cells (188). Thus, in order to investigate, whether MCF-7 cells, in general, are able to induce PD-L1 expression on their surface, the cells were treated with proinflammatory cytokines. Indeed, it was observed, that already 4 h treatment with a combination of IFN-γ and TNF-α resulted in a potent increase of PD-L1+ MCF-7 cells, which was in agreement with the killing dynamics observed in the RTCA assay (Figure 39). Most cytotoxic T cells are known to release IFN-γ and TNF-α (189), thus, the target cancer cells were also treated with the supernatants from antigen-activated CAR-T cells, and the effect of this treatment was even more significant when compared to the treatment with proinflammatory cytokines (Figure 40). The presence of the cytokines in the supernatants was confirmed, moreover, the results suggest that several other factors may contribute to the observed effect of the PD-L1 induction (Figure 41). Among the cytokines that were observed to be upregulated in the supernatants from activated

CAR-T using the cytokine array, for example, IL-6 was previously reported to increase PD-L1 expression on APCs (190) PMID: 21268011 and GM-CSF, on immature DCs (191) PMID: 12538684. Thus, massive PD-L1 induction on MCF-7 cells, which are PD-L1^{low} in steady-state, is a consequence of antigen-specific CAR activation and subsequent release of cytokines from CAR-T cells.

The observed effects of PD-L1-CAR-T cells on MCF-7 cells suggest, that the PD-L1-CAR construct may have a self-amplifying mechanism of action, which might have both positive and negative consequences. PD-L1-CAR-T cells may be effective not only in the elimination of breast cancer cells, regardless of their initial PD-L1 expression level, but as well eliminating other immunosuppressive cellular elements of the tumor microenvironment. For example, tumor-associated macrophages, which are the most prominent component of the breast cancer microenvironment (192), were shown to be able to upregulate PD-L1 expression following the treatment with IFN-γ (193). The recent studies also demonstrate, that dendritic cells represent a crucial source of PD-L1 in the TME, as PD-L1 deletion in DCs, but not more numerously presented macrophages, greatly restricted tumor growth and led to enhanced antitumor CD8+ T-cell responses (194). Additionally, PD-L1 expression on DCs can be as well upregulated by IFN-γ and T cells presence in general (195). Thus, this unique self-amplifying ability of the PD-L1-CAR-T cells would broaden their cytotoxic reaction towards the tumor stroma cells adjacent to the malignant cells, even if the stromal cells were initially PD-L1^{low}.

However, the self-amplification phenomenon of the PD-L1-CAR poses an even higher necessity to address the safety issues of this strategy. Especially considering the fact that the clinical trial conducted to evaluate PD-L1-CAR-T cells in patients with advanced lung cancer (NCT03330834) had to be terminated due to the serious adverse effects caused by the treatment. It is known, that vital organs such as lungs, spleen, and heart constitutively express PD-L1 protein (https://www.proteinatlas.org/) and thus can be severely damaged. Moreover, the potential ability of PD-L1-CAR-T cells to induce PD-L1 expression on various other cells and to further attack them makes the scale of the toxicity difficult to predict. Among all the parental cell lines evaluated in this study, only HEK293T cell line was resistant to the PD-L1-CAR-mediated toxicity, despite even an increased E:T ratio (Figure 48). HEK293T cells were PD-L1^{null} initially (Figure 45) and,

unlike MCF-7 cells, remained refractory to the induction of PD-L1 expression either by cytokines or supernatants derived from antigen-activated PD-L1-CAR-T cells (Figure 46). Interestingly, the genetic modification of HEK293T cells to overexpress PD-L1 (Figure 49) resulted in their sensitivity to the treatment with PD-L1-CAR-T cells (Figure 50). This observation excludes the possible resistance of HEK293T to cell-mediated cytotoxicity in general and suggests that this non-malignant cell line can be an interesting model to study in the future. However, the results obtained using non-malignant mammary cells indicate, that other non-transformed cells surrounding the tumor may have low basal PD-L1 expression (Figure 42) and additionally upregulated its expression in response to the molecules secreted by activated PD-L1-CAR-T cells (Figure 44), thus becoming targets for the CAR-T cell cytotoxicity (Figure 43).

5.2.1 Reported studies of the PD-L1-CAR-based treatment

Since 2018, several other research groups have published the results of their research evaluating the PD-L1-CAR-based approach. The effectiveness of the PD-L1-CAR-T cells was proved against human bronchioalveolar carcinoma cells (196), human non-small cell lung cancer and pancreatic cancer (197,198) and human leukemia and colorectal cancer cells (199,200). Additionally, two bispecific CAR constructs targeting PD-L1 as one of the antigens were shown to have a superior cytotoxic effect as compared to monovalent CAR-T cells. Dual CAR-T cells targeting PD-L1 and MUC16 antigens were demonstrated to efficiently eliminate ovarian cancer cells *in vitro* and to prolong the survival time of tumor-bearing mice *in vivo* (201). Whereas, bispecific CAR-T cells targeting PD-L1 and hepatocyte growth factor receptor (c-Met) were reported to have an improved cytotoxic effect against human hepatocellular carcinoma (202). In these studies, CAR-T cells targeting PD-L1 molecule were evaluated *in vitro* and *in vivo* in xenograft models. The mice used for the xenograft models establishment lack B and T cells, and also have other severe immune deficiencies in order to prevent tumor rejection (203). However, the defective immune cell populations of the animals as well prevent the CRS development, which is the major adverse effect caused by CAR-T cells applied in clinics (204). Thus, the issue of the toxicity of the PD-L1-CAR-based approach was not addressed directly.

In another study published in 2020, the PD-L1-CAR construct was used to modify irradiated human NK cells, which were then able to efficiently eliminate both human and mouse head and neck squamous cell carcinoma (HNSCC) cells. The approach was as well demonstrated to be effective in the treatment of immune-competent mice bearing syngeneic tumors, and lead to the rejection of the tumor or its growth delay**.** The use of the wild-type mice allowed to partially evaluate the ability of the PD-L1-CAR-bearing effector cells to eliminate the immune cells present in TME, such as macrophages and neutrophilic and monocytic myeloid cells**.** It was observed, that these cells, which endogenously expressed high levels of PD-L1, were eliminated not only in TME but also in the periphery. Nevertheless, any severe side effects were not observed in this study (205). Similarly, in the study with syngeneic models of aggressive melanoma, where murine PD-L1-CAR-T cells increased survival and decreased tumor growth, only moderate immunogenicity was noted (206). However, the lack of severe toxicity even in syngeneic mouse models cannot be interpreted as a possible outcome of the human patient treatment due to the differences in human and mouse biology, as well as in target and CAR sequences (207).

Currently, the HER-2/PD-L1 dual-targeting CAR-T cells are evaluated in patients with HER2 positive solid tumor serosal cavity metastases (NCT04684459). The early phase I of the study started in March 2021, and so far (in January 2022) neither the details of the study nor the primary results have been published yet. Thus, it is unclear what strategy was applied to overcome the possible severe side effects of the therapy, including the risk of damaging non-malignant tissues due to the self-amplifying mechanism of PD-L1-CAR-T cells action that was reported in the presented project.

5.2.2 Further improvement of the safety of PD-L1-CAR-based therapy

As mentioned above, the lack of antigens that are highly specific for tumor cells is one of the major challenges in solid cancer treatment with CAR-T cells. Thus, even the low-level expression of target antigens in non-malignant tissues often results in CAR-T cell “on-target/off-tumor” toxicity. A fatal example of this was the case of the patient treated with CAR-T cells specific for the cancer-associated antigen HER2, where the treatment led to rapid respiratory failure and multi-organ dysfunction, resulting in the death of the

patient (208). It is important to mention, that even though the majority of CAR-T cells, including PD-L1-CAR-T cells used in this study, recognize antigen through scFv derived from monoclonal antibodies, the toxicity profile of CAR-T cells and a particular corresponding mAb may not be identical. Such a conclusion was made based on the comparison of anti-HER2 mAb trastuzumab with HER2-CAR-T cells (208,209). Thus, even though the mAb atezolizumab, which is a base for scFv of the PD-L1-CAR evaluated in this study, was approved by FDA for PD-L1 positive unresectable TNBC in 2019 (210), the optimizations increasing the safety of the PD-L1-CAR-T cells need to be considered.

The studies of the CAR-T therapies for solid tumors revealed that both chosen method of T cell modification and the method of CAR-T cell administration into the patient may have a significant impact on the therapy outcome. For example, despite the initial concerns, HER2-CAR-T cell therapy was proven safe at significantly lower CAR T-cell doses (211). To even further reduce off-target toxicity, the T cells may be engineered with transient CAR expression by using *in vitro* transcribed mRNA encoding a CAR. The method was evaluated in a study using CAR-T cells targeting mesothelin, and a positive clinical effect without evidence of off-tumor toxicity was demonstrated in two out of eighteen patients (212). The PD-L1-CAR may also be introduced into primary T cells via mRNA electroporation, and the construct expression may be thus limited to 48 h post-modification (Figure 24). Additionally, CAR-T cells may be administered by direct intra-tumoral injection to boost their infiltration and safety (213). For example, treating metastatic breast cancer with intra-tumoral administration of mRNA-transfected c-Met-CAR T cells in a phase 0 clinical trial (NCT01837602) resulted in extensive tumor necrosis at the injection site, while none of the six patients had drug-related adverse effects greater than grade 1 (214).

The more advanced technique of CAR expression control is based on using the tetracycline regulatory system, which may be incorporated into a CAR construct. Inducible CD19-CARs were evaluated in a few studies, where introduced into the construct tetracycline regulation system was supposed to be activated only in the presence of doxycycline. The obtained results demonstrated the promising potential of this approach, as in both studies the CAR expression significantly decreased after doxycycline removal, while in the drug presence CD19-CAR-T cells with a tetracycline

system exhibited unaltered cytotoxicity and cytokine production both *in vitro* and *in vivo* (215,216). Recently, the same approach was used in an attempt to improve the safety of the CAR-T cells targeting CD38 molecule, and the results also indicated increased safety of the therapy (217). Moreover, the *iCasp9*-system, which enables the conditional elimination of gene-modified cells, can also be tested, however, the recently conducted clinical trial demonstrated that this approach may still not protect the patient from the delayed CRS development (218).

Another way to address the issue of "on-target/off-tumor" cytotoxicity of CAR-T cells is engineering chimeric receptors that require a signal from combinatorial antigens to activate the T cell, meaning that only the tumor cells that co-express more than one TAA would be attacked. One of the solutions proposed in 2013 was based on the physical separation of two signaling domains: the CD3ζ and CD28 signals were assembled into separate CAR constructs individually targeting two different antigens. The trans-signaling CAR-T cells exhibited low activation against the cells expressing only one of the targeted proteins, which were mesothelin and folate receptor α (FRα), but demonstrated potent functional response encountering epithelial ovarian tumor cells co-expressing both antigens (219). The more recent approach is based on using a synthetic Notch receptor (synNotch), which recognizes one antigen and then induces the expression of a CAR targeting the second antigen (220). The mechanism of the synNotch receptor action is schematically presented in Figure 51.

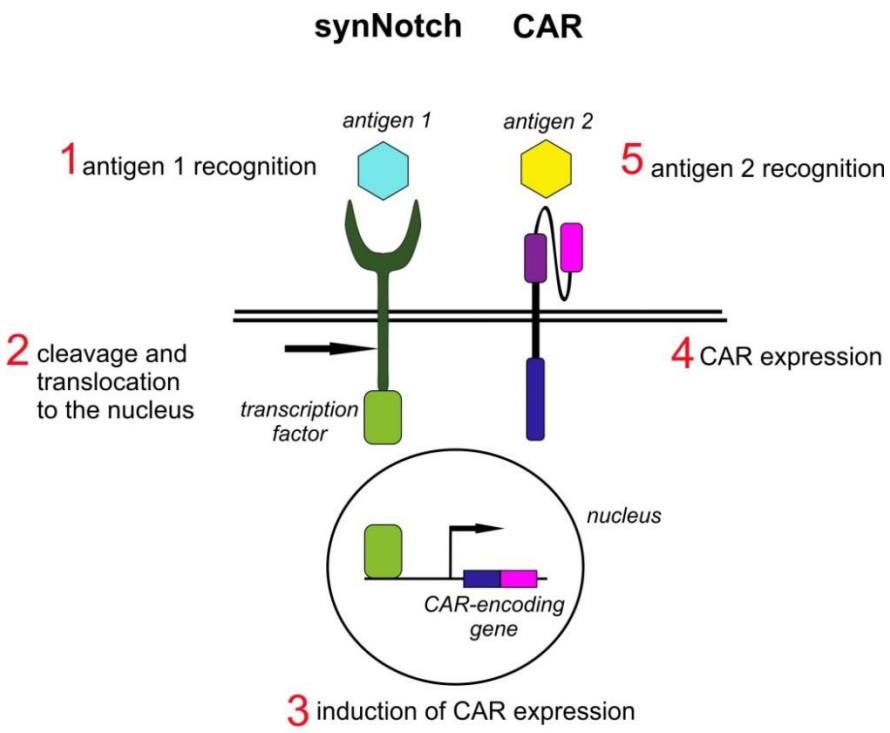

Figure 51 Two-step system of tumor cell recognition based on using a synthetic Notch receptor. Based on (221).

In the study published in 2021, synNotch CAR-T cells were shown to display superior control of the tumor burden in mouse models of human mesothelioma and ovarian cancer, when compared to the T cells constitutively expressing CARs targeting the same antigens. Alkaline phosphatase placental-like 2 (ALPPL2) was identified as a tumor-specific antigen expressed in various tumors, including mesothelioma and ovarian cancer, and it was used as a primary antigen for the synthetic Notch receptor. The study demonstrated, that the synNotch receptor targeting ALPPL2 can be combined with CARs targeting other tumor-associated antigens, such as melanoma cell adhesion molecule (MCAM), mesothelin, or HER2. Moreover, synNotch-controlled expression prevented CAR-mediated tonic signaling in T cells, maintaining their non-exhausted phenotype (222). A similar effect was observed in the study, where synNotch CAR-T cells were used in glioblastoma treatment. The synNotch-CAR circuit applied was primed by the specific for the central nervous system MOG antigen, which led to the local induction of the expression of a CAR targeting tumor-specific glioblastoma neo-antigen epidermal growth factor receptor splice variant III (EGFRvIII) (223). In the case of PD-L1-CAR-based therapy, the conditioning of the CAR construct expression with other TAAs recognition could significantly reduce the risk of non-malignant tissues damage. The earlier

mentioned examples of bispecific CARs targeting PD-L1 (combined with targeting MUC16 in ovarian cancer or c-Met in human hepatocellular carcinoma) suggest that the effectiveness of the approach would also increase. There are several molecules reported being upregulated in breast tumors, which could be potentially exploited as priming antigens for synNotch-PD-L1-CAR. For example, surface molecules mesothelin, FRα, FRa, tumor endothelial marker 8 (TEM8), chondroitin sulfate proteoglycan 4 (CSPG4), receptor-tyrosine-kinase-like orphan receptor 1 (ROR1), c-Met, MUC1, NKG2D ligands, epidermal growth factor receptor (EGFR), intercellular adhesion molecule-1 (ICAM-1) and receptor tyrosine kinase AXL were found to be upregulated in a high percentage of TNBC samples, while being expressed on a low level in non-malignant tissues (182). Additionally, recent studies demonstrate that even intracellularly overexpressed TAAs can be recognized by modified T cells. The expression of New York esophageal squamous cell carcinoma-1 (NY-ESO-1) and Wilms tumor antigen (WT-1) was detected in 18% and 54% of TNBC samples, respectively (224), and both these molecules can be targeted in the HLA context using modified TCR (225,226). The self-amplifying mechanism of PD-L1-CAR-T cells action allows for targeting also other breast tumor types, as the PD-L1 expression may be induced on initially PD-L1^{low} cancer cells. Thus, HER2 antigen, which is overexpressed in 25–30% of all breast cancers (227), may as well be exploited.

Except signaling from combinatorial antigens, the specific characteristics of the solid tumor microenvironment could be used as factors conditioning the induction of a CAR expression. High proliferation rate, and thus, high metabolic demands of the tumor cells often result in a state of inadequate oxygen supply in the TME, where oxygen concentration may be lower than 2% while in healthy tissues it is usually between 5 and 10% (228). Hypoxia is an outstanding feature of most solid tumors and in the case of breast cancer, approximately 25–40% of cases exhibit hypoxic regions (229).

Thus, hypoxia may be used as a marker for induction of a CAR expression, and this is achievable due to the naturally existing mechanisms, which cells utilize to detect and rapidly respond to hypoxia. In particular, the constitutive expression of transcription factor hypoxia-inducible-1 factor-alpha (HIF1-α), which degrades under the normoxia conditions. When a CAR was fused with an oxygen-dependent degradation domain

(ODD) of HIF1-α**,** the normoxia conditions led to the CAR proteasomal degradation as well. However, in that first study, the residual tumor cell killing under normoxic conditions was observed (230). To solve this issue, a dual oxygen-sensing T4-CAR was generated. A more stringent hypoxia-regulated CAR expression system was designed by combining the fusion of ODD domain to the CAR encoding sequence with incorporating a series of 9 consecutive hypoxia-responsive elements (HREs) into the CAR promotor, which permitted HIF1-α-mediated transcription of the CAR. This dual hypoxia-sensing system was proved to be superior to single hypoxia-sensing modules of the 9xHRE cassette or ODD, which displayed leakiness in CAR expression (231).

Altogether, these findings may be considered in further studies aimed to improve PD-L1-CAR safety in breast cancer treatment.

6. CONCLUSIONS

The main aims of this thesis were to provide the "proof-of-concept" results for the strategy of targeting obtained PD-L1-CAR-T cells against PD-L1-expressing human breast cancer cells and to evaluate the safety of the approach *in vitro*.

The performed studies allow to conclude:

- *primary human T cells can be effectively modified to express PD-L1-CAR by both mRNA electroporation and lentiviral transduction methods;*
- *in contrast to unmodified primary T cells, PD-L1-CAR-T cells do not express PD-L1 protein on their surface following the stimulation;*
- *PD-L1-CAR-T cells recognize the target PD-L1 protein specifically and produce the inflammatory cytokines following the target recognition;*
- *PD-L1-CAR-T cells have an improved ability to specifically eliminate breast cancer cells constitutively expressing the PD-L1 protein;*
- *PD-L1-CAR-T cells can trigger the PD-L1 expression in the majority of initially PD-L1-negative malignant and non-malignant cells;*
- *PD-L1-CAR-T cells exhibit enhanced cytotoxicity against both malignant and non-malignant cells which have the ability to upregulate PD-L1 expression;*
- *the self-amplifying mechanism of PD-L1-CAR-T cells action potentially increases the approach effectiveness and universality allowing for the elimination of not only tumor cells, but also the cells composing the tumor microenvironment;*
- *the self-amplifying mechanism of PD-L1-CAR-T cells action poses the risk of increased toxicity towards non-malignant cells surrounding the tumor and therefore requires the significant improvement of the safety of the approach.*

Altogether, the results obtained within this study suggest that targeting PD-L1 molecule using CAR-T cells can be a promising strategy in breast cancer treatment. However, this approach requires further optimization in order to obtain improved safety and thus prevent the PD-L1-CAR-T cell cytotoxicity against non-malignant cells surrounding the treated tumor.

7. LITERATURE

1. Sung H, Ferlay J, Siegel RL, Laversanne M, Soerjomataram I, Jemal A, et al. Global Cancer Statistics 2020: GLOBOCAN Estimates of Incidence and Mortality Worldwide for 36 Cancers in 185 Countries. CA Cancer J Clin. 2021 May;71(3):209–49.

2. Mattiuzzi C, Lippi G. Current Cancer Epidemiology. J Epidemiol Glob Health. 2019 Dec;9(4):217–22.

3. Global Burden of Disease Cancer Collaboration, Fitzmaurice C, Abate D, Abbasi N, Abbastabar H, Abd-Allah F, et al. Global, Regional, and National Cancer Incidence, Mortality, Years of Life Lost, Years Lived With Disability, and Disability-Adjusted Life-Years for 29 Cancer Groups, 1990 to 2017: A Systematic Analysis for the Global Burden of Disease Study. JAMA Oncol. 2019 Dec 1;5(12):1749–68.

4. Seebacher NA, Stacy AE, Porter GM, Merlot AM. Clinical development of targeted and immune based anti-cancer therapies. J Exp Clin Cancer Res. 2019 Apr 11;38(1):156.

5. Ceelen W, Pattyn P, Mareel M. Surgery, wound healing, and metastasis: recent insights and clinical implications. Crit Rev Oncol Hematol. 2014 Jan;89(1):16–26.

6. Valentini V, Boldrini L, Mariani S, Massaccesi M. Role of radiation oncology in modern multidisciplinary cancer treatment. Mol Oncol. 2020 Jul;14(7):1431–41.

7. Orth M, Lauber K, Niyazi M, Friedl AA, Li M, Maihöfer C, et al. Current concepts in clinical radiation oncology. Radiat Environ Biophys. 2014 Mar;53(1):1–29.

8. Bergamo A, Sava G. Chemical and Molecular Approach to Tumor Metastases. Int J Mol Sci. 2018 Mar 14;19(3):E843.

9. Knezevic CE, Clarke W. Cancer Chemotherapy: The Case for Therapeutic Drug Monitoring. Ther Drug Monit. 2020 Feb;42(1):6–19.

10. Baldo BA, Pham NH. Adverse reactions to targeted and non-targeted chemotherapeutic drugs with emphasis on hypersensitivity responses and the invasive metastatic switch. Cancer Metastasis Rev. 2013 Dec;32(3–4):723–61.

11. Santhosh S, Kumar P, Ramprasad V, Chaudhuri A. Evolution of targeted therapies in cancer: opportunities and challenges in the clinic. Future Oncol. 2015;11(2):279–93.

12. Shagufta null, Ahmad I. Tamoxifen a pioneering drug: An update on the therapeutic potential of tamoxifen derivatives. Eur J Med Chem. 2018 Jan 1;143:515–31.

13. Xu MJ, Johnson DE, Grandis JR. EGFR-targeted therapies in the post-genomic era. Cancer Metastasis Rev. 2017 Sep;36(3):463–73.

14. Schirrmacher V. From chemotherapy to biological therapy: A review of novel concepts to reduce the side effects of systemic cancer treatment (Review). Int J Oncol. 2019 Feb;54(2):407–19.

15. Ichim CV. Revisiting immunosurveillance and immunostimulation: Implications for cancer immunotherapy. J Transl Med. 2005 Feb 8;3(1):8.

16. Dunn GP, Old LJ, Schreiber RD. The immunobiology of cancer immunosurveillance and immunoediting. Immunity. 2004 Aug;21(2):137–48.

17. Ribatti D. The concept of immune surveillance against tumors. The first theories. Oncotarget. 2017 Jan 24;8(4):7175–80.

18. Galluzzi L, Vacchelli E, Bravo-San Pedro J-M, Buqué A, Senovilla L, Baracco EE, et al. Classification of current anticancer immunotherapies. Oncotarget. 2014 Dec 30;5(24):12472–508.

19. Berraondo P, Sanmamed MF, Ochoa MC, Etxeberria I, Aznar MA, Pérez-Gracia JL, et al. Cytokines in clinical cancer immunotherapy. Br J Cancer. 2019 Jan;120(1):6–15.

20. van der Zanden SY, Luimstra JJ, Neefjes J, Borst J, Ovaa H. Opportunities for Small Molecules in Cancer Immunotherapy. Trends Immunol. 2020 Jun;41(6):493–511.

21. Husain B, Ellerman D. Expanding the Boundaries of Biotherapeutics with Bispecific Antibodies. BioDrugs. 2018 Oct;32(5):441–64.

22. Thomas A, Teicher BA, Hassan R. Antibody-drug conjugates for cancer therapy. Lancet Oncol. 2016 Jun;17(6):e254–62.

23. Marin-Acevedo JA, Soyano AE, Dholaria B, Knutson KL, Lou Y. Cancer immunotherapy beyond immune checkpoint inhibitors. J Hematol Oncol. 2018 Jan 12;11(1):8.

24. Zheng M, Huang J, Tong A, Yang H. Oncolytic Viruses for Cancer Therapy: Barriers and Recent Advances. Mol Ther Oncolytics. 2019 Dec 20;15:234–47.

25. Abbott M, Ustoyev Y. Cancer and the Immune System: The History and Background of Immunotherapy. Semin Oncol Nurs. 2019 Oct;35(5):150923.

26. Varadé J, Magadán S, González-Fernández Á. Human immunology and immunotherapy: main achievements and challenges. Cell Mol Immunol. 2021 Apr;18(4):805–28.

27. Rosenberg SA, Spiess P, Lafreniere R. A new approach to the adoptive immunotherapy of cancer with tumor-infiltrating lymphocytes. Science. 1986 Sep 19;233(4770):1318–21.

28. Rosenberg SA, Packard BS, Aebersold PM, Solomon D, Topalian SL, Toy ST, et al. Use of tumor-infiltrating lymphocytes and interleukin-2 in the immunotherapy of

patients with metastatic melanoma. A preliminary report. N Engl J Med. 1988 Dec 22;319(25):1676–80.

29. Gajewski TF, Schreiber H, Fu Y-X. Innate and adaptive immune cells in the tumor microenvironment. Nat Immunol. 2013 Oct;14(10):1014–22.

30. Schumacher TN, Schreiber RD. Neoantigens in cancer immunotherapy. Science. 2015 Apr 3;348(6230):69–74.

31. Gilboa E. The makings of a tumor rejection antigen. Immunity. 1999 Sep;11(3):263–70.

32. Walsh SR, Simovic B, Chen L, Bastin D, Nguyen A, Stephenson K, et al. Endogenous T cells prevent tumor immune escape following adoptive T cell therapy. J Clin Invest. 2019 Dec 2;129(12):5400–10.

33. Rosenberg SA, Restifo NP. Adoptive cell transfer as personalized immunotherapy for human cancer. Science. 2015 Apr 3;348(6230):62–8.

34. Perica K, Varela JC, Oelke M, Schneck J. Adoptive T cell immunotherapy for cancer. Rambam Maimonides Med J. 2015 Jan;6(1):e0004.

35. Rosenberg SA, Yang JC, Sherry RM, Kammula US, Hughes MS, Phan GQ, et al. Durable complete responses in heavily pretreated patients with metastatic melanoma using T-cell transfer immunotherapy. Clin Cancer Res. 2011 Jul 1;17(13):4550–7.

36. Walia V, Mu EW, Lin JC, Samuels Y. Delving into somatic variation in sporadic melanoma. Pigment Cell Melanoma Res. 2012 Mar;25(2):155–70.

37. Ruella M, Kalos M. Adoptive immunotherapy for cancer. Immunol Rev. 2014 Jan;257(1):14–38.

38. Sadelain M, Rivière I, Brentjens R. Targeting tumours with genetically enhanced T lymphocytes. Nat Rev Cancer. 2003 Jan;3(1):35–45.

39. Garrido F, Aptsiauri N. Cancer immune escape: MHC expression in primary tumours versus metastases. Immunology. 2019 Dec;158(4):255–66.

40. Singh AK, McGuirk JP. CAR T cells: continuation in a revolution of immunotherapy. Lancet Oncol. 2020 Mar;21(3):e168–78.

41. Curtsinger JM, Mescher MF. Inflammatory Cytokines as a Third Signal for T Cell Activation. Curr Opin Immunol. 2010 Jun;22(3):333–40.

42. Roselli E, Frieling JS, Thorner K, Ramello MC, Lynch CC, Abate-Daga D. CAR-T Engineering: Optimizing Signal Transduction and Effector Mechanisms. BioDrugs. 2019 Dec;33(6):647–59.

43. Eshhar Z, Waks T, Gross G, Schindler DG. Specific activation and targeting of cytotoxic lymphocytes through chimeric single chains consisting of antibody-binding domains and the gamma or zeta subunits of the immunoglobulin and T-cell receptors. Proc Natl Acad Sci U S A. 1993 Jan 15;90(2):720–4.

44. Stock S, Schmitt M, Sellner L. Optimizing Manufacturing Protocols of Chimeric Antigen Receptor T Cells for Improved Anticancer Immunotherapy. Int J Mol Sci. 2019 Dec 10;20(24):E6223.

45. Abate-Daga D, Davila ML. CAR models: next-generation CAR modifications for enhanced T-cell function. Mol Ther Oncolytics. 2016;3:16014.

46. Sadelain M, Brentjens R, Rivière I. The basic principles of chimeric antigen receptor design. Cancer Discov. 2013 Apr;3(4):388–98.

47. Rahbarizadeh F, Ahmadvand D, Moghimi SM. CAR T-cell bioengineering: Single variable domain of heavy chain antibody targeted CARs. Adv Drug Deliv Rev. 2019 Feb 15;141:41–6.

48. Dwivedi A, Karulkar A, Ghosh S, Rafiq A, Purwar R. Lymphocytes in Cellular Therapy: Functional Regulation of CAR T Cells. Front Immunol. 2018;9:3180.

49. Weinkove R, George P, Dasyam N, McLellan AD. Selecting costimulatory domains for chimeric antigen receptors: functional and clinical considerations. Clin Transl Immunology. 2019;8(5):e1049.

50. Maher J, Brentjens RJ, Gunset G, Rivière I, Sadelain M. Human T-lymphocyte cytotoxicity and proliferation directed by a single chimeric TCRzeta /CD28 receptor. Nat Biotechnol. 2002 Jan;20(1):70–5.

51. Brentjens RJ, Santos E, Nikhamin Y, Yeh R, Matsushita M, La Perle K, et al. Genetically targeted T cells eradicate systemic acute lymphoblastic leukemia xenografts. Clin Cancer Res. 2007 Sep 15;13(18 Pt 1):5426–35.

52. Kowolik CM, Topp MS, Gonzalez S, Pfeiffer T, Olivares S, Gonzalez N, et al. CD28 costimulation provided through a CD19-specific chimeric antigen receptor enhances in vivo persistence and antitumor efficacy of adoptively transferred T cells. Cancer Res. 2006 Nov 15;66(22):10995–1004.

53. Savoldo B, Ramos CA, Liu E, Mims MP, Keating MJ, Carrum G, et al. CD28 costimulation improves expansion and persistence of chimeric antigen receptor-modified T cells in lymphoma patients. J Clin Invest. 2011 May;121(5):1822–6.

54. Hombach AA, Abken H. Costimulation by chimeric antigen receptors revisited the T cell antitumor response benefits from combined CD28-OX40 signalling. Int J Cancer. 2011 Dec 15;129(12):2935–44.

55. Chmielewski M, Abken H. TRUCKs: the fourth generation of CARs. Expert Opin Biol Ther. 2015;15(8):1145–54.

56. Chmielewski M, Hombach AA, Abken H. Of CARs and TRUCKs: chimeric antigen receptor (CAR) T cells engineered with an inducible cytokine to modulate the tumor stroma. Immunol Rev. 2014 Jan;257(1):83–90.

57. Holzinger A, Abken H. CAR T Cells: A Snapshot on the Growing Options to Design a CAR. Hemasphere. 2019 Feb;3(1):e172.

58. Yu S, Li A, Liu Q, Li T, Yuan X, Han X, et al. Chimeric antigen receptor T cells: a novel therapy for solid tumors. J Hematol Oncol. 2017 Mar 29;10(1):78.

59. Murthy H, Iqbal M, Chavez JC, Kharfan-Dabaja MA. Cytokine Release Syndrome: Current Perspectives. Immunotargets Ther. 2019;8:43–52.

60. Wu C, Hong SG, Winkler T, Spencer DM, Jares A, Ichwan B, et al. Development of an inducible caspase-9 safety switch for pluripotent stem cell-based therapies. Mol Ther Methods Clin Dev. 2014;1:14053.

61. Gargett T, Brown MP. The inducible caspase-9 suicide gene system as a “safety switch” to limit on-target, off-tumor toxicities of chimeric antigen receptor T cells. Front Pharmacol. 2014;5:235.

62. Rafiq S, Hackett CS, Brentjens RJ. Engineering strategies to overcome the current roadblocks in CAR T cell therapy. Nat Rev Clin Oncol. 2020 Mar;17(3):147–67.

63. Vitale C, Strati P. CAR T-Cell Therapy for B-Cell non-Hodgkin Lymphoma and Chronic Lymphocytic Leukemia: Clinical Trials and Real-World Experiences. Front Oncol. 2020;10:849.

64. Mian A, Hill BT. Brexucabtagene autoleucel for the treatment of relapsed/refractory mantle cell lymphoma. Expert Opin Biol Ther. 2021 Apr;21(4):435–41.

65. Sadeqi Nezhad M, Yazdanifar M, Abdollahpour-Alitappeh M, Sattari A, Seifalian A, Bagheri N. Strengthening the CAR-T cell therapeutic application using CRISPR/Cas9 technology. Biotechnol Bioeng. 2021 Oct;118(10):3691–705.

66. Ying Z, Yang H, Guo Y, Li W, Zou D, Zhou D, et al. Relmacabtagene autoleucel (relma-cel) CD19 CAR-T therapy for adults with heavily pretreated relapsed/refractory large B-cell lymphoma in China. Cancer Med. 2021 Feb;10(3):999–1011.

67. Ortíz-Maldonado V, Rives S, Castellà M, Alonso-Saladrigues A, Benítez-Ribas D, Caballero-Baños M, et al. CART19-BE-01: A Multicenter Trial of ARI-0001 Cell Therapy in Patients with CD19+ Relapsed/Refractory Malignancies. Mol Ther. 2021 Feb 3;29(2):636–44.

68. Abramson JS. Anti-CD19 CAR T-Cell Therapy for B-Cell Non-Hodgkin Lymphoma. Transfus Med Rev. 2020 Jan;34(1):29–33.

69. Zhang J, Li J, Ma Q, Yang H, Signorovitch J, Wu E. A Review of Two Regulatory Approved Anti-CD19 CAR T-Cell Therapies in Diffuse Large B-Cell Lymphoma: Why

Are Indirect Treatment Comparisons Not Feasible? Adv Ther. 2020 Jul;37(7):3040–58.

70. Klebanoff CA, Khong HT, Antony PA, Palmer DC, Restifo NP. Sinks, suppressors and antigen presenters: how lymphodepletion enhances T cell-mediated tumor immunotherapy. Trends Immunol. 2005 Feb;26(2):111–7.

71. Frey N, Porter D. Cytokine Release Syndrome with Chimeric Antigen Receptor T Cell Therapy. Biol Blood Marrow Transplant. 2019 Apr;25(4):e123–7.

72. Tvedt THA, Vo AK, Bruserud Ø, Reikvam H. Cytokine Release Syndrome in the Immunotherapy of Hematological Malignancies: The Biology behind and Possible Clinical Consequences. J Clin Med. 2021 Nov 6;10(21):5190.

73. Siegler EL, Kenderian SS. Neurotoxicity and Cytokine Release Syndrome After Chimeric Antigen Receptor T Cell Therapy: Insights Into Mechanisms and Novel Therapies. Front Immunol. 2020;11:1973.

74. Zhylko A, Winiarska M, Graczyk-Jarzynka A. The Great War of Today: Modifications of CAR-T Cells to Effectively Combat Malignancies. Cancers (Basel). 2020 Jul 24;12(8):E2030.

75. Kochenderfer JN, Rosenberg SA. Treating B-cell cancer with T cells expressing anti-CD19 chimeric antigen receptors. Nat Rev Clin Oncol. 2013 May;10(5):267–76.

76. Khodadadi L, Cheng Q, Radbruch A, Hiepe F. The Maintenance of Memory Plasma Cells. Front Immunol. 2019;10:721.

77. Makita S, Yoshimura K, Tobinai K. Clinical development of anti-CD19 chimeric antigen receptor T-cell therapy for B-cell non-Hodgkin lymphoma. Cancer Sci. 2017 Jun;108(6):1109–18.

78. Hou B, Tang Y, Li W, Zeng Q, Chang D. Efficiency of CAR-T Therapy for Treatment of Solid Tumor in Clinical Trials: A Meta-Analysis. Dis Markers. 2019;2019:3425291.

79. Wagner J, Wickman E, DeRenzo C, Gottschalk S. CAR T Cell Therapy for Solid Tumors: Bright Future or Dark Reality? Mol Ther. 2020 Nov 4;28(11):2320–39.

80. Jiang X, Wang J, Deng X, Xiong F, Ge J, Xiang B, et al. Role of the tumor microenvironment in PD-L1/PD-1-mediated tumor immune escape. Mol Cancer. 2019 Jan 15;18(1):10.

81. Duan Q, Zhang H, Zheng J, Zhang L. Turning Cold into Hot: Firing up the Tumor Microenvironment. Trends Cancer. 2020 Jul;6(7):605–18.

82. Hanson EM, Clements VK, Sinha P, Ilkovitch D, Ostrand-Rosenberg S. Myeloid-derived suppressor cells down-regulate L-selectin expression on CD4+ and CD8+ T cells. J Immunol. 2009 Jul 15;183(2):937–44.

83. Grosser R, Cherkassky L, Chintala N, Adusumilli PS. Combination Immunotherapy with CAR T Cells and Checkpoint Blockade for the Treatment of Solid Tumors. Cancer Cell. 2019 Nov 11;36(5):471–82.

84. Trujillo JA, Sweis RF, Bao R, Luke JJ. T Cell-Inflamed versus Non-T Cell-Inflamed Tumors: A Conceptual Framework for Cancer Immunotherapy Drug Development and Combination Therapy Selection. Cancer Immunol Res. 2018 Sep;6(9):990–1000.

85. Chen DS, Mellman I. Oncology meets immunology: the cancer-immunity cycle. Immunity. 2013 Jul 25;39(1):1–10.

86. Zou W, Wolchok JD, Chen L. PD-L1 (B7-H1) and PD-1 pathway blockade for cancer therapy: Mechanisms, response biomarkers, and combinations. Sci Transl Med. 2016 Mar 2;8(328):328rv4.

87. Dermani FK, Samadi P, Rahmani G, Kohlan AK, Najafi R. PD-1/PD-L1 immune checkpoint: Potential target for cancer therapy. J Cell Physiol. 2019 Feb;234(2):1313–25.

88. Marcucci F, Rumio C. The tumor-promoting effects of the adaptive immune system: a cause of hyperprogressive disease in cancer? Cell Mol Life Sci. 2021 Feb;78(3):853–65.

89. Upadhyay S, Sharma N, Gupta KB, Dhiman M. Role of immune system in tumor progression and carcinogenesis. J Cell Biochem. 2018 Jul;119(7):5028–42.

90. Ma S, Li X, Wang X, Cheng L, Li Z, Zhang C, et al. Current Progress in CAR-T Cell Therapy for Solid Tumors. Int J Biol Sci. 2019;15(12):2548–60.

91. Chen L, Flies DB. Molecular mechanisms of T cell co-stimulation and co-inhibition. Nat Rev Immunol. 2013 Apr;13(4):227–42.

92. Attanasio J, Wherry EJ. Costimulatory and Coinhibitory Receptor Pathways in Infectious Disease. Immunity. 2016 May 17;44(5):1052–68.

93. Funes SC, Manrique de Lara A, Altamirano-Lagos MJ, Mackern-Oberti JP, Escobar-Vera J, Kalergis AM. Immune checkpoints and the regulation of tolerogenicity in dendritic cells: Implications for autoimmunity and immunotherapy. Autoimmun Rev. 2019 Apr;18(4):359–68.

94. Fife BT, Bluestone JA. Control of peripheral T-cell tolerance and autoimmunity via the CTLA-4 and PD-1 pathways. Immunol Rev. 2008 Aug;224:166–82.

95. Nandi D, Pathak S, Verma T, Singh M, Chattopadhyay A, Thakur S, et al. T cell costimulation, checkpoint inhibitors and anti-tumor therapy. J Biosci. 2020;45:50.

96. Jiang X, Liu G, Li Y, Pan Y. Immune checkpoint: The novel target for antitumor therapy. Genes Dis. 2021 Jan;8(1):25–37.

97. He X, Xu C. Immune checkpoint signaling and cancer immunotherapy. Cell Res. 2020 Aug;30(8):660–9.

98. Tsai H-F, Hsu P-N. Cancer immunotherapy by targeting immune checkpoints: mechanism of T cell dysfunction in cancer immunity and new therapeutic targets. J Biomed Sci. 2017 May 25;24(1):35.

99. Rotte A, Jin JY, Lemaire V. Mechanistic overview of immune checkpoints to support the rational design of their combinations in cancer immunotherapy. Ann Oncol. 2018 Jan 1;29(1):71–83.

100. Ishida Y, Agata Y, Shibahara K, Honjo T. Induced expression of PD-1, a novel member of the immunoglobulin gene superfamily, upon programmed cell death. EMBO J. 1992 Nov;11(11):3887–95.

101. Bally APR, Austin JW, Boss JM. Genetic and Epigenetic Regulation of PD-1 Expression. J Immunol. 2016 Mar 15;196(6):2431–7.

102. Judge SJ, Dunai C, Aguilar EG, Vick SC, Sturgill IR, Khuat LT, et al. Minimal PD-1 expression in mouse and human NK cells under diverse conditions. J Clin Invest. 2020 Jun 1;130(6):3051–68.

103. Davis Z, Felices M, Lenvik T, Badal S, Walker JT, Hinderlie P, et al. Low-density PD-1 expression on resting human natural killer cells is functional and upregulated after transplantation. Blood Adv. 2021 Feb 23;5(4):1069–80.

104. Solinas C, Aiello M, Rozali E, Lambertini M, Willard-Gallo K, Migliori E. Programmed cell death-ligand 2: A neglected but important target in the immune response to cancer? Transl Oncol. 2020 Oct;13(10):100811.

105. Sharpe AH, Wherry EJ, Ahmed R, Freeman GJ. The function of programmed cell death 1 and its ligands in regulating autoimmunity and infection. Nat Immunol. 2007 Mar;8(3):239–45.

106. Akinleye A, Rasool Z. Immune checkpoint inhibitors of PD-L1 as cancer therapeutics. J Hematol Oncol. 2019 Sep 5;12(1):92.

107. Keir ME, Butte MJ, Freeman GJ, Sharpe AH. PD-1 and its ligands in tolerance and immunity. Annu Rev Immunol. 2008;26:677–704.

108. Escors D, Gato-Cañas M, Zuazo M, Arasanz H, García-Granda MJ, Vera R, et al. The intracellular signalosome of PD-L1 in cancer cells. Signal Transduct Target Ther. 2018;3:26.

109. Ahmadzadeh M, Johnson LA, Heemskerk B, Wunderlich JR, Dudley ME, White DE, et al. Tumor antigen-specific CD8 T cells infiltrating the tumor express high levels of PD-1 and are functionally impaired. Blood. 2009 Aug 20;114(8):1537–44.

110. Pardoll DM. The blockade of immune checkpoints in cancer immunotherapy. Nat Rev Cancer. 2012 Mar 22;12(4):252–64.

111. Patel SP, Kurzrock R. PD-L1 Expression as a Predictive Biomarker in Cancer Immunotherapy. Mol Cancer Ther. 2015 Apr;14(4):847–56.

112. Marhelava K, Pilch Z, Bajor M, Graczyk-Jarzynka A, Zagozdzon R. Targeting Negative and Positive Immune Checkpoints with Monoclonal Antibodies in Therapy of Cancer. Cancers (Basel). 2019 Nov 8;11(11):E1756.

113. Chen Y, Pei Y, Luo J, Huang Z, Yu J, Meng X. Looking for the Optimal PD-1/PD-L1 Inhibitor in Cancer Treatment: A Comparison in Basic Structure, Function, and Clinical Practice. Front Immunol. 2020;11:1088.

114. Kim YJ. Subverting the adaptive immune resistance mechanism to improve clinical responses to immune checkpoint blockade therapy. Oncoimmunology. 2014 Dec;3(12):e954868.

115. Boyerinas B, Jochems C, Fantini M, Heery CR, Gulley JL, Tsang KY, et al. Antibody-Dependent Cellular Cytotoxicity Activity of a Novel Anti-PD-L1 Antibody Avelumab (MSB0010718C) on Human Tumor Cells. Cancer Immunol Res. 2015 Oct;3(10):1148–57.

116. Durrechou Q, Domblides C, Sionneau B, Lefort F, Quivy A, Ravaud A, et al. Management of Immune Checkpoint Inhibitor Toxicities. Cancer Manag Res. 2020;12:9139–58.

117. Johnson DB, Balko JM, Compton ML, Chalkias S, Gorham J, Xu Y, et al. Fulminant Myocarditis with Combination Immune Checkpoint Blockade. N Engl J Med. 2016 Nov 3;375(18):1749–55.

118. Xu X, Sun Q, Liang X, Chen Z, Zhang X, Zhou X, et al. Mechanisms of Relapse After CD19 CAR T-Cell Therapy for Acute Lymphoblastic Leukemia and Its Prevention and Treatment Strategies. Front Immunol. 2019;10:2664.

119. Cader FZ, Schackmann RCJ, Hu X, Wienand K, Redd R, Chapuy B, et al. Mass cytometry of Hodgkin lymphoma reveals a CD4+ regulatory T-cell-rich and exhausted T-effector microenvironment. Blood. 2018 Aug 23;132(8):825–36.

120. Wang H, Kaur G, Sankin AI, Chen F, Guan F, Zang X. Immune checkpoint blockade and CAR-T cell therapy in hematologic malignancies. J Hematol Oncol. 2019 Jun 11;12(1):59.

121. Roemer MGM, Advani RH, Ligon AH, Natkunam Y, Redd RA, Homer H, et al. PD-L1 and PD-L2 Genetic Alterations Define Classical Hodgkin Lymphoma and Predict Outcome. J Clin Oncol. 2016 Aug 10;34(23):2690–7.

122. Xie W, Medeiros LJ, Li S, Yin CC, Khoury JD, Xu J. PD-1/PD-L1 Pathway and Its Blockade in Patients with Classic Hodgkin Lymphoma and Non-Hodgkin Large-Cell Lymphomas. Curr Hematol Malig Rep. 2020 Aug;15(4):372–81.

123. Cioroianu AI, Stinga PI, Sticlaru L, Cioplea MD, Nichita L, Popp C, et al. Tumor Microenvironment in Diffuse Large B-Cell Lymphoma: Role and Prognosis. Anal Cell Pathol (Amst). 2019;2019:8586354.

124. Vincent-Fabert C, Roland L, Zimber-Strobl U, Feuillard J, Faumont N. Pre-clinical blocking of PD-L1 molecule, which expression is down regulated by NF-κB, JAK1/JAK2 and BTK inhibitors, induces regression of activated B-cell lymphoma. Cell Commun Signal. 2019 Aug 5;17(1):89.

125. Yoon DH, Osborn MJ, Tolar J, Kim CJ. Incorporation of Immune Checkpoint Blockade into Chimeric Antigen Receptor T Cells (CAR-Ts): Combination or Built-In CAR-T. Int J Mol Sci. 2018 Jan 24;19(2):E340.

126. Park SH, You E, Park C-J, Cho Y-U, Jang S, Im H-J, et al. Increased expression of immune checkpoint programmed cell death protein-1 (PD-1) on T cell subsets of bone marrow aspirates in patients with B-Lymphoblastic leukemia, especially in relapse and at diagnosis. Cytometry B Clin Cytom. 2020 Jul;98(4):336–47.

127. Williams P, Basu S, Garcia-Manero G, Hourigan CS, Oetjen KA, Cortes JE, et al. The distribution of T-cell subsets and the expression of immune checkpoint receptors and ligands in patients with newly diagnosed and relapsed acute myeloid leukemia. Cancer. 2019 May 1;125(9):1470–81.

128. Berthon C, Driss V, Liu J, Kuranda K, Leleu X, Jouy N, et al. In acute myeloid leukemia, B7-H1 (PD-L1) protection of blasts from cytotoxic T cells is induced by TLR ligands and interferon-gamma and can be reversed using MEK inhibitors. Cancer Immunol Immunother. 2010 Dec;59(12):1839–49.

129. Kochenderfer JN, Dudley ME, Kassim SH, Somerville RPT, Carpenter RO, Stetler-Stevenson M, et al. Chemotherapy-refractory diffuse large B-cell lymphoma and indolent B-cell malignancies can be effectively treated with autologous T cells expressing an anti-CD19 chimeric antigen receptor. J Clin Oncol. 2015 Feb 20;33(6):540–9.

130. Brudno JN, Somerville RPT, Shi V, Rose JJ, Halverson DC, Fowler DH, et al. Allogeneic T Cells That Express an Anti-CD19 Chimeric Antigen Receptor Induce Remissions of B-Cell Malignancies That Progress After Allogeneic Hematopoietic Stem-Cell Transplantation Without Causing Graft-Versus-Host Disease. J Clin Oncol. 2016 Apr 1;34(10):1112–21.

131. McClanahan F, Hanna B, Miller S, Clear AJ, Lichter P, Gribben JG, et al. PD-L1 checkpoint blockade prevents immune dysfunction and leukemia development in a mouse model of chronic lymphocytic leukemia. Blood. 2015 Jul 9;126(2):203–11.

132. Shen C, Zhang Z, Zhang Y. Chimeric Antigen Receptor T Cell Exhaustion during Treatment for Hematological Malignancies. Biomed Res Int. 2020;2020:8765028.

133. Binnewies M, Roberts EW, Kersten K, Chan V, Fearon DF, Merad M, et al. Understanding the tumor immune microenvironment (TIME) for effective therapy. Nat Med. 2018 May;24(5):541–50.

134. Cherkassky L, Morello A, Villena-Vargas J, Feng Y, Dimitrov DS, Jones DR, et al. Human CAR T cells with cell-intrinsic PD-1 checkpoint blockade resist tumor-mediated inhibition. J Clin Invest. 2016 Aug 1;126(8):3130–44.

135. John LB, Devaud C, Duong CPM, Yong CS, Beavis PA, Haynes NM, et al. Anti-PD-1 antibody therapy potently enhances the eradication of established tumors by gene-modified T cells. Clin Cancer Res. 2013 Oct 15;19(20):5636–46.

136. Tanoue K, Rosewell Shaw A, Watanabe N, Porter C, Rana B, Gottschalk S, et al. Armed Oncolytic Adenovirus-Expressing PD-L1 Mini-Body Enhances Antitumor Effects of Chimeric Antigen Receptor T Cells in Solid Tumors. Cancer Res. 2017 Apr 15;77(8):2040–51.

137. Huemer F, Leisch M, Geisberger R, Melchardt T, Rinnerthaler G, Zaborsky N, et al. Combination Strategies for Immune-Checkpoint Blockade and Response Prediction by Artificial Intelligence. Int J Mol Sci. 2020 Apr 19;21(8):E2856.

138. Titov A, Zmievskaya E, Ganeeva I, Valiullina A, Petukhov A, Rakhmatullina A, et al. Adoptive Immunotherapy beyond CAR T-Cells. Cancers (Basel). 2021 Feb 11;13(4):743.

139. Meyers DE, Bryan PM, Banerji S, Morris DG. Targeting the PD-1/PD-L1 axis for the treatment of non-small-cell lung cancer. Curr Oncol. 2018 Aug;25(4):e324–34.

140. Bellucci R, Martin A, Bommarito D, Wang K, Hansen SH, Freeman GJ, et al. Interferon-γ-induced activation of JAK1 and JAK2 suppresses tumor cell susceptibility to NK cells through upregulation of PD-L1 expression. Oncoimmunology. 2015 Jun;4(6):e1008824.

141. Lei Q, Wang D, Sun K, Wang L, Zhang Y. Resistance Mechanisms of Anti-PD1/PDL1 Therapy in Solid Tumors. Front Cell Dev Biol. 2020;8:672.

142. Ping Y, Li F, Nan S, Zhang D, Shi X, Shan J, et al. Augmenting the Effectiveness of CAR-T Cells by Enhanced Self-Delivery of PD-1-Neutralizing scFv. Front Cell Dev Biol. 2020;8:803.

143. Sharma GN, Dave R, Sanadya J, Sharma P, Sharma KK. Various types and management of breast cancer: an overview. J Adv Pharm Technol Res. 2010 Apr;1(2):109–26.

144. Mittendorf EA, Philips AV, Meric-Bernstam F, Qiao N, Wu Y, Harrington S, et al. PD-L1 expression in triple-negative breast cancer. Cancer Immunol Res. 2014 Apr;2(4):361–70.

145. Barrett MT, Anderson KS, Lenkiewicz E, Andreozzi M, Cunliffe HE, Klassen CL, et al. Genomic amplification of 9p24.1 targeting JAK2, PD-L1, and PD-L2 is enriched in high-risk triple negative breast cancer. Oncotarget. 2015 Sep 22;6(28):26483–93.

146. McKinnon KM. Flow Cytometry: An Overview. Curr Protoc Immunol. 2018 Feb 21;120:5.1.1-5.1.11.

147. Platelets - 3rd Edition [Internet]. [cited 2022 Jan 30]. Available from: https://www.elsevier.com/books/platelets/michelson/978-0-12-387837-3

148. Adan A, Alizada G, Kiraz Y, Baran Y, Nalbant A. Flow cytometry: basic principles and applications. Crit Rev Biotechnol. 2017 Mar;37(2):163–76.

149. Ibrahim SF, van den Engh G. Flow cytometry and cell sorting. Adv Biochem Eng Biotechnol. 2007;106:19–39.

150. Givan AL. Flow cytometry: an introduction. Methods Mol Biol. 2011;699:1–29.

151. Roederer M. Compensation in Flow Cytometry. Current Protocols in Cytometry [Internet]. 2002 Oct [cited 2022 Jan 30];22(1). Available from: https://onlinelibrary.wiley.com/doi/10.1002/0471142956.cy0114s22

152. Szalóki G, Goda K. Compensation in multicolor flow cytometry. Cytometry A. 2015 Nov;87(11):982–5.

153. Kurien BT, Scofield RH. Western blotting: an introduction. Methods Mol Biol. 2015;1312:17–30.

154. Mahmood T, Yang P-C. Western blot: technique, theory, and trouble shooting. N Am J Med Sci. 2012 Sep;4(9):429–34.

155. Lee PY, Costumbrado J, Hsu C-Y, Kim YH. Agarose gel electrophoresis for the separation of DNA fragments. J Vis Exp. 2012 Apr 20;(62):3923.

156. Stephenson FH. Chapter 5 - Nucleic Acid Quantification. In: Stephenson FH, editor. Calculations for Molecular Biology and Biotechnology (Third Edition) [Internet]. Boston: Academic Press; 2016 [cited 2022 Jan 30]. p. 97–129. Available from: https://www.sciencedirect.com/science/article/pii/B9780128022115000059

157. Johnston C, Martin B, Fichant G, Polard P, Claverys J-P. Bacterial transformation: distribution, shared mechanisms and divergent control. Nat Rev Microbiol. 2014 Mar;12(3):181–96.

158. Hasegawa H, Suzuki E, Maeda S. Horizontal Plasmid Transfer by Transformation in Escherichia coli: Environmental Factors and Possible Mechanisms. Front Microbiol. 2018;9:2365.

159. Uzman A. Molecular Cell Biology (4th edition): Harvey Lodish, Arnold Berk, S. Lawrence Zipursky, Paul Matsudaira, David Baltimore and James Darnell; Freeman & Co., New York, NY, 2000, 1084 pp., list price $102.25, ISBN 0-7167-3136-3. 2001;

160. Sambrook J, Russell DW. Molecular cloning: a laboratory manual. 3rd ed. Cold Spring Harbor, N.Y: Cold Spring Harbor Laboratory Press; 2001. 3 p.

161. Demaison C, Parsley K, Brouns G, Scherr M, Battmer K, Kinnon C, et al. High-level transduction and gene expression in hematopoietic repopulating cells using a human immunodeficiency [correction of imunodeficiency] virus type 1-based lentiviral vector containing an internal spleen focus forming virus promoter. Hum Gene Ther. 2002 May 1;13(7):803–13.

162. Sæbøe-Larssen S, Fossberg E, Gaudernack G. mRNA-based electrotransfection of human dendritic cells and induction of cytotoxic T lymphocyte responses against the telomerase catalytic subunit (hTERT). Journal of Immunological Methods. 2002 Jan 1;259(1):191–203.

163. Muttach F, Muthmann N, Rentmeister A. Synthetic mRNA capping. Beilstein J Org Chem. 2017;13:2819–32.

164. Fleiss A, Sarkisyan KS. A brief review of bioluminescent systems (2019). Curr Genet. 2019 Aug;65(4):877–82.

165. Gregor C, Pape JK, Gwosch KC, Gilat T, Sahl SJ, Hell SW. Autonomous bioluminescence imaging of single mammalian cells with the bacterial bioluminescence system. Proc Natl Acad Sci U S A. 2019 Dec 2;201913616.

166. Hamidi H, Lilja J, Ivaska J. Using xCELLigence RTCA Instrument to Measure Cell Adhesion. Bio Protoc. 2017 Dec 20;7(24):e2646.

167. Cerignoli F, Abassi YA, Lamarche BJ, Guenther G, Santa Ana D, Guimet D, et al. In vitro immunotherapy potency assays using real-time cell analysis. PLoS One. 2018;13(3):e0193498.

168. Harris E, Elmer JJ. Optimization of electroporation and other non-viral gene delivery strategies for T cells. Biotechnol Prog. 2021 Jan;37(1):e3066.

169. Pohl-Guimarães F, Hoang-Minh LB, Mitchell DA. RNA-electroporated T cells for cancer immunotherapy. Oncoimmunology. 2020 Oct 7;9(1):1792625.

170. Van Tendeloo VF, Ponsaerts P, Lardon F, Nijs G, Lenjou M, Van Broeckhoven C, et al. Highly efficient gene delivery by mRNA electroporation in human hematopoietic cells: superiority to lipofection and passive pulsing of mRNA and to electroporation of plasmid cDNA for tumor antigen loading of dendritic cells. Blood. 2001 Jul 1;98(1):49–56.

171. Okazaki T, Chikuma S, Iwai Y, Fagarasan S, Honjo T. A rheostat for immune responses: the unique properties of PD-1 and their advantages for clinical application. Nat Immunol. 2013 Dec;14(12):1212–8.

172. Qu Q-X, Xie F, Huang Q, Zhang X-G. Membranous and Cytoplasmic Expression of PD-L1 in Ovarian Cancer Cells. Cell Physiol Biochem. 2017;43(5):1893–906.

173. Martinez M, Moon EK. CAR T Cells for Solid Tumors: New Strategies for Finding, Infiltrating, and Surviving in the Tumor Microenvironment. Front Immunol. 2019;10:128.

174. Han Y, Liu D, Li L. PD-1/PD-L1 pathway: current researches in cancer. Am J Cancer Res. 2020;10(3):727–42.

175. Li X, Shao C, Shi Y, Han W. Lessons learned from the blockade of immune checkpoints in cancer immunotherapy. J Hematol Oncol. 2018 Feb 27;11(1):31.

176. Sabatier R, Finetti P, Mamessier E, Adelaide J, Chaffanet M, Ali HR, et al. Prognostic and predictive value of PDL1 expression in breast cancer. Oncotarget. 2015 Mar 10;6(7):5449–64.

177. Samanta D, Park Y, Ni X, Li H, Zahnow CA, Gabrielson E, et al. Chemotherapy induces enrichment of CD47+/CD73+/PDL1+ immune evasive triple-negative breast cancer cells. Proc Natl Acad Sci U S A. 2018 Feb 6;115(6):E1239–48.

178. Brockhoff G, Seitz S, Weber F, Zeman F, Klinkhammer-Schalke M, Ortmann O, et al. The presence of PD-1 positive tumor infiltrating lymphocytes in triple negative breast cancers is associated with a favorable outcome of disease. Oncotarget. 2018 Jan 19;9(5):6201–12.

179. Huang W, Ran R, Shao B, Li H. Prognostic and clinicopathological value of PD-L1 expression in primary breast cancer: a meta-analysis. Breast Cancer Res Treat. 2019 Nov;178(1):17–33.

180. Oner G, Önder S, Karatay H, Ak N, Tükenmez M, Müslümanoğlu M, et al. Clinical impact of PD-L1 expression in triple-negative breast cancer patients with residual tumor burden after neoadjuvant chemotherapy. World J Surg Oncol. 2021 Sep 2;19(1):264.

181. Schmid P, Adams S, Rugo HS, Schneeweiss A, Barrios CH, Iwata H, et al. Atezolizumab and Nab-Paclitaxel in Advanced Triple-Negative Breast Cancer. N Engl J Med. 2018 Nov 29;379(22):2108–21.

182. Xie Y, Hu Y, Zhou N, Yao C, Wu L, Liu L, et al. CAR T-cell therapy for triple-negative breast cancer: Where we are. Cancer Lett. 2020 Oct 28;491:121–31.

183. Callard RE, Stark J, Yates AJ. Fratricide: a mechanism for T memory-cell homeostasis. Trends Immunol. 2003 Jul;24(7):370–5.

184. Breman E, Demoulin B, Agaugué S, Mauën S, Michaux A, Springuel L, et al. Overcoming Target Driven Fratricide for T Cell Therapy. Front Immunol. 2018;9:2940.

185. Brochez L, Meireson A, Chevolet I, Sundahl N, Ost P, Kruse V. Challenging PD-L1 expressing cytotoxic T cells as a predictor for response to immunotherapy in melanoma. Nat Commun. 2018 Jul 26;9(1):2921.

186. Diskin B, Adam S, Cassini MF, Sanchez G, Liria M, Aykut B, et al. PD-L1 engagement on T cells promotes self-tolerance and suppression of neighboring macrophages and effector T cells in cancer. Nat Immunol. 2020 Apr;21(4):442–54.

187. Chen J, Jiang CC, Jin L, Zhang XD. Regulation of PD-L1: a novel role of pro-survival signalling in cancer. Ann Oncol. 2016 Mar;27(3):409–16.

188. Chen S, Crabill GA, Pritchard TS, McMiller TL, Wei P, Pardoll DM, et al. Mechanisms regulating PD-L1 expression on tumor and immune cells. J Immunother Cancer. 2019 Nov 15;7(1):305.

189. Jr CAJ, Travers P, Walport M, Shlomchik MJ, Jr CAJ, Travers P, et al. Immunobiology. 5th ed. Garland Science; 2001.

190. Wölfle SJ, Strebovsky J, Bartz H, Sähr A, Arnold C, Kaiser C, et al. PD-L1 expression on tolerogenic APCs is controlled by STAT-3. Eur J Immunol. 2011 Feb;41(2):413–24.

191. Brown JA, Dorfman DM, Ma F-R, Sullivan EL, Munoz O, Wood CR, et al. Blockade of programmed death-1 ligands on dendritic cells enhances T cell activation and cytokine production. J Immunol. 2003 Feb 1;170(3):1257–66.

192. Roux C, Jafari SM, Shinde R, Duncan G, Cescon DW, Silvester J, et al. Reactive oxygen species modulate macrophage immunosuppressive phenotype through the up-regulation of PD-L1. Proc Natl Acad Sci U S A. 2019 Mar 5;116(10):4326–35.

193. Zhang X, Zeng Y, Qu Q, Zhu J, Liu Z, Ning W, et al. PD-L1 induced by IFN-γ from tumor-associated macrophages via the JAK/STAT3 and PI3K/AKT signaling pathways promoted progression of lung cancer. Int J Clin Oncol. 2017 Dec;22(6):1026–33.

194. Oh SA, Wu D-C, Cheung J, Navarro A, Xiong H, Cubas R, et al. PD-L1 expression by dendritic cells is a key regulator of T-cell immunity in cancer. Nat Cancer. 2020 Jul;1(7):681–91.

195. Peng Q, Qiu X, Zhang Z, Zhang S, Zhang Y, Liang Y, et al. PD-L1 on dendritic cells attenuates T cell activation and regulates response to immune checkpoint blockade. Nat Commun. 2020 Sep 24;11(1):4835.

196. Xie J, Zhou Z, Jiao S, Li X. Construction of an anti-programmed death-ligand 1 chimeric antigen receptor and determination of its antitumor function with transduced cells. Oncol Lett. 2018 Jul;16(1):157–66.

197. Liu M, Wang X, Li W, Yu X, Flores-Villanueva P, Xu-Monette ZY, et al. Targeting PD-L1 in non-small cell lung cancer using CAR T cells. Oncogenesis. 2020 Aug 13;9(8):72.

198. Yang C-Y, Fan MH, Miao CH, Liao YJ, Yuan R-H, Liu CL. Engineering Chimeric Antigen Receptor T Cells against Immune Checkpoint Inhibitors PD-1/PD-L1 for Treating Pancreatic Cancer. Mol Ther Oncolytics. 2020 Jun 26;17:571–85.

199. Peng Q, Zhu X, Li C, Xin P, Zheng Y, Liu S. APDL1-CART cells exhibit strong PD-L1-specific activity against leukemia cells. Aging (Albany NY). 2021 Feb 26;13(5):7199–210.

200. Liu L, Liu Y, Xia Y, Wang G, Zhang X, Zhang H, et al. Synergistic killing effects of PD-L1-CAR T cells and colorectal cancer stem cell-dendritic cell vaccine-sensitized T cells in ALDH1-positive colorectal cancer stem cells. J Cancer. 2021;12(22):6629–39.

201. Li T, Wang J. Therapeutic effect of dual CAR-T targeting PDL1 and MUC16 antigens on ovarian cancer cells in mice. BMC Cancer. 2020 Jul 20;20(1):678.

202. Jiang W, Li T, Guo J, Wang J, Jia L, Shi X, et al. Bispecific c-Met/PD-L1 CAR-T Cells Have Enhanced Therapeutic Effects on Hepatocellular Carcinoma. Front Oncol. 2021;11:546586.

203. Xu C, Li X, Liu P, Li M, Luo F. Patient-derived xenograft mouse models: A high fidelity tool for individualized medicine. Oncol Lett. 2019 Jan;17(1):3–10.

204. Sentman M-L, Murad JM, Cook WJ, Wu M-R, Reder J, Baumeister SH, et al. Mechanisms of Acute Toxicity in NKG2D Chimeric Antigen Receptor T Cell–Treated Mice. The Journal of Immunology. 2016 Dec 15;197(12):4674–85.

205. Robbins Y, Greene S, Friedman J, Clavijo PE, Van Waes C, Fabian KP, et al. Tumor control via targeting PD-L1 with chimeric antigen receptor modified NK cells. Elife. 2020 Jul 7;9:e54854.

206. Xie YJ, Dougan M, Jailkhani N, Ingram J, Fang T, Kummer L, et al. Nanobody-based CAR T cells that target the tumor microenvironment inhibit the growth of solid tumors in immunocompetent mice. Proc Natl Acad Sci U S A. 2019 Apr 16;116(16):7624–31.

207. Zhao R, Cui Y, Li S, Qin L, Li P. Current status and hurdles for CAR-T cell immune therapy. Blood Science. 2019 Oct;1(2):148–55.

208. Morgan RA, Yang JC, Kitano M, Dudley ME, Laurencot CM, Rosenberg SA. Case report of a serious adverse event following the administration of T cells transduced with a chimeric antigen receptor recognizing ERBB2. Mol Ther. 2010 Apr;18(4):843–51.

209. Zhao Y, Wang QJ, Yang S, Kochenderfer JN, Zheng Z, Zhong X, et al. A herceptin-based chimeric antigen receptor with modified signaling domains leads to enhanced

survival of transduced T lymphocytes and antitumor activity. J Immunol. 2009 Nov 1;183(9):5563–74.

210. Kwapisz D. Pembrolizumab and atezolizumab in triple-negative breast cancer. Cancer Immunol Immunother. 2021 Mar;70(3):607–17.

211. Ahmed N, Brawley VS, Hegde M, Robertson C, Ghazi A, Gerken C, et al. Human Epidermal Growth Factor Receptor 2 (HER2) -Specific Chimeric Antigen Receptor-Modified T Cells for the Immunotherapy of HER2-Positive Sarcoma. J Clin Oncol. 2015 May 20;33(15):1688–96.

212. Beatty GL, Haas AR, Maus MV, Torigian DA, Soulen MC, Plesa G, et al. Mesothelin-specific chimeric antigen receptor mRNA-engineered T cells induce anti-tumor activity in solid malignancies. Cancer Immunol Res. 2014 Feb;2(2):112–20.

213. Guo F, Cui J. CAR-T in solid tumors: Blazing a new trail through the brambles. Life Sci. 2020 Nov 1;260:118300.

214. Tchou J, Zhao Y, Levine BL, Zhang PJ, Davis MM, Melenhorst JJ, et al. Safety and Efficacy of Intratumoral Injections of Chimeric Antigen Receptor (CAR) T Cells in Metastatic Breast Cancer. Cancer Immunol Res. 2017 Dec;5(12):1152–61.

215. Gu X, He D, Li C, Wang H, Yang G. Development of Inducible CD19-CAR T Cells with a Tet-On System for Controlled Activity and Enhanced Clinical Safety. Int J Mol Sci. 2018 Nov 3;19(11):E3455.

216. Sakemura R, Terakura S, Watanabe K, Julamanee J, Takagi E, Miyao K, et al. A Tet-On Inducible System for Controlling CD19-Chimeric Antigen Receptor Expression upon Drug Administration. Cancer Immunol Res. 2016 Aug;4(8):658–68.

217. Drent E, Poels R, Mulders MJ, van de Donk NWCJ, Themeli M, Lokhorst HM, et al. Feasibility of controlling CD38-CAR T cell activity with a Tet-on inducible CAR design. PLoS One. 2018;13(5):e0197349.

218. Zhang P, Raju J, Ullah MA, Au R, Varelias A, Gartlan KH, et al. Phase I Trial of Inducible Caspase 9 T Cells in Adult Stem Cell Transplant Demonstrates Massive Clonotypic Proliferative Potential and Long-term Persistence of Transgenic T Cells. Clin Cancer Res. 2019 Mar 15;25(6):1749–55.

219. Lanitis E, Poussin M, Klattenhoff AW, Song D, Sandaltzopoulos R, June CH, et al. Chimeric antigen receptor T Cells with dissociated signaling domains exhibit focused antitumor activity with reduced potential for toxicity in vivo. Cancer Immunol Res. 2013 Jul;1(1):43–53.

220. Roybal KT, Rupp LJ, Morsut L, Walker WJ, McNally KA, Park JS, et al. Precision Tumor Recognition by T Cells With Combinatorial Antigen-Sensing Circuits. Cell. 2016 Feb 11;164(4):770–9.

221. Si W, Li C, Wei P. Synthetic immunology: T-cell engineering and adoptive immunotherapy. Synth Syst Biotechnol. 2018 Sep;3(3):179–85.

222. Hyrenius-Wittsten A, Su Y, Park M, Garcia JM, Alavi J, Perry N, et al. SynNotch CAR circuits enhance solid tumor recognition and promote persistent antitumor activity in mouse models. Sci Transl Med. 2021 Apr 28;13(591):eabd8836.

223. Choe JH, Watchmaker PB, Simic MS, Gilbert RD, Li AW, Krasnow NA, et al. SynNotch-CAR T cells overcome challenges of specificity, heterogeneity, and persistence in treating glioblastoma. Sci Transl Med. 2021 Apr 28;13(591):eabe7378.

224. Curigliano G, Bagnardi V, Ghioni M, Louahed J, Brichard V, Lehmann FF, et al. Expression of tumor-associated antigens in breast cancer subtypes. Breast. 2020 Feb;49:202–9.

225. Rapoport AP, Stadtmauer EA, Binder-Scholl GK, Goloubeva O, Vogl DT, Lacey SF, et al. NY-ESO-1-specific TCR-engineered T cells mediate sustained antigen-specific antitumor effects in myeloma. Nat Med. 2015 Aug;21(8):914–21.

226. Chapuis AG, Egan DN, Bar M, Schmitt TM, McAfee MS, Paulson KG, et al. T cell receptor gene therapy targeting WT1 prevents acute myeloid leukemia relapse post-transplant. Nat Med. 2019 Jul;25(7):1064–72.

227. Carlsson J, Nordgren H, Sjöström J, Wester K, Villman K, Bengtsson NO, et al. HER2 expression in breast cancer primary tumours and corresponding metastases. Original data and literature review. Br J Cancer. 2004 Jun 14;90(12):2344–8.

228. Muz B, de la Puente P, Azab F, Azab AK. The role of hypoxia in cancer progression, angiogenesis, metastasis, and resistance to therapy. Hypoxia (Auckl). 2015;3:83–92.

229. Lundgren K, Holm C, Landberg G. Hypoxia and breast cancer: prognostic and therapeutic implications. Cell Mol Life Sci. 2007 Dec;64(24):3233–47.

230. Semenza GL, Wang GL. A nuclear factor induced by hypoxia via de novo protein synthesis binds to the human erythropoietin gene enhancer at a site required for transcriptional activation. Mol Cell Biol. 1992 Dec;12(12):5447–54.

231. Kosti P, Opzoomer JW, Larios-Martinez KI, Henley-Smith R, Scudamore CL, Okesola M, et al. Hypoxia-sensing CAR T cells provide safety and efficacy in treating solid tumors. Cell Rep Med. 2021 Apr 20;2(4):100227.

8. ATTACHMENTS

- study approval of the Local Bioethics Committee;

- bibliometric profile of the candidate.

Komisja Bioetyczna
przy Warszawskim Uniwersytecie Medycznym

Tel.: 022/ 57 - 20 -303
Fax: 022/ 57 - 20 -165

ul. Żwirki i Wigury nr 61
02-091 Warszawa

e-mail: komisja.bioetyczna@wum.edu.pl
www.komisja-bioetyczna.wum.edu.pl

Warszawa, dnia 19 listopada 2018 r

AKBE/ 194 / 2018

Dr hab. n. med. Radosław Zagożdżon
Zakład Immunologii Klinicznej
ul. Nowogrodzka 59
02-006 Warszawa

OŚWIADCZENIE

Niniejszym oświadczam, że Komisja Bioetyczna przy Warszawskim Uniwersytecie Medycznym w dniu 19 listopada 2018r. przyjęła do wiadomości informację na temat badania pt. „Ocena skuteczności przeciwnowotworowej nowego chimerycznego receptora antygenowego ukierunkowanego na cząsteczkę PD-L1." Przedstawione badanie nie stanowi eksperymentu medycznego w rozumieniu art. 21 ust. 1 ustawy z dnia 5 grudnia 1996 r. o zawodach lekarza i lekarza dentysty (Dz.U. z 2018 r. poz. 617) i nie wymaga uzyskania opinii Komisji Bioetycznej przy Warszawskim Uniwersytecie Medycznym, o której mowa w art. 29 ust. 1 ww. ustawy.

Przewodnicząca Komisji Bioetycznej

Prof. dr hab. n. med. Magdalena Kuźma –Kozakiewicz

WARSZAWSKI
UNIWERSYTET
MEDYCZNY

BIBLIOTEKA UCZELNIANA

Nr referencyjny
BIBG/Punktacja/ 46 /2022/DG

Warszawa, 28.01.2022

Sz. Pani
Katsiaryna Marhelava

ANALIZA BIBLIOMETRYCZNA CAŁOKSZTAŁTU DOROBKU PUBLIKACYJNEGO
PANI KATSIARYNA MARHELAVA,
W POSTĘPOWANIU O NADANIE STOPNIA NAUKOWEGO DOKTORA

Lp.	Opis bibliograficzny	Impact Factor	MEiN
I. Artykuły opublikowane w czasopismach naukowych lub w recenzowanych materiałach z konferencji międzynarodowych ujętych w aktualnym wykazie MEiN[1]			
1.	Bajor M, Graczyk-Jarzynka A, **Marhelava K**, Burdzinska A, Muchowicz A, Goral A, Zhylko A, Soroczynska K, Retecki K, Krawczyk M, Klopotowska M, Pilch Z, Paczek L, Malmberg KJ, Wälchli S, Winiarska M, Zagozdzon R. PD-L1 CAR effector cells induce self-amplifying cytotoxic effects against target cells. Journal for ImmunoTherapy of Cancer. 2022 Jan;10(1):e002500. (Rodzaj publikacji: praca oryginalna)	13,751	140
2.	Kłopotowska M, Bajor M, Graczyk-Jarzynka A, Kraft A, Pilch Z, Zhylko A, Firczuk M, Baranowska I, Lazniewski M, Plewczynski D, Góral A, Soroczyńska K, Domagała J, **Marhelava K**, Ślusarczyk A, Retecki K, Ramji K, Krawczyk M, Temples M, Sharma B, Lachota M, Netskar H, Malmberg K, Zagożdżon R, Winiarska M. PRDX-1 supports the survival and antitumor activity of primary and CAR-modified NK cells under oxidative stress. Cancer Immunology Research. 2021. doi: 10.1158/2326-6066.CIR-20-1023. [ahead-of-print] (Rodzaj publikacji: praca oryginalna)	11,151	200
3.	Bajor M, Graczyk-Jarzynka A, **Marhelava K**, Kurkowiak M, Rahman A, Aura C, Russell N, Zych A, Firczuk M, Winiarska M, Gallagher W, Zagożdżon R. Triple Combination of Ascorbate, Menadione and the Inhibition of Peroxiredoxin-1 Produces Synergistic Cytotoxic Effects in Triple-Negative Breast Cancer Cells. Antioxidants. 2020;9(4):320 (Rodzaj publikacji: praca oryginalna)	6,313	100

[1] Wykaz sporządzony zgodnie z przepisami wydanymi na podstawie art. 267 ust. 2 pkt 2 lit. b Ustawy z dnia 20 lipca 2018 r. - Prawo o szkolnictwie wyższym i nauce (Dz. U. z 2021 r. poz. 478, z późn. zm.). Wykaz stanowi załącznik do komunikatu MEiN z 21 grudnia 2021 r. o zmianie i sprostowaniu komunikatu w sprawie wykazu czasopism naukowych i recenzowanych materiałów z konferencji międzynarodowych.

ul. Żwirki i Wigury 63
02-091 Warszawa
www.biblioteka.wum.edu.pl
tel.: +48 22 116 60 11
biblioteka@wum.edu.pl

4.	Bobrowicz M, Ślusarczyk A, Domagała J, Dwojak M, Ignatova D, Chang Y, Iselin C, Miazek-Zapala N, **Marhelava K**, Guenova E, Winiarska M. Selective inhibition of HDAC6 sensitizes cutaneous T-cell lymphoma to PI3K inhibitors. Oncology Letters. 2020;20(1):533-540 (Rodzaj publikacji: praca oryginalna)	2,967	70
5.	**Marhelava K**, Pilch Z, Bajor M, Graczyk-Jarzynka A, Zagożdżon R. Targeting Negative and Positive Immune Checkpoints with Monoclonal Antibodies in Therapy of Cancer. Cancers. 2019;11(11):1756 (Rodzaj publikacji: praca poglądowa)	6,126	140
6.	Adamska I, **Marhelava K**, Walkiewicz D, Kedzierska U, Markowska M, Majewski P. All genes encoding enzymes participating in melatonin biosynthesis in the chicken pineal gland are transcribed rhythmically. Journal of Physiology and Pharmacology. 2016;67(4):521-530 (Rodzaj publikacji: praca oryginalna)	2,883	25
	Łącznie:	43,191	675
II. Artykuły opublikowane przed 1.01.2019 r. w czasopismach ujętych w wykazie czasopism MNiSW z dnia 25.01.2017 r., o ile czasopismo uzyskało co najmniej 10 pkt.			
brak		-	-
	Łącznie:	-	-
III. Pozostałe artykuły			
brak		-	-
	Łącznie:	-	-
	Łącznie (cz. I- III):	43,191	675
IV. Monografie naukowe/rozdziały w monografiach wydane przez wydawnictwa ujęte w wykazie MEiN[2] lub jednostki organizacyjne podmiotów, których wydawnictwa są ujęte w tym wykazie			
brak			
V. Pozostałe monografie lub rozdziały w monografiach			
brak			
VI. Patenty			
brak			

DYREKTOR BIBLIOTEKI

mgr Irmina Utrata

[2] Wykaz sporządzony zgodnie z przepisami wydanymi na podstawie art. 267 ust. 2 pkt 2 lit. a Ustawy z dnia 20 lipca 2018 r. - Prawo o szkolnictwie wyższym i nauce (Dz. U. z 2021 r. poz. 478, z późn. zm.). Wykaz ogłoszony komunikatem MEiN z dnia 22 lipca 2021 r. w sprawie wykazu wydawnictw publikujących recenzowane monografie naukowe.

ul. Żwirki i Wigury 63
02-091 Warszawa
www.biblioteka.wum.edu.pl
tel.: +48 22 116 60 11
biblioteka@wum.edu.pl